

Review

# Relativistic Effects from Heavy Main Group p-Elements on the NMR Chemical Shifts of Light Atoms: From Pioneering Studies to Recent Advances

Irina L. Rusakova \*  and Yuriy Yu. Rusakov

A. E. Favorsky Irkutsk Institute of Chemistry, Siberian Branch of the Russian Academy of Sciences, Favorsky St. 1, 664033 Irkutsk, Russia

\* Correspondence: i-rusakova@bk.ru

**Abstract:** This review represents a compendium of computational studies of relativistic effects on the NMR chemical shifts of light nuclei caused by the presence of heavy main group p-block elements in molecules. The narration starts from a brief discussion of the relativistic theories and quantum chemical methods for the calculation of NMR chemical shifts at the relativistic level of the electronic theory. The main part of the review contains a survey on the relativistic calculations of NMR shielding constants of the most popular NMR-active light nuclei such as  $^1\text{H}$ ,  $^{13}\text{C}$ ,  $^{19}\text{F}$ ,  $^{29}\text{Si}$ ,  $^{15}\text{N}$ , and  $^{31}\text{P}$  of compounds containing heavy p-elements. A special focus is placed on the relativistic effects initiated by the 16th and 17th group elements. Different factors governing the behavior of the relativistic effects on the chemical shifts of light atoms are discussed. In particular, the stereochemistry of the relativistic “heavy atom on the light atom” effect and the influence of the spin–orbit relativistic effects on the vibrational contributions to the shielding constants of light nuclei are considered.

**Keywords:** NMR; relativistic effects; spin–orbit coupling; NMR chemical shift; NMR shielding constant; heavy atom on light atom effect; spin–orbit HALA effect; SO-HALA; scalar-HALA; heavy p-elements



**Citation:** Rusakova, I.L.; Rusakov, Y.Y. Relativistic Effects from Heavy Main Group p-Elements on the NMR Chemical Shifts of Light Atoms: From Pioneering Studies to Recent Advances. *Magnetochemistry* **2023**, *9*, 24. <https://doi.org/10.3390/magnetochemistry9010024>

Academic Editor: Sangdoon Ahn

Received: 5 December 2022

Revised: 3 January 2023

Accepted: 4 January 2023

Published: 7 January 2023



**Copyright:** © 2023 by the authors. Licensee MDPI, Basel, Switzerland. This article is an open access article distributed under the terms and conditions of the Creative Commons Attribution (CC BY) license (<https://creativecommons.org/licenses/by/4.0/>).

## 1. Introduction

Nuclear Magnetic Resonance (NMR) spectroscopy represents one of the most powerful tools for chemical structure studies. In the current moment, it has become common practice to combine high-quality quantum chemical modeling of spectra with the experimental NMR technique, which implies the assignment of the signals of an experimental spectrum to those of a simulated one. In this sense, much effort has been made to work out accurate and efficient quantum chemical computational protocols for NMR parameters [1–33]. In this respect, the investigation of different factors affecting the accuracy of theoretical modeling of the NMR spectra for the most popular spin-1/2 “light nuclei,” such as  $^1\text{H}$ ,  $^{13}\text{C}$ ,  $^{15}\text{N}$ ,  $^{19}\text{F}$ ,  $^{29}\text{Si}$ , and  $^{31}\text{P}$ , of the compounds containing heavy elements is nowadays of paramount importance. One of such factors of accuracy is the effects of special relativity [34], which may have a significant impact on the NMR parameters of light nuclei, if there are one or more heavy atoms in the vicinity.

The relativistic influence of heavy atom(s) (HAs) on the nuclear shielding constant of a light spectator atom (LA) is known as the relativistic HALA effect, coined more than 50 years ago by Nomura, Takeuchi, and Nakagawa [35], who were the first to propose an explanation of the anomalous magnitudes of the chemical shifts of the ortho- and meta-protons of monosubstituted halobenzenes via the so-called “spin polarization shift” or *LS* shift. This idea has received very close attention due to its importance in the NMR computational methodology. Indeed, ignoring the relativistic effects in the computation of the NMR spectra of light nuclei for the molecules containing heavy atoms usually results in erroneous results. In this way, the investigation of the electronic structure

factors influencing the magnitudes of the relativistic HALA effect as well as the related computational aspects affecting the accuracy of the calculation of the HALA effect is of practical importance today [36,37].

This review focuses on the calculations of the relativistic HALA effect due to the presence of heavy p-block elements on chemical shifts of popular NMR-active nuclei of 1–3 periods. It is worth noting that, in general, the HALA effect is a very important and extensively studied field of research per se that is not restricted by the consideration of heavy p-element compounds. In particular, in the compounds containing heavy d-elements (transition-metal complexes) [36–54], f-elements (lanthanide and actinide complexes) [55–57] and s-elements (alkaline and alkaline-earth group hydrides) [58,59], the manifestation of the relativistic HALA effect may be very pronounced. These works have been covered in two salient reviews by Vicha et al. [36,37].

The relativistic HALA effect due to the presence of heavy main group p-block elements is a very important issue that deserves separate consideration. In this way, the present review covers the works on this topic in much detail, starting from early studies to recent advances.

## 2. Brief Notes on Developing the Relativistic Theory and Computational Methods for NMR Shielding Constants

Notwithstanding how several decades have passed since the appearance of the first theoretical studies on the effects of special relativity manifesting in NMR parameters [35,60–68], the challenge of their accurate prediction still strikingly arises whenever one deals with heavy element compounds. The relativistic theory of NMR chemical shifts (CSs) originates from the first attempts to include the spin–orbit (SO) coupling (SOC) in its simplest form into the perturbation theory for the NMR shielding tensor [35,60,69,70]. The so-called “spin-polarization shift” or *LS* shift was originally determined as a chemical shift related to the third-order perturbational correction to the energy containing the couplings of the external field with the electron orbital momentum, of the electron orbital momentum with the electron spin, and of the electron spin with the nuclear spin [35]. The lowest order of relativistic corrections due to the SOC occurred sufficiently enough to interpret the experimental data for the proton CSs in hydrogen halides [60] and carbon CSs in methyl halides [61] to support the motivation for further development of the relativistic theory as applied to the NMR CSs.

Pyper [62–65], Pyykkö [67,68], and Zhang and Webb [66] independently presented the four-component relativistic theory of NMR CSs for the first time. Thus, Pyper [62–64] introduced the relativistic theory of NMR CSs for the closed-shell systems that were described within the single-determinant Dirac–Fock wavefunctions. The equation for the shielding tensor was derived without taking into account the two-electron Breit interaction [71,72] by expressing the field-dependent orbitals in terms of the field-independent orbitals by using the first-order perturbational theory. Apart from the finite summation over the occupied orbitals, the most important term of Pyper’s theory contained an infinite summation over the negative-energy electronic states. Thus, to develop a consistent theory that is physically transparent and computationally convenient, Pyper applied the Gordon decomposition [73] to the relativistic current operator in the expectation value of the electron–nuclear spin–dipole interaction over the field-dependent many-electron wavefunctions. As a result, he obtained an expression where the contributions from the negative-energy electronic states were reduced to the order  $1/c^6$ . This provided the diamagnetic term in an explicit form and gave the exact relativistic analogue of the non-relativistic paramagnetic term.

Pyykkö et al. [67,68] presented a fully relativistic analogue to Ramsey’s theory of NMR chemical shifts [74] formulated for the four-component one-electron wavefunctions and relativistic magnetic Hamiltonian. The gauge origin problem [1,21] issue has arisen within the framework of Pyykkö’s four-component relativistic theory, and an idea was proposed to treat this problem via the use of the gauge-including atomic orbitals (GIAO) formalism [75,76]. Zhang and Webb [66] did actually incorporate London’s gauge invari-

ant atomic orbitals formalism [75] into the four-component relativistic theory for NMR shielding tensors.

The pioneering works of Pyper, Pyykkö, Zhang, Webb, and Quiney et al. [77–79] laid the foundation of modern relativistic four-component random phase approximation (RPA), 4RPA, or a coupled perturbed Dirac–Hartree–Fock (CP-DHF) method for shielding constants. Aucar et al. worked out the full four-component polarization propagator theory (4c-PPT) for nuclear shielding constants [80–88]. It should be mentioned that in the pioneering work on 4c-PPT [80], the concepts of paramagnetic- and diamagnetic-type contributions to the magnetic response properties were generalized. To treat the gauge-origin problem, Iliaš et al. [89] developed the theory of relativistic localized atomic orbitals (RLAO) and implemented it into the four-component CP-DHF (4RPA) approach, demonstrating the efficiency of the presented methodology on the example of the calculation of  $\sigma(^1\text{H})$  and  $\sigma(^{127}\text{I})$  in the HI molecule. Further, the developments of the 4RPA method were concentrated on the correct inclusion of the magnetic balance (MB) condition [90] in the formalism of relativistic localized atomic orbitals, which is necessary for all relativistic four-component methods for calculating the NMR shielding constants. This issue has been thoroughly investigated for some time, and, finally, Cheng et al. [91] presented the theory of the so-called magnetically balanced gauge-including atomic orbitals (MB-GIAOs), in which each “magnetically balanced” atomic orbital has its own local origin located in its center. The calculations of nuclear shielding constants within the 4RPA formalism were presented in a number of papers [84,88,92,93]; however, this method has not received very much popularity yet.

A scientific group of Sauer [94] presented the second-order polarization-propagator-approximation (SOPPA) method [95,96] within the relativistic framework. The equations for the relativistic SOPPA method were deduced in their most general form, that is, in a non-canonical spin–orbital basis, which can be reduced to the canonical case. The obtained equations are one-index transformed, giving more compact expressions that correspond to those already available for the four-component RPA. Thereby, a possible scheme has been outlined for the implementation of the presented equations in a program that already contains the RPA code. Overall, the relativistic SOPPA theory represents a very important computational ab initio highly correlated relativistic approach to the calculation of NMR chemical shifts of molecules containing heavy elements, especially if the magnetically balanced GIAO formalism will be embedded into this theory.

Another branch of development of the general four-component relativistic theory of the NMR shielding constants that already have received much greater popularity than the 4RPA method is the Dirac–Kohn–Sham (DKH) or four-component density functional theory (4DFT). Studies in this field were incepted by Malkin et al. [97], who circumvented the problem of using the complex arithmetic in the self-consistent field (SCF) procedure by employing the Fermi-contact (FC) operator as a real finite field perturbation operator. An approximate four-component density functional sum-over-states (SOS-DFPT) method has been elaborated for the straightforward calculation of shielding tensors, including scalar and spin–orbit coupling effects. The authors also employed the individual gauge for the localized orbitals (IGLO) method [98] to handle the gauge origin problem. The pioneering works of Malkin et al. laid the foundation of the state-of-the-art relativistic four-component DFT theory that is described in the works of Komorovsky et al. [99,100]. Komorovsky and colleagues proposed the most general relativistic four-component density functional theory (4DFT) for the calculations of NMR shielding constants. Their theory is based on the matrix formulation of the Dirac–Kohn–Sham (mDKS) method and on the use of the restricted magnetic balance (RMB) condition for the small molecular spinor components (the mDKS-RMB methodology). At the present moment, their methodology can be regarded as one of the most efficient approaches to the calculation of the NMR parameters within the four-component DFT method. Apart from the mDKS-RMB methodology, there is another approach for the relativistic DKS calculations of nuclear shielding tensors, which was proposed by Xiao et al., namely, the orbital decomposition approach (ODA) [101,102]. The

ODA also goes beyond the kinetic balance and treats the magnetic part of the response of the small components. Notwithstanding how the ODA approach deals with more complicated equations, it has an advantage that one can use the basis set for the large components only.

Four-component methods constitute a relativistic “golden standard” that gives highly accurate results, provided that a suitable approximation for the electronic wave function is employed [103], though, they are characterized by a high computational cost. Moreover, in the four-component formalism, the physically tractable relativistic effects of different types cannot be distinguished in an explicit way. In order to lower the computation costs of the four-component methods, the Dirac–Fock operator was decoupled using different strategies to give the relativistic two-component theories. At that, different types of relativistic corrections to the shielding tensor were deduced in an explicit form. Generally, a transition to the two-component theories can be done by transforming the many-body four-component relativistic Hamiltonian to the block-diagonal form, resulting in the elimination of the small spinor components. The other way that also gives the expressions for different types of relativistic corrections lies in a straightforward treatment of the relativistic terms as the perturbations operating on a nonrelativistic reference wave function, on the same footing as the magnetic perturbation operators.

In that way, Nakatsuji et al. [69,104] proposed a computational method for accounting for the spin–orbit effects on the magnetic shielding constant using the *ab initio* unrestricted Hartree–Fock (UHF) wavefunction in the finite perturbation theory (FPT) [105]. Both the one-electron term of the spin–orbit operator and the external magnetic field were included in that theory as finite perturbations. However, in the mentioned pioneering work, the spin–orbit operator did not include any vector potentials coming from an external magnetic field and nuclear magnetic moments. In particular, this resulted in a disadvantage that there was no gauge invariance reached. Fukui et al. [106–108] was the first to include the vector potential into the mechanical momentum in the SO interaction operator and derived the lowest-order relativistic theory for the nuclear magnetic shielding constants from the two-component positive-energy Hamiltonian. As a result, final gauge-invariant expressions for many types of relativistic corrections have been derived. Later on, Ballard et al. [109] presented an extension of the method of Nakatsuji et al. by combining Nakatsuji’s SO-UHF method with the spin-free relativistic no-pair theory of Sucher [110] and Hess [111,112], thus accounting for both the spin–orbit and scalar relativistic effects. Fukuda et al. [113,114] also presented a quasirelativistic theory of magnetic shielding constants based on the Sucher–Hess method, solving the gauge-origin problem with the GIAO formalism. As a result, they worked out the gauge-origin-independent theory of the so-called GIAO-FP-QR-GUHF method that uses the generalized UHF (GUHF) wavefunction [115,116] within the finite perturbation technique.

Another two-component gauge-invariant theory was proposed by Wolf and Ziegler [117] on the basis of the nonrelativistic DFT theory of Schreckenbach and Ziegler [118]. The authors presented the extension of the original work by including into the Hamiltonian the one-electron spin–orbit operator together with the Darwin and mass-velocity terms and the Fermi–contact interaction. The authors resorted to a frozen-core approximation [119] and to the GIAO formalism. The effect of magnetic fields on the MOs was taken into account within the first-order perturbation theory (FOPT).

Vaara et al. [120,121] presented the *ab initio* correlated theory of the electronic spin–orbit contribution to the nuclear magnetic shielding tensors for the first time. This was the first theory to describe the heavy atom-induced relativistic SO corrections to the chemical shifts of the light nuclei located in the vicinity of the heavy elements (i.e., the heavy atom SOC-induced HALA effect or simply the SO-HALA effect) within the *ab initio* correlated MCSCF approach [122,123]. The SO contribution was calculated as the sum of analytical quadratic response functions, calculated by taking into account both the one- and two-electron parts of the spin–orbit Hamiltonian and considering the interaction through both the Fermi-contact (FC) and the spin-dipolar (SD) mechanisms. Vaara et al. has also showed that, apart from the third-order perturbation terms (those expressed with quadratic

response), there are the terms originating from the magnetic field-dependent spin-orbit Hamiltonian that requires the consideration within the second-order perturbation theory and, therefore, the calculation of linear response functions only [121]. For the hydrogen chalcogenides, contributions of this type are often negligibly small [121]. Subsequently, Vaara et al. [124] reported on a new approach to calculate both scalar and SO effects on the nuclear shielding constants of light nuclei in molecules containing heavy atoms. In that approach, the scalar relativistic effects were incorporated into a conventional shielding calculation via the quasi-relativistic effective-core potentials (ECPs) [125]. This calculation was combined with the third-order perturbation theory treatment of the SO effect using the so-called SO-ECPs. They also implemented the second-order SO term due to the magnetic field dependence of the one-electron part of the SO Hamiltonian interacting with the Fermi contact mechanism. The method was implemented at the DFT level of theory, and the IGLO scheme for treating the gauge origin problem was employed.

Manninen et al. [126–128] presented the ab initio calculations of the full set of leading-order one-electron relativistic contributions to the NMR shielding tensor based on the Breit–Pauli perturbational theory (BPPT). The corrections were evaluated using the relativistic and magnetic operators as perturbations on an equal footing by means of the analytical linear and quadratic response theory applied on top of a nonrelativistic reference state provided by self-consistent field calculations. In terms of BPPT, the relativistic effects on the NMR parameters were classified into two conceptually different categories: the “passive” and “active” relativistic effects. The “passive” relativistic effects were determined as those that modify the perturbational expressions of the terms that are present in the non-relativistic consideration via the first-order relativistic modification of the wavefunction. For example, the second-order Ramsey expression [74] for the nonrelativistic (NR) paramagnetic shielding tensor can be modified to include the scalar mass-velocity or Darwin correction as an additional third perturbation operator. The “active” corrections are those which contain the relativistic operators bearing a functional dependence on the explicit degrees of freedom in the effective NMR spin-Hamiltonian, that is, the nuclear magnetic moment, and/or the external magnetic field. For example, the second-order SO effects that originate from the magnetic field-dependent spin-orbit Hamiltonian, which were also noticed by Vaara et al. [121] and Fukui [106], contribute precisely to the “active” relativistic corrections.

The expressions for the perturbation treatment of the relativistic effects were also presented by Jaszunski and Ruud [129], who demonstrated that the BPPT can be successfully applied to analyze the relativistic effects on both light- and heavy-atom shielding constants. In particular, the authors showed that the relativistic shielding constants obtained within the perturbational treatment were in satisfying agreement with the results obtained within the four-component relativistic calculations: the differences were practically negligible for the compounds containing the elements of the first five rows of the periodic table.

Kudo and Fukui [130] presented two expressions for the NMR shielding tensor components based on the analytical differentiation of the electronic energy of a system. The first approach was based on the second-order Douglas–Kroll–Hess (DKH) transformation [112,131], in which the off-diagonal block terms of the transformed Dirac Hamiltonian were diminished to the second order with respect to both the electrostatic nuclear attraction potential and the magnetic vector potential. The second expression was based on the method of Barysz–Sadlej–Snijders (BSS) [132–135], where the off-diagonal block terms in the transformed Dirac Hamiltonian were completely eliminated with respect to the electrostatic potential terms and to the second order with respect to the terms bearing the magnetic vector potential.

To conclude, the two-component theories resulted in two-component methods of calculation of the relativistic effects on the NMR chemical shifts. Sun et al. [136] has published a thorough review, devoted to the two-component schemes for calculating the NMR parameters, surveying in detail various two-component Hamiltonians, both of the exact two-component (X2C) and approximate two-component (A2C) types.

It is generally accepted that X2C schemes imply that the eigenvalues of a given two-component Hamiltonian exactly reproduce the solutions of the four-component ana-

logue. According to the recent reviews by Autschbach [137] and Peng and Reicher [103], one can distinguish two different types of X2C schemes, namely those which split the Hamiltonian into large and small subblocks via the one- and more-than-one-step procedure. Among the most well-known X2Cs are the following schemes: normalized elimination of the small component (NESC) [138–145], the infinite-order Douglas–Kroll–Hess (DKH) [146], and the Barysz–Sadlej–Snijders (BSS) or the infinite-order two-component (IOTC) approach [132–135].

The other two-component schemes, which give solutions that are unequal to those of the original four-component problem, are called quasirelativistic or approximate two-component schemes, A2C. These include the following most well-known approaches: zero-order regular approximation (ZORA) [147–149], second-order regular approximation to normalized elimination of the small component (SORA-NESC) [150], finite-order Douglas–Kroll–Hess approximations (DKH) [112,131,151–156], and the infinite-order regular approximation (IORA) [157,158]. Among the two-component techniques, ZORA-DFT approach has attained the most popularity in the calculations of NMR properties, especially in the solid-state NMR [159–162].

A separate two-component “linear response within the elimination of small component” (LRESC) approach for calculating the relativistic corrections to the nuclear magnetic shielding constants was presented by Aucar et al. [83,86,163–166]. The final expressions for the relativistic corrections to the shielding tensor, obtained by Aucar et al. within the LRESC approach, were equivalent to those of Fukui [106], though some other additional terms correcting both the paramagnetic and the diamagnetic parts of shielding tensors were introduced.

Various methods for the inclusion of relativistic effects in the calculation of NMR parameters have been discussed in a number of salient reviews by Visscher et al. [167], Autschbach et al. [168–171], Oprea [172], Aucar et al. [80,83,86–88,163,173–182], and Rusakova et al. [22–24,183].

It is helpful to briefly discuss here a set of the leading-order perturbational one-electron relativistic contributions to the NMR shielding tensor in terms of the Breit–Pauli perturbational theory [126–128] and LRESC theory [83,86,163]. Thus, 16 types of the leading-order relativistic corrections are as follows:

$$\begin{aligned} \Delta\sigma^{\text{BPTT}} = & \sigma^{\text{con}} + \sigma^{\text{dip}} + \sigma^{\text{d-KE}} + \sigma^{\text{p-OZ}} \quad (\text{first order}) \\ & + \sigma^{\text{d/mv}} + \sigma^{\text{d/Dar}} + \sigma^{\text{p/OZ-KE}} + \sigma^{\text{p-KE/OZ}} \quad (\text{second order, singlet}) \\ & + \sigma^{\text{FC-II}} + \sigma^{\text{SD-II}} + \sigma^{\text{FC/SZ-KE}} + \sigma^{\text{SD/SZ-KE}} \quad (\text{second order, triplet}) \\ & + \sigma^{\text{p/mv}} + \sigma^{\text{p/Dar}} \quad (\text{third order, singlet}) \\ & + \sigma^{\text{FC-I}} + \sigma^{\text{SD-I}} \quad (\text{third order, triplet}) \end{aligned} \quad (1)$$

These relativistic corrections can be divided into two main categories. The first category includes the effects that contribute to the shielding tensor of a light atom due to a neighboring heavy atom, that is, to the very same HALA effect that is the subject of the present review. The second category includes the relativistic corrections to the shielding tensor of a heavy atom itself (HAHA effects) [173]. Among the terms, presented in Equation (1), typically only five terms are responsible for the majority of relativistic corrections. The main terms which provide the leading contributions to the HAHA effect are  $\sigma^{\text{p-KE/OZ}}$ ,  $\sigma^{\text{p/mv}}$ ,  $\sigma^{\text{p/Dar}}$ ,  $\sigma^{\text{FC-I}}$ , and  $\sigma^{\text{SD-I}}$ , with the last two contributions,  $\sigma^{\text{FC-I}}$  and  $\sigma^{\text{SD-I}}$ , also being responsible for the HALA effect. The first three terms,  $\sigma^{\text{p-KE/OZ}}$ ,  $\sigma^{\text{p/mv}}$ ,  $\sigma^{\text{p/Dar}}$ , represent the scalar corrections and are of minor importance for the HALA effect. The  $\sigma^{\text{FC-I}}$ , and  $\sigma^{\text{SD-I}}$  represent the third-order “passive” (those corrections which are due to the relativistic operators with no dependence on external or nuclear magnetic field) triplet properties which can be expressed through the quadratic response function of orbital Zeeman (OZ), one-electron spin-orbit (SO(1)) and Fermi-contact/spin-dipole (FC/SD) operators [129]:

$$\sigma_{K,\epsilon\tau}^{\text{FC-I}} = \gamma_K^{-1} \left\langle \left\langle h_{K,\epsilon}^{\text{FC}}; h_{B,\tau}^{\text{OZ}}, h_{\epsilon}^{\text{SO(1)}} \right\rangle \right\rangle_{0,0} \quad (2)$$

$$\sigma_{K,\epsilon\tau}^{SD-I} = \gamma_K^{-1} \sum_{\mu=x,y,z} \left\langle \left\langle h_{K,\epsilon}^{SD,\mu}; h_{B,\tau}^{OZ}; h_{\mu}^{SO(1)} \right\rangle \right\rangle_{0,0} \quad (3)$$

There are also “active” counterparts (the contributions involving relativistic operators carrying an explicit reference to the external field or nuclear spin) of these terms, namely  $\sigma^{FC-II}$  and  $\sigma^{SD-II}$ , which originate from the active second-order SO effects. They represent triplet linear response functions of FC or SD hyperfine operators and the external field-dependent SO counterparts.

In general, the  $\sigma^{FC-II}$  and  $\sigma^{SD-II}$  can be expressed as follows [129]:

$$\sigma_{K,\epsilon\tau}^{FC-II} = \gamma_K^{-1} \left\langle \left\langle h_{K,\epsilon}^{FC}; h_{B,\tau}^{SO(1),\epsilon} \right\rangle \right\rangle_0 \quad (4)$$

$$\sigma_{K,\epsilon\tau}^{SD-II} = \gamma_K^{-1} \sum_{\mu=x,y,z} \left\langle \left\langle h_{K,\epsilon}^{SD,\mu}; h_{B,\tau}^{SO(1),\mu} \right\rangle \right\rangle_0 \quad (5)$$

It should be noted that the FC-I and FC-II, as well as the SD-I and SD-II terms are not by themselves gauge-invariant, but the sums of the corresponding third- and second-order terms are [129]. That is why Nakatsuji et al. [69,104] did not achieve the gauge invariance when presenting the theory that omitted the dependence of the momentum operator included into the SO operator on the vector potential of the external magnetic field. The influence of the  $\sigma^{FC-II}$  and  $\sigma^{SD-II}$  on the HALA effect is very much diminished as compared to the  $\sigma^{FC-I}$  and  $\sigma^{SD-I}$  contributions. This can be demonstrated by the first calculations by Fukui et al. [106], performed for hydrogen halides at the experimental geometries. Thus, for example, in the HX (X = F to I) series, the  $\sigma^{FC-I}$  contribution to the hydrogen shielding constant exceeds the  $\sigma^{FC-II}$  contribution by *ca.* 23, 110, 350, and 765 times for X = F, Cl, Br, I, respectively [106]. Even for the heaviest molecule of the HX series, HI, the contribution of the  $\sigma^{FC-II}$  term to the hydrogen shielding constant accounts only to 0.02 ppm.

It is also worth noting that the scalar and SO effects on molecular properties are not additive; for example, the scalar-induced changes in the nodal structure of the wave function typically increase the magnitude of the SO effect [44,104,108,109].

The main contribution which is known to be responsible for the most part of the HALA effect is  $\sigma^{FC-I}$ . This term is said to embody the FC/OZ/SO, or briefly, the SO/FC mechanism that determines the spin-orbit HALA (SO-HALA) effect. The main expression for the SO-HALA correction in terms of molecular orbitals (MOs) that helps to deduce the physical meaning of this phenomenon and some of its properties is as follows [36,37,184]:

$$\begin{aligned} \sigma_{SO/FC}^{\mu\mu}(LA) &\sim \sum_{ab}^{vac} \sum_i^{occ} \left( \frac{\langle \varphi_i | \delta_{LA} | \varphi_a \rangle \langle \varphi_a | \Delta r_{HA}^{-3} \hat{I}_{HA}^{\mu} | \varphi_b \rangle \langle \varphi_b | \hat{I}_{HA}^{\mu} | \varphi_i \rangle}{(\epsilon_i - \epsilon_a)(\epsilon_i - \epsilon_b)} + perms \right) \\ &- \sum_a^{vac} \sum_{ij}^{occ} \left( \frac{\langle \varphi_i | \delta_{LA} | \varphi_a \rangle \langle \varphi_a | \Delta r_{HA}^{-3} \hat{I}_{HA}^{\mu} | \varphi_j \rangle \langle \varphi_j | \hat{I}_{HA}^{\mu} | \varphi_i \rangle}{(\epsilon_i - \epsilon_a)(\epsilon_j - \epsilon_a)} + perms \right) \end{aligned} \quad (6)$$

The denominators in Equation (6) represent the energy gaps of the occupied (*i, j*) and vacant (*a, b*) MOs (indices *p* and *q* will be used to designate an arbitrary type of MOs). The numerators of Equation (6) represent the products of three spatial one-electron molecular integrals, namely, the one-electron spin-orbit (SO) integrals,  $\langle \varphi_p | \Delta r_{HA}^{-3} \hat{I}_{HA}^{\mu} | \varphi_q \rangle$ , Dirac's  $\delta$ -function (FC) integrals,  $\langle \varphi_i | \delta_{LA} | \varphi_a \rangle$ , and angular momentum or orbital Zeeman (OZ) integrals,  $\langle \varphi_b | \hat{I}_{HA}^{\mu} | \varphi_i \rangle$ . The subscripts “HA” and “LA” refer to a particular operator that is centered on the heavy and light atom under consideration, respectively. The physical mechanism that underlies the expression (6) can be described as follows [37,185]: in the presence of an external magnetic field, SOC on the HA mixes some triplet character into the closed-shell singlet ground-state wavefunction, and thereby spin-polarizes the density distribution in the core and valence shells of the heavy atom, even in a closed-shell molecule. The induced spin density propagates to LA and provides an additional magnetic interaction with a magnetic dipole of LA via the Fermi-contact mechanism changing the LA NMR chemical shift,  $\delta(LA)$ .

The main factors that can affect the magnitude of the SO-HALA effect on the shielding constants of light nuclei can readily be established from the expression (6). The first factor is the rate of involvement of the valence  $s$  orbitals of the LA in the HA–LA bond. This determines the efficiency of the SO/FC mechanism, which requires the involvement of the LA atomic  $ns$  orbitals to bring the SO-induced spin-polarization in contact with the LA nucleus [186]. As a consequence, the most pronounced SO-HALA effect is expected for the  $^1\text{H}$  NMR shielding constants of protons directly bonded to HA, because in this case the hydrogen  $1s$  orbital predominates in bonding. The second factor is the energy gaps between the involved occupied and vacant molecular orbitals (usually several frontier highest occupied MOs (HOMO) and lowest unoccupied MOs (LUMO) contribute to a large extent) [186]. The third factor is the magnitude of the SOC at HA. In particular, the occupation of orbitals with  $l \geq 1$  and the partial charge on the heavy atom (entering through the SO integrals in Equation (6)) play a decisive role in the magnitude of the spin–orbit splitting (SOC coupling) [186]. In this respect, the spin–orbit contributions should increase from fluorine to iodine substituents, and from left to right within a given row of the p-block main group elements (e.g., from chalcogen to halogen) [186]. These considerations to a high extent can also be attributed to the SO-HALA effect on NMR chemical shifts of light nuclei. This is due to the fact that the relativistic correction to the chemical shift of a light nucleus (e.g.,  $^1\text{H}$ ,  $^{13}\text{C}$ ) of a compound can simply be expressed as the difference between the relativistic correction to the shielding constant of a light spectator nucleus in the reference compound and that in the compound under consideration:

$$\Delta_{rel}(\delta_{LA}^{sample}) = \Delta_{rel}(\sigma_{LA}^{ref}) - \Delta_{rel}(\sigma_{LA}^{sample}) \quad (7)$$

Taking into account that in most cases the relativistic effects on the NMR shielding constants of light nucleus in reference compounds,  $\Delta_{rel}(\sigma_{LA}^{ref})$ , are small (take, for example, the relativistic correction of only  $-0.02$  ppm to proton-shielding constant in TMS [187]), one can roughly attribute the facts established for the negative  $\Delta_{rel}(\sigma_{LA}^{sample})$ , including  $\Delta_{SO-HALA}(\sigma_{LA}^{sample})$ , to  $\Delta_{rel}(\delta_{LA}^{sample})$ .

### 3. Studies of the Relativistic Effects on NMR Shielding Constants of Light Nuclei from Heavy Main Group p-Elements

#### 3.1. Relativistic Effects on $^1\text{H}$ and $^{13}\text{C}$ NMR Chemical Shifts

For a very long time, so-called normal halogen dependence (NHD) [188–192] has been observed in NMR experimental studies. The NHD consists of a decrease in the proton and carbon chemical shifts (increasing of the shielding constants) ongoing from chloride to bromide to iodide substituents. For the hydrogen halides, HF, HCl, HBr and HI, despite their similarity from a chemical point of view, the hydrogen chemical shift changes significantly from HF to HI. The nucleus of the hydrogen atom in the HI molecule is extremely shielded [188] and the difference between the proton chemical shifts of HF and HI molecules reaches up to 15 ppm [188]. Thus, the chemical shift of HI molecule is noticeably out of the common range. This phenomenon was extensively studied by many. In particular, Nakatsuji and coworkers [69,104,109,193–197] observed significant changes in the  $^1\text{H}$ ,  $^{13}\text{C}$  and the other nuclei NMR chemical shifts in various halogenated molecules with an increasing atomic number of the halogen substituent.

From first sight, the NHD phenomenon may seem to be straightforward with regard to the rationale: the shielding increases along the series from F to I because the halogen electronegativity decreases, presumably leading to more electron density on the atom bound to it [198]. However, the NMR shielding constant is a response property of the second order, which implies that there is no direct relation to the electron density, and that this property depends not only on the bonding in the ground state but also on how the electronic system responds to the magnetic field.

Anomalous high-field shifted experimental chemical shifts of light nuclei in organic compounds containing heavy elements and a dubious situation with the NHD phenomenon, in particular, led to a number of attempts to include the SOC into the non-relativistic electronic theory of NMR chemical shifts. The first investigation accounting for the relativistic effects of the spin-orbit origin was carried out by Nomura, Takeuchi, and Nakagawa [35]. They recognized the lack of qualitative explanation of the substituent effect on the proton NMR chemical shifts of monosubstituted benzenes and tried to solve the problem. In particular, there was no rationale for the anomalous shifts of the halogen-substituted benzene for that time. To shed some light on the problem, Nomura et al. proposed an explanation based on the notion of the “spin-polarization shift” or *LS* shift, introduced earlier by Nakagawa et al. [199]. Nomura et al. [35] presented the sum-over-states (SOS) expression for the *LS* shift, which was derived from the third-order perturbation theory. For today, this term is known to be responsible for the most part of the relativistic spin-orbit heavy-atom effect on the light-atom shielding constant (SO-HALA). Nomura et al. successfully explained anomalous values of the observed proton chemical shifts with the SO-HALA effect and suggested that, for the ortho- and meta-protons in halobenzenes, the *LS* shift would be relatively large, giving rise to the contributions of the increasing magnitude from Cl to Br to I.

Morishima et al. [60] developed the ideas of Nomura et al. [35] and conducted a comprehensive investigation of the spin-polarization shift. Morishima et al. applied the molecular orbital formalism to the exact sum-over-excited-states expression of the *LS* shift, derived earlier by Nomura et al. In particular, the authors presented numerical results for the proton and carbon-shielding constants of hydrogen halides and methyl halides, respectively, that demonstrated nonlinearly increasing contributions due to the *LS* shift ongoing from F to I. Moreover, a clearer physical explanation of the *LS* shift was coined [60]: “A localized triplet exciton is induced on the heavy atom by the spin-orbit interaction, which is in turn transmitted to the neighboring atom through the bond. Thus, the *LS* shift arises on the neighboring atom through the Fermi-contact interaction of a nucleus with electrons”.

Cheremisin and Schastnev [61] also made pioneering calculations of the *LS* shift contribution to the  $^{13}\text{C}$  NMR shielding constants of halogen-substituted methanes and pointed out that carbon-shielding constants increase with the atomic number of adjacent halogens and become anomalously high for  $\text{Cl}_4$ . Moreover, they also showed that the substitution effects turned out to be nonadditive for bromine- and iodine-substituted methanes.

Pyykkö et al. [68] gave a transparent interpretation of the relativistic contributions to  $^1\text{H}$  and  $^{13}\text{C}$  chemical shifts of hydrogen halides and of methyl halides and haloacetylenes, respectively. He applied the second-order perturbation theory to obtain the relativistic analogue of the Ramsey's equations [74] for the shielding tensor, using the molecular wavefunctions derived from the relativistically parameterized extended Hückel method (REX-EHT) [200]. The REX-EHT results were compared with those calculated within the ordinary nonrelativistic extended Hückel theory (EHT) [201] and it was found that the SO-HALA effect, induced by halogen, gives nonlinearly increasing positive contributions to the neighbor proton and carbon-shielding constants with an increase in the atomic number of the adjacent halogen.

Fukui et al. [106] presented the gauge invariant lowest-order relativistic theory for nuclear magnetic shielding constants derived from a two-component positive-energy Hamiltonian. A great number of new contributions to the relativistic magnetic shielding tensor have been obtained, among which there was the third-order perturbation term, FC-I, representing the *LS* shift. A numerical estimation for this term was performed on the example of four hydrogen halides, HF, HCl, HBr, and HI. The FC-I was found to rapidly increase from 0.17 ppm for HF to 15.61 ppm for HI.

Malkin et al. [97] presented a different method for the calculation of the SO correction (using the one-electron SO operator) to the NMR shielding constants and tested this method on the calculations of the SO corrections to hydrogen chemical shifts of HF, HCl, HBr and HI molecules and carbon chemical shifts of  $\text{CH}_n\text{Cl}_{4-n}$ ,  $\text{CH}_n\text{Br}_{4-n}$ ,

$\text{CH}_n\text{I}_{4-n}$  (for  $n = 0, 1, 2, 3$ ) series [97] and of halomethyl cations,  $\text{CX}_3^+$  ( $X = \text{F}, \text{Cl}, \text{Br}, \text{I}$ ) [202]. Malkin et al. considered the existing approaches to be seriously spoiled by several disadvantages. To be more precise, from Malkin's point of view, the third-order Rayleigh–Schrödinger perturbation approach, proposed earlier by Morishima et al. [60], Cheremisin et al. [61], and Fukui et al. [106], required a proper description of singlet–triplet transitions in the framework of a sum-over-states approach, while the second-order perturbation approach, introduced by Pyper [62–65], Pyykkö [67,68], and Zhang and Webb [66], involved complex arithmetic due to the inclusion of the SO operators. Malkin et al. developed an approach that avoids complex arithmetic and, therefore, is more efficient from a computational point of view. Their approach was based on the sum-over-states density-functional-perturbation-theoretical (SOS-DFPT) method developed earlier for the chemical shift calculations [203–205]. The results of SOS-DFPT calculations carried out by Malkin et al. with and without taking into account the SO corrections in comparison with experimental data are presented in Figure 1.

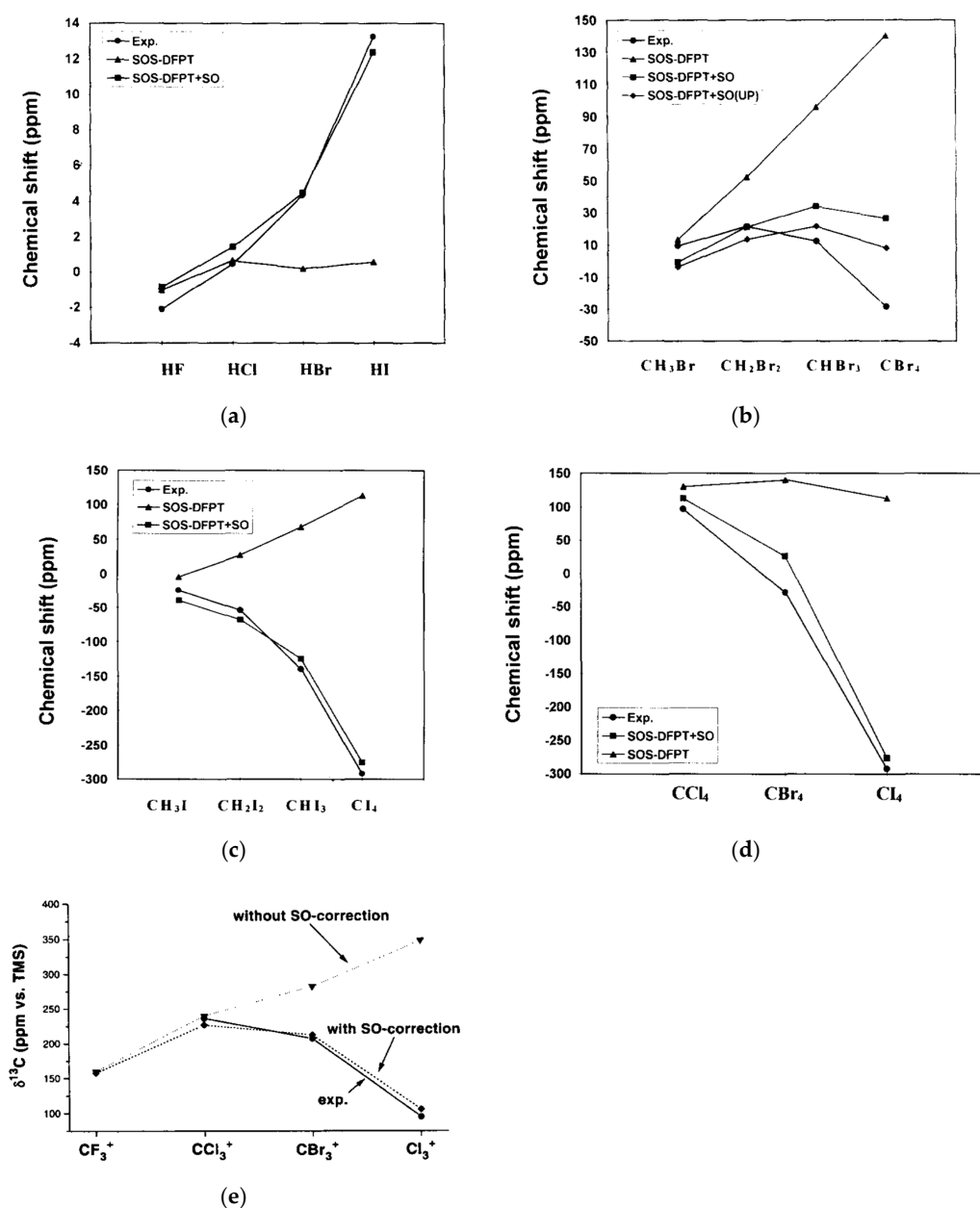


**Figure 1.** A comparison of theoretical and experimental chemical shifts. Theoretical values were obtained within the IGLO-SOS-DFPT approach, with and without taking into account the SO corrections:

(a)  $^1\text{H}$  chemical shifts in HF, HCl, HBr and HI with respect to  $\text{CH}_4$  (these values should come with the opposite sign); (b)  $^{13}\text{C}$  chemical shifts in bromo-substituted methanes with respect to TMS; (c)  $^{13}\text{C}$  chemical shifts in iodo-substituted methanes with respect to TMS; (d)  $^{13}\text{C}$  chemical shifts in tetrahalogenomethanes with respect to TMS; (e)  $^{13}\text{C}$  chemical shifts in halomethyl cations with respect to TMS. Reproduced from Malkin et al. [97,202] with the permission of Elsevier.

These results demonstrate the importance of the SO correction for reliable calculations of the proton and carbon chemical shifts in molecules containing heavy halogens, and clearly indicate the responsibility of the SO-HALA effect for their steep up-field shift ongoing from F to I. Moreover, from Figure 1c, one can conclude that the SO-HALA effect from multiple iodine atoms on a carbon chemical shift is cumulative and it increases nonlinearly with the number of adjacent iodine atoms.

The SOS-DFPT study of the SO-HALA effect on proton and carbon chemical shifts has been continued by Kaupp et al. [186] on the example of iodoethane, iodoethylene, iodoacetylene, and iodobenzene. That paper reported on the major trends of the SO-HALA effect and delineated the interpretation of this effect. The main idea of the paper was to juxtapose the behavior of the SO-HALA mechanism with that of the multiple-bond spin–spin coupling constants by density functional calculations. The authors suggested that the propagation mechanisms of both phenomena are similar, see Figure 2.

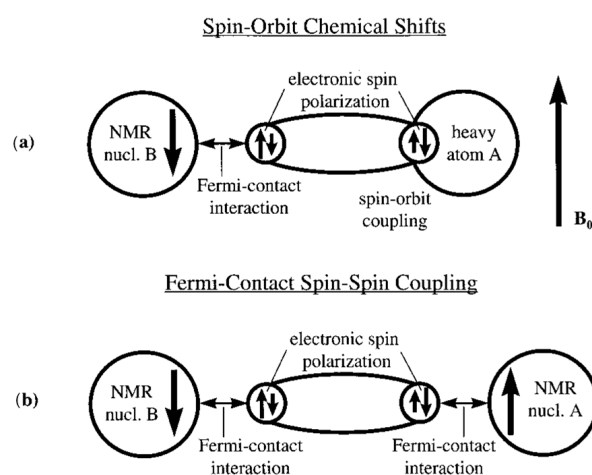


**Figure 2.** Schematic illustration of the analogy between the spin–orbit shifts and the Fermi-contact mechanism of indirect spin–spin coupling: (a) Qualitative interaction of the mechanism for spin–orbit shifts; (b) qualitative Fermi-contact interaction mechanism for spin–spin coupling constant. The schemes correspond to the simplest situation of the one-bond SO-HALA shift and the one-bond coupling  $^1K_{\text{FC}}(\text{HA,LA})$  in the absence of lone pairs. In the presence of lone pairs or in the case of longer-range interactions, both schemes are to be modified. Reproduced from Kaupp et al. [186] with the permissions of John Wiley and Sons.

Based on the semblance of the propagation mechanisms of the SO-HALA effect and the indirect spin–spin coupling interaction, Kaupp et al. came to several important conclusions regarding the main features of the SO-HALA effect: (i) the spin–orbit shift of nuclei directly attached to the heavy atom ( $\alpha$ -SO-HALA effect) should predominantly (but not exclusively) depend on the involvement of valence *s*-orbitals of the NMR atom in bonding to the heavy atom; (ii) in contrast to spin–spin coupling, the *s*-orbital contribution of the heavy atom is not a major factor in the spin–orbit shift; (iii) owing to the energy denominators in the sum-over-states terms (see Equation (2)), the effects that decrease (increase) the energy difference between the most important excited states and the ground state will enhance (diminish) the spin–orbit effects; (iv) for the light atom that is separated by several bonds from the heavy atom, one can expect that many of the rules governing the multiple-bond spin–spin coupling constant between these two atoms will also hold for the distant SO-HALA effect on the light atom.

As was suggested by Kaupp et al., the conclusion (i) unfolds into several important issues: (i-i) the one-bond spin-orbit SO-HALA shifts increases from  $sp^3$  to  $sp^2$  to  $sp$  hybridized carbon; (i-ii) the  $^1\text{H}$  shifts are the most sensitive ones to the spin-orbit effects from neighboring heavy atoms as the hydrogen  $1s$ -orbital predominates in bonding; (i-iii) in the case of  $p$ -block main-group central atoms considered as the light NMR spectator atoms, the valence  $s$ -orbitals are fully involved in bonding when these atoms are in their highest oxidation states, therefore, one should expect large shielding spin-orbit effects for them.

The importance of the two-electron SO contributions for a reliable calculation of the NMR chemical shifts was clarified by Malkina et al. [206] and Kaupp et al. [207]. Malkina et al. [206] reported on the explicit implementation of the two-electron SO integrals in the DFT-based deMon-NMR code and performed the calculations within the SOS-DFPT approach with IGLO scheme of the  $^1\text{H}$  chemical shifts in the hydrogen halides ( $\text{HX}$ ,  $\text{X} = \text{F-I}$ ) and  $^{13}\text{C}$  chemical shifts in halogenomethanes ( $\text{CH}_3\text{X}$ ,  $\text{X} = \text{F-I}$ ), and  $^{13}\text{C}$  and  $^1\text{H}$  chemical shifts in iodobenzene. In virtue of the fact that the explicit calculations of the two-electron SO matrix elements quickly become computationally demanding, Malkina et al. also have developed, implemented and tested the mean-field approximation to the two-electron SO integrals. Overall, the two-electron contributions were found to be far from being negligible. Namely, they amount to ca. 30% of the one-electron contributions for the proton and carbon-shielding constants. For the heavier halogens, their relative importance is decreased, down to ca. 6–7% in iodine compounds. Figure 3 shows theoretical NHD dependences for the proton-shielding constants of hydrogen halides (Figure 3a) and carbon-shielding constants of halogenomethanes (Figure 3b), calculated at both nonrelativistic SOS-DFPT and relativistic SOS-DFPT levels, by taking into account the SO-HALA corrections (both with and without two-electron SO terms), against the experimental NHDs.

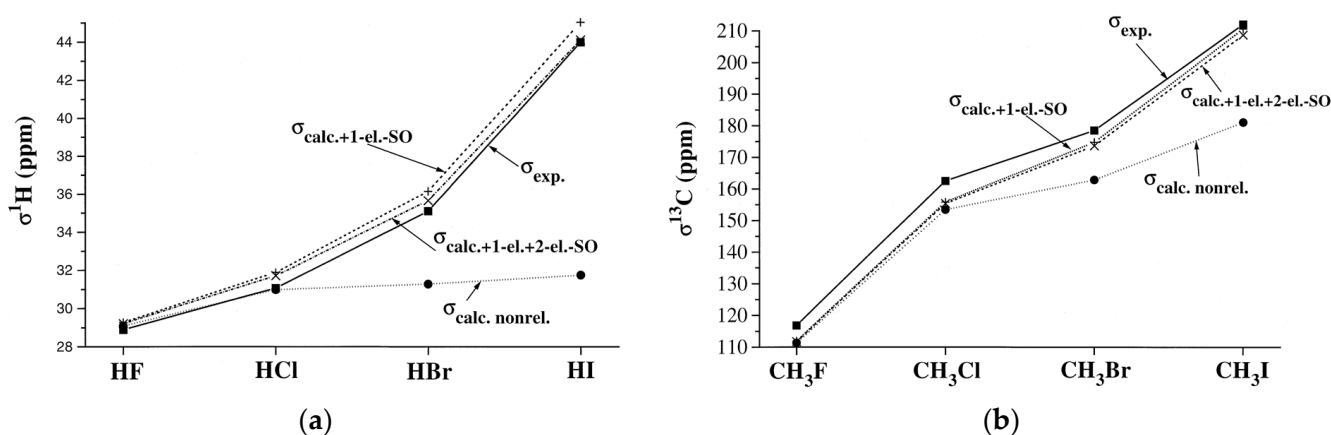


**Figure 3.** Calculated and experimental NHD dependences of: (a) proton-shielding constants of hydrogen halides; (b) carbon-shielding constants of halogenomethanes. The SO corrections were calculated within the mean-field approximation. Reproduced from Malkina et al. [206] with the permission of Elsevier.

As can be seen from these figures, the SO-corrected results reproduce the experimental trends very well, by contrast to the nonrelativistic results that seemed to be unable to model the large increase in the proton and carbon-shielding constants or chemical shifts ongoing from F to I. The two-electron SO corrections are opposite in sign to the one-electron contributions, and, thus, reduce to some extent the overall magnitude of the SO corrections. On average, the SO corrections improve the agreement of the theoretical results with the experimental data.

Malkina et al. [206] also made first attempts to investigate the importance of the basis set quality for the description of the SO-HALA effect. As was exemplified on hydrogen halides, for the correct description of the SO-HALA-induced proton-shielding constants, it is more

important to have a large basis set on hydrogen, as the FC operator probes the spin density at the NMR nucleus, while the basis set on the heavy neighboring atom is of less importance.

The study of the spin–orbit relativistic effects on the nuclear proton and carbon-shielding constants has also been carried out by Vaara et al. [120,121,124] and by Wolff and Ziegler [117], using the density-functional theory. Analytical calculations of the spin–orbit interaction contribution to nuclear magnetic shielding tensors using linear and quadratic response theory have been presented for the HX (X = F, Cl, Br, and I), and CH<sub>3</sub>X (X = F, Cl, Br, and I) systems [121]. In addition, the authors introduced a correlated study of the spin–orbit-induced contributions to shielding tensors arising from the magnetic field dependence of the spin–orbit Hamiltonian. For both nuclei, hydrogen and carbon, the second-order SO effects appeared to be negligible. For example, the second-order SO contributions to the carbon-shielding constant in CH<sub>3</sub>X (X = F, Cl, Br, I) series give almost constant deshielding-type effect of about 0.45 ppm, while the original third-order SO term gives the increasing contributions from 0.25 ppm for CH<sub>3</sub>F to 31.78 ppm for CH<sub>3</sub>I. The total SO corrections to <sup>1</sup>H and <sup>13</sup>C shielding constants rapidly increase when going from light to heavy substituents.

First attempts to explain the increase of proton and carbon-shielding constants when going from light to heavy halogen substituents, as illustrated by Figures 1 and 3, within the molecular orbital analysis were made by Pyykkö et al. [68]. They analyzed the relativistic contributions to the proton-shielding constants of hydrogen halides within the REX-EHT approach and found that  $\pi$ -type nonbonding MOs appear to be largely responsible for the negative SO contributions to hydrogen shielding constants induced by heavy halide substituents. This idea was examined and confirmed by DFT calculations of <sup>13</sup>C chemical shifts of trifluoromethyl compounds CF<sub>3</sub>IF<sub>*n*</sub> (*n* = 0, 2, 4, 6) including both one- and two-electron spin–orbit corrections by Kaupp et al. [208]. The examination implied the removal or delocalization of the  $\pi$ -type lone pairs of iodine atom that would lead to a dramatic decrease of the SO shifts. This study was carried out by means of considering the molecules that are different in the formal number of  $\pi$ - and  $\sigma$ -type nonbonding orbitals on iodine. Figure 4 provides a graphical comparison of experimental and theoretical <sup>13</sup>C chemical shifts, calculated at the DFT-PW91 [209,210] level with IGLO-II(BII) [98] and uncontracted Partridge’s (UP) [211–213] basis sets.

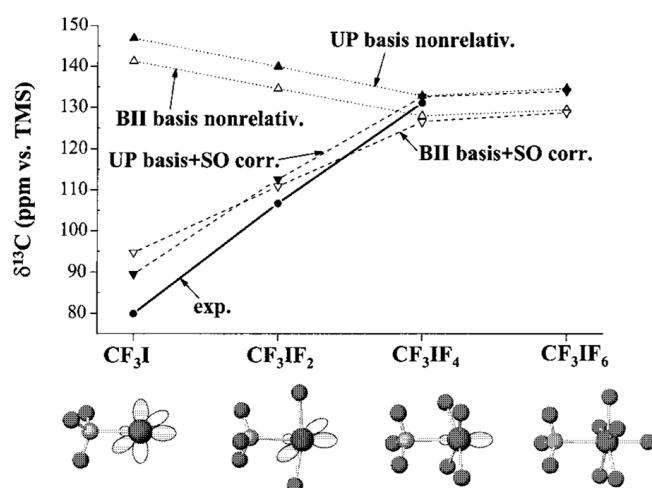


**Figure 4.** Comparison of calculated and experimental <sup>13</sup>C chemical shifts. The SO-corrected data include both one- and two-electron contributions. At the bottom of the figure, the presence of iodine lone pairs is shown schematically. Reproduced from Kaupp et al. [208] with the permission of John Wiley and Sons.

The experimentally observed increase of the <sup>13</sup>C chemical shifts of CF<sub>3</sub>IF<sub>*n*</sub> (*n* = 0, 2, 4, 6) with the increasing of the oxidation state of iodine, that is, with the increasing of *n* (see Figure 4), was explained by the diminishing of the SO effects in going from *n* = 0 to *n* = 4.

At that, the carbon chemical shifts calculated at the nonrelativistic level decrease from  $n = 0$  to  $n = 4$  and increase very slightly from  $n = 4$  to  $n = 6$ . The remarkably large SO corrections inverted this trend, and thus the experimental behavior was recovered. This confirms the idea that the removal of iodine lone pairs dramatically diminishes the SO-HALA contributions to carbon chemical shifts and makes it evident that  $\pi$ -type nonbonding MOs are largely responsible for the negative SO contributions.

The authors of the work [208] have also plotted the  $^{13}\text{C}$  SO-HALA shifts against the FC contributions of the reduced one-bond I-C coupling constants,  $^1K(\text{I,C})$ , in  $\text{CH}_3\text{I}$  and  $\text{CF}_3\text{IF}_n$  ( $n = 0, 2, 4, 6$ ) molecules, see Figure 5. It shows that ongoing from  $\text{CH}_3\text{I}$  to  $\text{CF}_3\text{I}$  the two quantities correlate with each other. However, starting from  $\text{CF}_3\text{IF}_2$  molecule, the discrepancy in their behaviors rapidly increase. This was attributed to the removal of the iodine nonbonding orbitals.

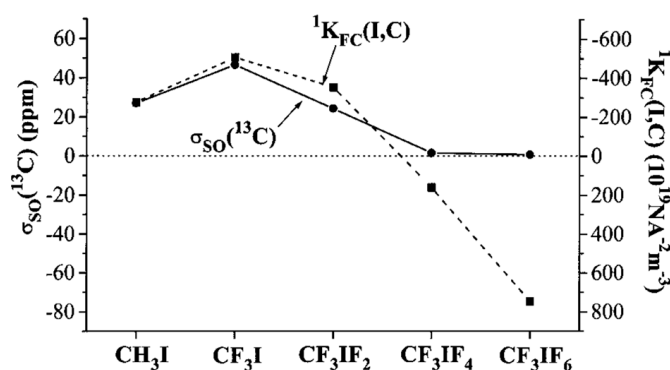


**Figure 5.** Comparison of the SO contributions to  $^{13}\text{C}$  shielding constants,  $\sigma_{\text{SO}}$ , and Fermi-contact contributions to the reduced spin–spin coupling constants,  $^1K(\text{I,C})$ , in the series of trifluoromethyl compounds  $\text{CF}_3\text{IF}_n$  ( $n = 0, 2, 4, 6$ ). Reproduced from Kaupp et al. [208] with the permission of John Wiley and Sons.

Indeed, while the SO contributions are already negligible for both  $\text{CF}_3\text{IF}_4$  and  $\text{CF}_3\text{IF}_6$  due to the lack of  $\pi$ -type lone pairs on iodine, the reduced coupling constants still changed significantly, and the removal of the remaining  $\sigma$ -type nonbonding electron pairs ongoing from  $\text{CF}_3\text{IF}_4$  to  $\text{CF}_3\text{IF}_6$  did not affect the SO shifts much. However, at the same time, the iodine  $s$ -character of the I-C bond was enhanced significantly, and this affects the  $^1K(\text{I,C})$  to a large extent. Kaupp et al. carried out the MO analysis and showed that the iodine  $\sigma$ -type nonbonding MO provides a significant negative contribution to the reduced spin–spin coupling constant  $^1K(\text{I,C})$  of  $\text{CF}_3\text{IF}_4$  but does not contribute much to the  $^{13}\text{C}$  SO-HALA chemical shift.

Visscher et al. [167] discussed various methods for the inclusion of the relativistic effects of different types into the calculation of NMR parameters and carried out benchmark calculations of the proton NMR shielding constants of hydrogen halides at the 4RPA level. The NHD trend was confirmed to be due to the spin–orbit coupling effects initiated by halogen atoms. A very interesting achievement of that study consisted in establishing the role of scalar relativistic effects, namely those due to the mass-velocity and Darwin corrections. They appeared to be negligible for the proton-shielding constants in hydrogen halides, see Figure 6.

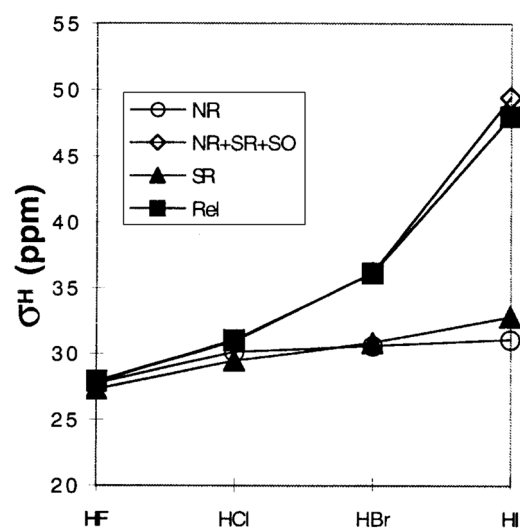


**Figure 6.** Isotropic hydrogen shielding constants of hydrogen halides HX (X = F, Cl, Br, I) calculated within the nonrelativistic (NR) RPA method, within the nonrelativistic RPA method with perturbative inclusion of scalar relativistic and spin–orbit relativistic effects (NR + SR + SO), within the four-component scalar relativistic RPA method (SR), and within the fully relativistic 4RPA formalism (Rel). Reproduced from Visscher et al. [167] with the permission of John Wiley and Sons.

As can be seen from Figure 6, the inclusion of scalar relativistic (or SR) effects into the calculation of hydrogen shielding constants does not affect the NHD trend. Only the perturbational inclusion of the SO corrections (see the graph “NR + SR + SO”) gives the proper behavior and, apparently, reproduces the full four-component results with very good accuracy.

Vaara et al. [124] also studied the role of scalar relativistic effects on the chemical shifts of hydrogen and carbon atoms. The authors presented an approach that combines a perturbational treatment of the spin–orbit effects via the spin–orbit pseudopotentials (SO-ECP) and the self-consistent treatment of the scalar relativistic effects using the quasirelativistic pseudopotentials (SR-ECP). With this technique, the scalar and FC–I-type (SO-HALA) corrections were calculated. The <sup>1</sup>H shielding constants of HX and <sup>13</sup>C shielding constants of CH<sub>3</sub>X (X = F, Cl, Br, I) series, calculated by taking into account the relativistic effects within the ECPs, were compared with the values obtained using an all-electron (AE) approach (in the latter case, the SO effects were taken into account via the atomic mean-field approximation (AMFI-AE) [204]). Selected results are presented in Table 1.

**Table 1.** Comparison of ECP and all-electron (AE) results for the <sup>1</sup>H shielding constants in HX and <sup>13</sup>C shielding constants in CH<sub>3</sub>X (X = F, Cl, Br, I). The SO contributions were obtained with the common gauge origin placed on X.

X	σ <sub>NR</sub>	σ <sub>SR</sub>	σ <sub>SO/FC-I</sub>		σ <sub>tot</sub>	
	AE	ECP	AMFI-AE	SO-ECP	AE	ECP
HX series						
F	30.04	29.09	0.11	0.13	30.15	29.22
Cl	31.72	30.82	0.65	0.70	32.37	31.52
Br	31.25	31.14	3.76	3.78	35.01	34.92
I	31.65	31.69	10.78	11.38	42.43	43.07
CH <sub>3</sub> X series						
F	119.98	116.59	0.48	0.47	120.46	117.06
Cl	162.78	162.77	1.82	2.07	164.60	164.84
Br	171.09	168.49	10.14	10.46	181.23	178.95
I	188.76	183.00	26.99	27.81	215.75	210.81

The results of the ECP calculations presented in Table 1 indicate that the SR-ECP/SO-ECP approach provides sufficient accuracy for the NMR chemical shifts as compared to the AE results, and it can be regarded as a useful and efficient alternative for larger systems.

The SR effects give only minor contributions to the proton and carbon-shielding constants, while the SO effects are responsible for the most part of the relativistic contributions for heavier substituents, agreeably providing the correct behavior of the shielding constants with an increasing atomic number of halogen substituents, see Figure 7.

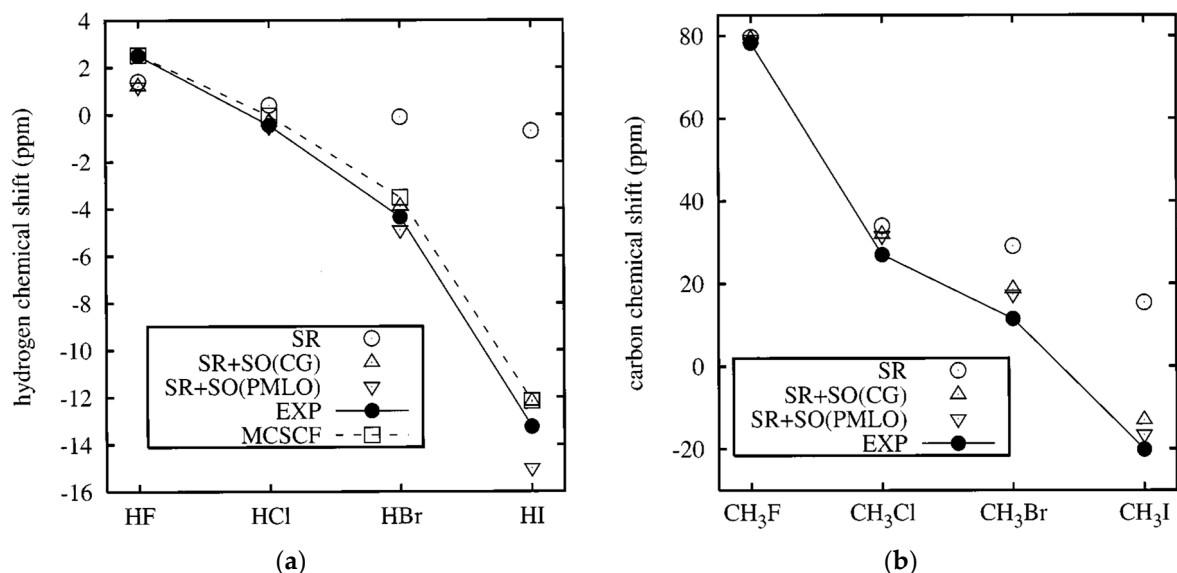


**Figure 7.** Scalar relativistic (SR) and spin-orbit (SO)-corrected DFT results for common gauge [SR + SO(CG)] and for IGLO PM calculation [SR + SO(PMLO)], as well as the experimental results: (a) <sup>1</sup>H chemical shifts in HX (X = F, Cl, Br, I); (b) <sup>13</sup>C chemical shifts in CH<sub>3</sub>X (X = F, Cl, Br, I). Reproduced from Vaara et al. [124] with the permission of AIP Publishing.

Kudo and Fukui [130] carried out the calculations of nuclear magnetic shielding constants of HX (X = F, Cl, Br, I) within the DKH2 and BSS approaches. In line with the classical NHD trend, the hydrogen shielding constant increased from *ca.* 27 to 46 ppm for X = F to I. The results appeared to be in poor agreement with the four-component RPA calculations of Visscher et al. [167], the GIAO-FP-GUHF/DKH2 calculations of Fukuda et al. [113] and LRESC calculations by Melo et al. [83]. For example, the difference between the results obtained by Kudo and Fukui with that calculated at the 4RPA level by Visscher et al. [167] is as much as *ca.* 10 ppm for the hydrogen shielding constant in the HF molecule. Apparently, such a significant discrepancy does not speak in favor of two-component methods for the calculation of the relativistic values of proton-shielding constants. However, one of the advantages of Kudo and Fukui's calculations consisted in the fact that the dependence of the evaluated shielding constants on the gauge origin was very weak. This indicates the fact that large basis sets like that used in their calculations are capable of alleviating the gauge origin problem.

Manninen et al. [126,128] presented the application of BPPT using SCF and complete active space SCF (CASSCF) wave functions to the calculation of proton-shielding constants in different systems, including HX (X = F, Cl, Br, I, At) series. All significant types of relativistic corrections were analyzed. Active non-spin-orbit corrections to <sup>1</sup>H nuclear magnetic shielding constants of HX series were found to be negligible. Passive scalar relativistic corrections vary from 0.018 ppm for X = F to -0.557 ppm for X = At. Passive spin-orbit corrections involving the FC mechanism provide the main contribution to the total relativistic effect on the proton-shielding constants in HX series with an increasing X atom weight; namely, it is only 0.129 ppm for F, while it is 11.876 ppm for X = I and 36.573 ppm for X = At.

Melo et al. tested the LRESC theory on the representative series of halogenated compounds, calculating the shielding constants of heavy and light nuclei of HX and CH<sub>3</sub>X (X = Br, I) systems [163]. The newly introduced contributions to the HALA effect on proton magnetic shielding constants appeared to be negligibly small. However, for the carbon nucleus directly bonded to the heavy atom in CH<sub>3</sub>X series, the overall value of that contribution to its shielding constant was calculated as about 2.70 ppm (X = Br, I), which cannot be said to be negligible in comparison with the typical spin-orbit contributions of about 10–15 ppm for X = Br and 20–45 ppm for X = I [117,120,124,130]. Numerical calculations of the relativistic effects on nuclear magnetic shielding constants corresponding to all one-particle operators obtained within the formalism developed by Melo et al. [163] were carried out in the Ref. [83]. In these calculations, the elimination of small component scheme was applied to evaluate all quantities entering to a four-component RSPT expression of the NMR shielding tensor. The HX and CH<sub>3</sub>X (X = Br, I) were taken as model compounds. It was found that the most important corrections to the hydrogen and carbon-shielding constants are the SO/FC-I corrections, which become significant for the compounds containing heavier halogens, especially with iodine atoms. In particular, the SO/FC-I contribution to the hydrogen shielding constant of HI is *ca.* 19.72 ppm with the total nonrelativistic value of 31.21 ppm, while that for the carbon-shielding constant in CH<sub>3</sub>I molecule is *ca.* 47.09 ppm with the total nonrelativistic value of 190.06 ppm. Total scalar relativistic corrections to the hydrogen and carbon-shielding constants originating from the mass-velocity and one-particle Darwin operators appeared to be of less importance as compared to the SO contributions. Though, based on Melo's results, one cannot say that these are negligible, especially for the iodine compounds. For instance, the passive scalar corrections to the proton-shielding constant in HI and carbon-shielding constant in CH<sub>3</sub>I were calculated as −3.71 and −6.31 ppm, respectively.

Kantola et al. [214] studied the carbon and proton-shielding tensors in methyl halides, CH<sub>3</sub>X (X = F, Cl, Br, and I). A uniqueness of the work [214] consisted in the fact that a systematic liquid crystalline and gas-phase experimental NMR study of methyl halides has been carried out, providing constant experimental conditions, which constitute a solid ground for considering the relative magnitudes and trends of the NMR parameters of these compounds. The calculations were performed at the HF, MP2 [215,216], CCSD [217], and CCSD(T) [218–222] levels of theory, as well as using the DFT methods with B3LYP [223,224] and BHandHLYP [225] exchange-correlation functionals. Relativistic corrections were calculated with the BPPT. Both scalar and spin-orbit relativistic contributions were included. The results revealed the importance of both types of relativistic corrections to the <sup>13</sup>C shielding constants. Rovibrational effects were also shown to be significant and mandatory for the correct juxtaposing with the experimental trends. The dependences of the <sup>1</sup>H and <sup>13</sup>C NMR isotropic shielding constants in the series of methyl halides CH<sub>3</sub>X (X = F, Cl, Br, and I) on the atomic number of the substituent halogen are shown in Figure 8. In each figure there are five plots, corresponding to different levels of calculation: (i) the nonrelativistic MP2 level without accounting for any corrections (the equilibrium geometry is used) (NR(*r*<sub>e</sub>)); (ii) nonrelativistic MP2 level by taking into account the relativistic corrections via the BPPT approach (TOT(*r*<sub>e</sub>)); (iii) nonrelativistic MP2 level by taking into account the relativistic and rovibrational corrections (TOT(300 K)); (iv) BPPT corrections *per se* (BPPT(*r*<sub>e</sub>)); (v) the experimental data (EXP(GAS)).

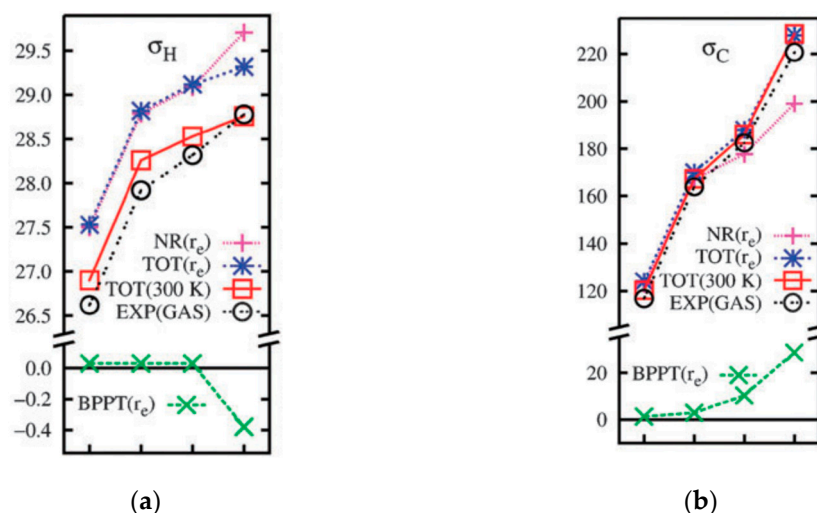


**Figure 8.** Experimental and calculated shielding constants of: (a)  $^1\text{H}$  and (b)  $^{13}\text{C}$  nuclei. Magenta, blue, red, black and green lines correspond to: (i) the nonrelativistic MP2 level without accounting for any corrections (the equilibrium geometry is used) ( $\text{NR}(r_e)$ ); (ii) nonrelativistic MP2 level by taking into account the relativistic corrections via the BPPT approach ( $\text{TOT}(r_e)$ ); (iii) nonrelativistic MP2 level by taking into account the relativistic and rovibrational corrections ( $\text{TOT}(300\text{ K})$ ); (iv) BPPT corrections per se ( $\text{BPPT}(r_e)$ ); (v) the experimental data ( $\text{EXP}(\text{GAS})$ ). Reproduced from Kantola et al. [214] with permission from the Royal Society of Chemistry.

Relativistic corrections to the proton nuclear magnetic shielding constants of  $\text{MH}_{4-n}\text{Y}_n$  ( $n = 1-3$ ;  $\text{M} = \text{Si, Ge, Sn}$ , and  $\text{Y} = \text{H, F, Cl, Br, I}$ ) model compounds were investigated by Maldonado et al. [85] using the LRESC formalism. For the Si-containing molecules,  $\sigma(\text{H})$  increases as the weight of each heavy halogen substituent increases, though the increase is not substantial. In particular, for the  $\text{SiH}_3\text{Y}$  series, there was only a small rise of  $\sigma(\text{H})$  in going from F to Br (26.76 and 28.02 ppm, respectively), and then a somewhat larger rise when going to I (32.02 ppm). Similar patterns were observed for the  $\text{SiH}_2\text{Y}_2$  and  $\text{SiHY}_3$  molecules; the largest difference in shielding appeared to be between  $\text{SiHF}_3$  (27.67 ppm) and  $\text{SiHI}_3$  (39.71 ppm). Among the Sn-series, the most rapid growth of the  $\sigma(\text{H})$  with the weight of the halogen substituent was observed for the  $\text{SnH}_3\text{Y}$  molecules. In particular, the difference between the proton-shielding constant of  $\text{SnHI}_3$  ( $\sigma(\text{H}) = 37.24$  ppm) and that of  $\text{SnHF}_3$  ( $\sigma(\text{H}) = 23.15$  ppm) is about 14.09 ppm.

Another interesting moment of that study consisted in the analysis of  $\sigma(\text{H})$  upon rising the number of heavy eponymous halogen substituents. Namely, there are very small changes in the proton-shielding constants with an increase in the amount of fluorine, chlorine, or bromine atoms. For example, for the  $\text{SiH}_{4-n}\text{Y}_n$  series ( $\text{Y} = \text{F, Cl, and Br}$ ), this change is less than 1 ppm upon shifting from  $\text{SiH}_3\text{Y}$  to  $\text{SiHY}_3$ . Only for the iodine series this change is essential in magnitude; namely, the increase of the number of iodine atoms from one to three results in rising of the proton-shielding constant from 32.02 ppm (for  $\text{SiH}_3\text{I}$ ) to 39.71 ppm (for  $\text{SiHI}_3$ ) that corresponds to an increase of 24%.

Casella et al. [226] calculated the  $^{13}\text{C}$  NMR chemical shifts of a large ensemble of halogenated organic molecules (81 molecules in total), ranging from small rigid organic compounds, used for testing the performances of various levels of theory, to natural substances of marine origin with conformational degrees of freedom. The authors showed that the NMR spectra of molecules with heavy halogen atoms are strongly affected by large relativistic effects, and the well-established nonrelativistic protocols used for organic molecules containing only light atoms, such as C, H, N, and O, dramatically fail in the prediction of the chemical shifts of carbon atoms bonded to one or more halogen atoms. The inclusion of spin-orbit coupling was demonstrated to be mandatory; therefore, both nonrelativistic and scalar relativistic approaches, which in fact give rather similar results, cannot be used, not even for a qualitative prediction of the  $^{13}\text{C}$  NMR spectrum. The highest level of accuracy

was reached within the framework of the four-component relativistic description. Remarkably, a very small corrected mean absolute error ( $\text{CMAE} = \sum_n |\delta_{scaled} - \delta_{exp}| / n$ , where  $\delta_{scaled} = (\delta_{calc} - b) / a$ —measures the distance between the experimental value and the value predicted by the linear fitting) of about 3–5 ppm was obtained at the four-component Dirac–Kohn–Sham level with the PBE functional, that, together with the other statistical parameters, demonstrates a high predictive power of the used computational methodology.

Neto et al. [227] performed a qualitative analysis of the spin–orbit operator in order to predict the types of organic compounds, where large relativistic SO/FC–I correction to  $^{13}\text{C}$  shielding constants could be expected. The following approaches were used: nonrelativistic DFT, scalar ZORA-DFT, scalar PAULI-DFT, SO-ZORA-DFT, and SO-PAULI-DFT. Qualitatively, Neto et al. had come to several important conclusions, that were based on a simple assumption that one considers a system for which the frontier NBO orbitals (e.g., highest occupied bonding and lone-pair orbitals and lowest vacant antibonding orbitals) presumably give the main contributions to the SO/FC–I cross term. Under these prerequisites, the SO/FC–I cross term should be significant whenever both of the following two conditions hold:

- The overlaps of the  $90^\circ$  rotated occupied frontier MOs with the lowest vacant frontier MOs are significant (see the numerators in Equation (6));
- The relevant energy gaps between the frontier occupied and vacant MOs are not “very large” (see the denominators in Equation (6)).

Some cases where the frontier  $90^\circ$  rotated occupied MO (lone pair of a heavy atom X, LP(X)) effectively overlaps with the antibonding orbital  $\sigma^*_{\text{C-X}}$  are shown in Figure 9.

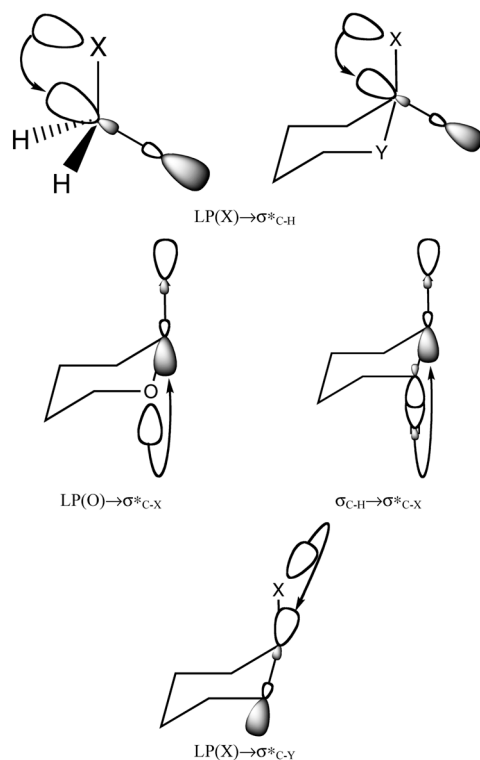


**Figure 9.** Relevant NBO interactions for methane, cyclohexane, and pyran derivatives, where X = F, Cl, Br, and I, and Y =  $\text{CH}_2$  and O. Reproduced from Neto et al. [227] with the permission of American Chemical Society.

Studies confirming the inverse relationship between the energy gaps and  $\sigma_{\text{SO}}$ , as stated above in option (b), have also been performed in several works [117,186,228,229]. Thus, one can say that any stereoelectronic interactions that increases a relevant energy gap

between the ground and the excited states have the potential to decrease the corresponding SO/FC–I contribution [230].

Demissie et al. [231] has reported high-level calculations of  $^{13}\text{C}$  chemical shifts of six representative organic compounds (see Figure 10), with and without heavy elements, at both non-relativistic and four-component relativistic Kohn–Sham DFT levels. The performances of different pure GGA exchange–correlation functionals (PBE [232,233], SVWN5 [234,235], BP86 [236,237], PW91 [238]) were compared at both the non-relativistic and relativistic levels of theory. According to Demissie et al., the structural elucidation of naturally occurring organic molecules with heavy atoms, like those containing iodine atoms, with database approaches [239,240] is problematic due to the lack of information of relevant NMR properties of such compounds in such databases. In such cases as these, four-component relativistic calculations are a promising concomitant means of the structure elucidation via the NMR experiment. Demissie et al. showed that pure GGA functionals perform better than the hybrid B3LYP functional, providing high-accuracy results within the advanced relativistic four-component DFT theory applied in combination with the restricted magnetic balance condition and gauge-including atomic orbitals approach (GIAO–mDKS–RMB). The four-component calculations were found to be highly efficient, but not significantly more expensive than the corresponding non-relativistic calculations. Of all the GGA functionals considered by Demissie et al., the PBE functional demonstrated the best performance, though, the results obtained with the BP86 functional appeared to be very close to those obtained with the PBE functional. For the iodine compounds (see Figure 10), the relativistic effect on the NMR chemical shift of carbon directly bonded to the iodine atom ( $\alpha$ -HALA effect) appeared to be substantial, about  $-38$  ppm, while the relativistic correction to the same chemical shift in a parent compound in which there is no iodine substituent was found to be only  $-2$  ppm. The bromine atom induces the  $\alpha$ -HALA shielding (negative) contributions to the carbon chemical shifts of about  $10$ – $12$  ppm, depending on the attached subunit.

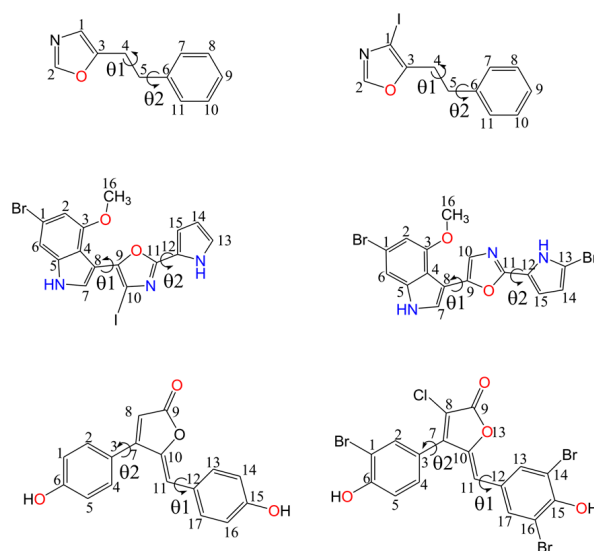


**Figure 10.** Compounds considered in the Ref. [231]. Reproduced with the permission of John Wiley and Sons.

Samultsev et al. [241] revisited the NHD of the  $^{13}\text{C}$  NMR chemical shifts using different computational schemes. Carbon chemical shifts have been calculated in 70 halogenomethanes at the four-component RPA and DFT levels of theory using the OPW91 [242,243] exchange–correlation functional and at the nonrelativistic MP2 level in combination with the 4RPA and 4DFT relativistic corrections. The dependence of the relativistic effects on  $^{13}\text{C}$  NMR shielding constants on the sum of atomic numbers of the substituents in the series of halogenomethanes obtained by Samultsev et al. is shown in Figure 11.

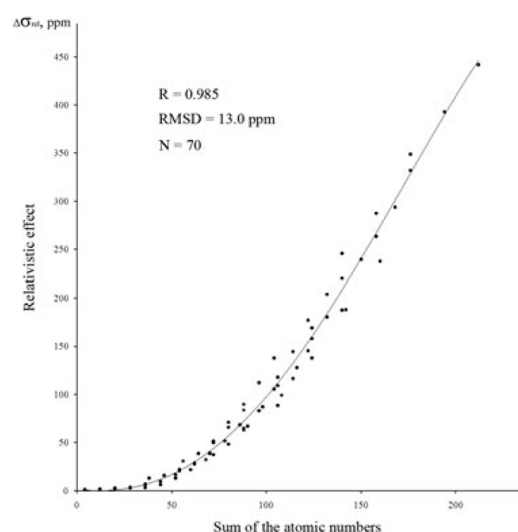


**Figure 11.** The dependence of the relativistic corrections to  $^{13}\text{C}$  NMR shielding constants calculated at the 4DFT(OPW91)/dyall.av3z level on the sum of the atomic numbers of the substituents in the series of halogenomethanes CWXYZ (W, X, Y, Z = {H, F, Cl, Br, I}). Approximation curve is described by the equation  $Y = aX^4 + bX^3 + cX^2 + dX + e$  with  $a = -2.16 \cdot 10^{-7}$ ,  $b = 5.98 \cdot 10^{-5}$ ,  $c = 8.00 \cdot 10^{-3}$ ,  $d = -0.21$ ,  $e = 1.55$ . Reproduced from Samultsev et al. [241] with the permission of John Wiley and Sons.

It can be seen from Figure 11 that the relativistic contribution to the carbon-shielding constant rapidly increases with the number of heavy halogens and that this increase is not linear. The most obvious tendency can be found in the series of iodomethanes. Thus, for iodomethane, the total relativistic effect on the shielding constant of  $^{13}\text{C}$  nucleus is around 30 ppm; for diiodomethane, it is about 100 ppm; for triiodomethane, it is about 250 ppm; and for tetraiodomethane, the relativistic correction to the carbon-shielding constant was calculated as *ca.* 440 ppm. From the results illustrated by Figure 11, one can conclude that the non-relativistic calculations of carbon chemical shifts are inadequate when the total atomic number of directly attached halogens exceeds 30 (for example, treating the systems with two chlorine atoms already requires the inclusion of the relativistic effects).

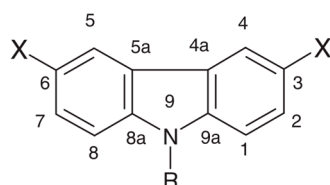
The relativistic geometry factor was also studied in the Ref. [241]. This factor provides the correction to carbon chemical shifts of about 1 ppm for monoiodomethanes, around 2–3 ppm for diiodomethanes, around 3–5 ppm for triiodomethanes, and reaches as much as 11.2 ppm for tetraiodomethane. Thus, one can conclude that the relativistic level of geometry optimization is worth applying when one deals with compounds with at least two iodine atoms.

Viesser et al. [198] presented the study of X–R-substituted benzenes (R =  $\text{NH}_2$ ,  $\text{NO}_2$ ; X = F, Cl, Br or I). The effect of X and R groups on  $^{13}\text{C}$  NMR chemical shifts in X–R-benzenes was investigated by the density functional calculations and localized molecular orbital analyses. An observation was made that the X atom causes deshielding-type effects on the directly bonded carbon nucleus for F and Cl derivatives due to the paramagnetic coupling between occupied  $\pi$  orbitals and unoccupied  $\sigma^*_{\text{C-X}}$  antibonding orbitals. SO coupling plays an important role in the carbon magnetic shielding of Br and I derivatives. The nature of the X substituent was also found to modulate the  $^{13}\text{C}$  paramagnetic shielding contributions.

A crucial importance of the spin–orbit-induced heavy atom effect of iodine on the  $^{13}\text{C}$  NMR chemical shifts was reported in the NMR study of the halogen-bonding of haloarenes [244]. Systematic large deviations for chemical shifts of carbons directly attached to iodine ( $\text{C}_i$ ) in iodine–halogen-bonded DMSO complexes were observed between theoretical values obtained at the nonrelativistic GIAO-DFT(B3LYP) level of theory and the corresponding experimental data. The experimental values were measured as 90–100 ppm in DMSO, while the calculations resulted in much higher values of about 130–140 ppm. Moreover, the comparison of the nonrelativistically calculated chemical shifts in the free molecules and their complexes showed noticeable chemical shift changes for carbons di-

rectly bonded to iodine atoms, while the measurements showed hardly any change. These discrepancies were attributed to the neglect of the spin–orbit-induced heavy atom effect of iodine. Indeed, the calculated SO corrections to chemical shifts of  $C_i$  atoms appeared to be very close in magnitude to that of iodobenzene [186] and reduced the computed  $C_i$  shifts from *ca.* 130–140 ppm to *ca.* 90–100 ppm, thus bringing them into much better agreement with experiment.

Radula-Janik et al. [245] studied the halogen effect on the structure and  $^{13}\text{C}$  NMR chemical shifts of 3,6-disubstituted-N-alkyl carbazoles (see Figure 12).



$R = \text{H}, \text{C}(10)\text{H}_3, \text{C}(10)\text{H}_2\text{C}(11)\text{H}_3$

$X = \text{H}, \text{F}, \text{Cl}, \text{Br}, \text{I}$

**Figure 12.** 3,6-disubstituted-N-alkyl carbazoles studied by Radula-Janik et al. [245]. Reproduced with the permission of John Wiley and Sons.

The investigation has been carried out within the GIAO-DFT formalism using the VSXC [246]/STO-3G<sub>mag</sub> and KT2/DZP schemes for the nonrelativistic level, and the SO-ZORA-KT2/DZP schemes for the relativistic level of theory. The impact of the alkyl substitution at N9 on the chemical shifts of ring carbons appeared to be negligible, while the effect of X-substituent on the C3 and C6 chemical shifts is essential for X = Br and I. Namely, the HALA effect is about  $-10$  and  $-30$  ppm for the C3/6 carbons attached to Br and I, respectively. The authors have also plotted the chemical shifts of C3/6 calculated at the SO-ZORA-KT2/DZP against the electronegativity of X substituent and found that the calculated results correlate with electronegativity with the Pearson correlation coefficient of 0.9553. The nonrelativistic theoretical results did not show the correlation with the electronegativity.

A crucial role of the relativistic effects on the carbon chemical shifts was also demonstrated for the biologically relevant heteroaromatic compounds containing heavy halogen atoms [247]. To be more precise, the study was carried out for the series of 6-halopurines (see Figure 13):

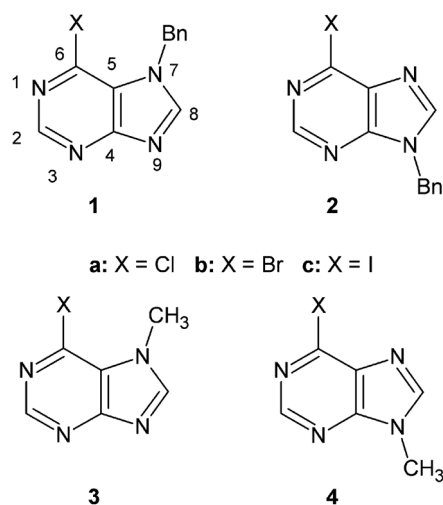


**Figure 13.** 6-halopurines studied in the Ref. [247]. Reproduced with the permission of Royal Society of Chemistry.

All sixteen types of BPPT leading-order relativistic corrections (see Equation (1)) were calculated for the chemical shifts of all  $^{13}\text{C}$  nuclei. The most pronounced relativistic effects were observed for the carbon chemical shifts of C-6 atom. They were found to decrease in going from compounds **a** to **c**, in line with the NHD trend. In particular, the differences in  $\delta(\text{C-6})$  in both regioisomers **3** and **4** between chloro- (**a**) and bromo- (**b**) and between bromo- (**b**) and iodo- (**c**) compounds were calculated approximately as 10 and 20 ppm, respectively. Out of all sixteen relativistic contributions, the prevailing effect was shown to be provided by the third-order spin-orbit contribution  $\sigma^{\text{FC-I}}$ , which was slightly compensated by its two-electron counterpart  $\sigma^{\text{FC-II}}$ . This is a pronounced classical  $\alpha$ -SO-HALA effect. The  $\beta$ -HALA effect for the chemical shift of C-5 was found to be remarkably smaller in magnitude and opposite in sign. It caused the increase of  $\delta(\text{C-5})$  along the series **a-c** by *ca.* 6 ppm. In general, the authors concluded that the inclusion of the relativistic corrections to  $^1\text{H}$  and  $^{13}\text{C}$  NMR chemical shifts of 6-halopurines is essential to correctly reproduce the experimental trends.

Ariai and Saielli [248] carried out the first detailed investigation of the occurrence of the “through-space” relativistic effects on the  $^1\text{H}$  and  $^{13}\text{C}$  chemical shifts on the example of 1-methylpyridinium halides [MP][X] and 1-butyl-3-methylpyridinium trihalides [BMP][X<sub>3</sub>] ionic liquids (ILs) (X = Cl, Br, I). These relativistic effects were attributed to the non-covalent interaction with the heavy anions. The studies were carried out using the two-component SO-ZORA-DFT(BP86) and SO-ZORA-DFT(PBE0) levels. In summary, they revealed that relativistic effects on light atom NMR chemical shifts manifest themselves in ion pairs and thus are not restricted to covalently HA-LA bonded systems. Indeed, on the contrary to common halogenated organic molecules, iodide and triiodide ( $\text{I}^-$  and  $\text{I}_3^-$ ), engaged in ion pairs with pyridinium-like cations, cause an increase of the  $^{13}\text{C}$  NMR chemical shifts (relativistic deshielding-type effect) of about 1 ppm at particular pyridinium atoms interacting with  $\text{I}^-$  and  $\text{I}_3^-$ . The authors also concluded that this would be hard to observe experimentally and urged for further studies.

Further study of a “through-space” spin-orbit heavy atom effect on  $^1\text{H}$  NMR chemical shifts was carried out by Vícha et al. [249]. The authors investigated the effect in the 4-dimethylaminopyridinium (DMAPH<sup>+</sup>) salts containing iodide, bromide and chloride as the counter ions (see [DMAPH]<sup>+</sup> $\text{I}^-$  in Figure 14) experimentally and theoretically at the SO-ZORA-DFT(PBE0)/TZP level using MO analysis and spin-orbit induced electron density difference (SO-EDD) approach. The authors stated that notwithstanding the observation of “through-space” SO-HALA chemical shifts is not possible via direct experimental observation due to the fact that it is an integral part of the total chemical shift measured, its role can be revealed with the help of theoretical calculations agreeable with experiment.

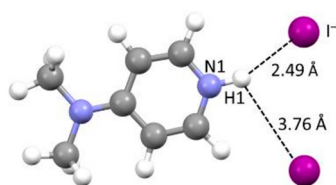


**Figure 14.** 4-dimethylaminopyridinium salts containing iodide [DMAPH]<sup>+</sup> $\text{I}^-$ . Partially reproduced from Vícha et al. [249] with the permission of John Wiley and Sons.

A correlation analysis of the experimental proton chemical shifts of [DMAPH]<sup>+</sup> $\text{I}^-$  system and the corresponding data calculated via the gauge-including projector-augmented wave (GIPAW) method [250,251] revealed that the signal of H1 proton (see Figure 14) was a clear outlier. Initially, the outlier was assumed to be due to the well-known disadvantage of the GIPAW approach which consists in the fact that it currently is implemented only for the general-gradient-approximation (GGA) family of exchange-correlation functionals, such as the PBE. Hence, the authors tried to apply a simple correction to the GIPAW result calculated on an isolated molecule using the PBE0 functional, though in vain: this correction did not improve the predicted proton chemical shifts in the DMAPH salts. In that way,

Vícha et al. turned to the calculations of the relativistic SO correction and this improved the agreement with the experiment at all computational levels resorted to.

In the same work [249], Vícha et al. studied the N–H $\cdots$ I interaction with the Quantum Theory of Atoms in Molecules (QTAIM) [252] approach. It was revealed that there is a bond critical point between H1 and I $^-$  characterized by electron density  $\zeta = 0.024 \text{ e.bohr}^{-3}$  and positive Laplacian of  $0.04 \text{ e.bohr}^{-5}$ , which is consistent with a moderate-strength hydrogen bond [253]. The calculated QTAIM delocalization index (indicator of electron sharing between two atoms) of 0.15 electrons also confirmed a certain degree of electron sharing between H1 and I $^-$  which is necessary for the propagation of the SO-HALA effect [254]. Molecular orbital analysis revealed that  $\delta_{\text{SO}}(\text{H1})$  originates mainly from the HOMO orbital, which is a mix of iodine 6p lone electron pairs (LEPs) with  $\sigma_{\text{N1-H1}}$  bonding orbitals, while the spin-orbit induced electron density difference (SO-EDD) approach gave a vivid picture of the mechanism of the “through-space”  $\delta_{\text{SO}}(\text{H1})$ , see Figure 15.

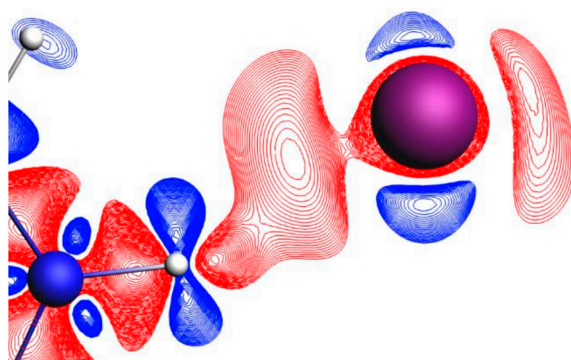


**Figure 15.** Detail of Spin-orbit Induced Electron Density Difference (SO-EDD) along the N1–H1 $\cdots$ I $^-$  interaction in the [DMAPH] $^+$ I $^-$  system. The plot was obtained as the difference between 2c and 1c-PBE0/TZP electron density. Red/blue colors correspond to a depletion/increase of electron density, respectively. Reproduced from Vícha et al. [249] with the permission of John Wiley and Sons.

Figure 15 shows the action of the SO operator, which causes depletion of electron density from the  $\sigma$ -space of the N1–H1 and H1 $\cdots$ I $^-$  bonds (red color), towards  $\pi$ -space of N1, H1 and LEPs of iodine (blue color). To resume, the action of the SO operator “weakens” the  $\sigma$ -character of the hydrogen bond, which leads to a weakening of the local paramagnetic couplings by causing the deshielding-type SO-HALA effect on the H1 nucleus (the values for the “through-hydrogen bond”  $\delta_{\text{SO}}(\text{H1})$  lie between  $-0.35$  and  $-0.6$  ppm, depending on the computational level).

The relativistic effects from chalcogen atoms on the hydrogen and carbon-shielding constants have been studied in a wide series of papers [84,126,128,130,183,184,187,255–258]. In particular, Manninen et al. [126,128] evaluated all possible types of relativistic corrections to hydrogen shielding constants of H $_2$ X (X = O, S, Se, Te, Po) using analytical linear and quadratic response theory applied on top of the nonrelativistic SCF reference state. Analogically to HX series, the active non-spin-orbit corrections to  $^1\text{H}$  nuclear magnetic shielding constants of HX series were found to be next to negligible. Passive scalar relativistic corrections vary from 0.004 ppm for X = O to  $-0.631$  ppm for X = Po [126]. Passive spin-orbit corrections that involve the FC mechanism provide the main contribution to the total relativistic effect on the proton-shielding constants with an increase in the atomic number of chalcogen, namely, it is 0.063 ppm for oxygen, 8.272 ppm for tellurium, and 23.229 ppm polonium [126].

Analytical calculations of the spin-orbit interaction contribution to nuclear magnetic shielding tensors using linear and quadratic response theory were also carried out for the H $_2$ X (X = O, S, Se, and Te) systems by Vaara et al. [121]. Total SO corrections to  $^1\text{H}$  shielding constant in this series rapidly increase when going from light to heavy chalcogen substituents. Figure 16 shows the chalcogen dependence (CD) of  $^1\text{H}$  nuclear shielding constant in H $_2$ X series with an increase in the atomic number of chalcogen X.

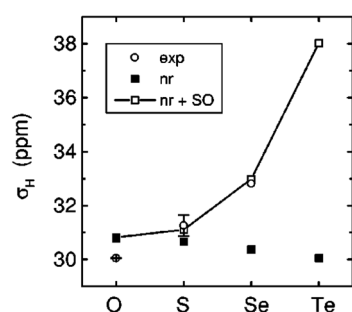


**Figure 16.** Calculated and experimental  $^1\text{H}$  nuclear shielding constants in the  $\text{H}_2\text{X}$  ( $\text{X} = \text{O}, \text{S}, \text{Se}, \text{Te}$ ) series. Both the non-relativistic (nr) and spin-orbit corrected results are shown (nr + SO). Reproduced from Vaara et al. [121] with the permission of AIP Publishing.

The first fully relativistic calculations of proton NMR shielding constants in group-15 and -16 hydrides were carried out by Gomez et al. [84]. The authors calculated  $\sigma(\text{H})$  of  $\text{XH}_3$  ( $\text{X} = \text{N}, \text{P}, \text{As}, \text{Sb}, \text{Bi}$ ) and  $\text{XH}_2$  ( $\text{X} = \text{O}, \text{S}, \text{Se}, \text{Te}, \text{Po}$ ) compounds both at the nonrelativistic RPA and relativistic four-component RPA (4RPA) levels of theory with common gauge origin placed at the heavy nucleus. In all shielding calculations, the authors used manually modified uncontracted basis sets of different types (Sadlej [259], Faegri [211–213]) for each element. Actually, the basis sets were prepared for the spin–spin coupling constant calculations, which also were the primary objects of the study [84] in the sense of the manifestation of the relativistic effects. However, the authors did not explain why they used the same basis sets for the nuclear magnetic shielding constant and spin–spin coupling constant calculations. The main results pertaining the manifestation of the HALA effect on the  $\sigma(\text{H})$  of  $\text{XH}_3$  and  $\text{XH}_2$  molecules are presented in Table 2.

**Table 2.** Isotropic shielding constants  $\sigma_{\text{iso}}(^1\text{H})$  of  $\text{XH}_3$  ( $\text{X} = \text{N}, \text{P}, \text{As}, \text{Sb}, \text{Bi}$ ) and  $\text{XH}_2$  ( $\text{X} = \text{O}, \text{S}, \text{Se}, \text{Te}, \text{Po}$ ) series calculated at the nonrelativistic RPA and relativistic 4RPA levels of theory (in ppm).

Molecule	$\sigma_{\text{RPA}}$	$\sigma_{\text{4RPA}}$	HALA Effect
$\text{NH}_3$	31.8986	30.3269	−1.5717
$\text{PH}_3$	29.7512	28.6462	−1.1050
$\text{AsH}_3$	29.5515	28.6451	−0.9064
$\text{SbH}_3$	28.9133	28.1719	−0.7414
$\text{BiH}_3$	27.5737	15.4135	−12.1602
$\text{H}_2\text{O}$	31.0213	29.1499	−1.8714
$\text{H}_2\text{S}$	31.1767	30.7105	−0.4662
$\text{H}_2\text{Se}$	30.4243	33.2876	2.8633
$\text{H}_2\text{Te}$	29.8316	39.8276	9.9960
$\text{H}_2\text{Po}$	28.1430	42.4056	14.2626

As one can see from Table 2, the HALA effect on  $\sigma_{\text{iso}}(\text{H})$  in pnictogen series is negative in all cases, reaching *ca.* −12 ppm in  $\text{BiH}_3$  molecule, while for the chalcogen series, this effect is slightly negative for the lightest chalcogens, namely, oxygen and sulfur, though, starting from Se, it rapidly growth in positive scale reaching *ca.* 14 ppm for  $\text{H}_2\text{Po}$  molecule. Thus, one can see that in pnictogen series  $\text{XH}_3$ , the HALA effect gives the deshielding-type contributions with the largest effect from bismuth. It is worth noting that the latter in is in agreement with the results of Berger et al. [260], who calculated  $\alpha$ -HALA effect from bismuth on  $^{13}\text{C}$  chemical shift in triphenylbismuth to be about 18 ppm. At the same time, in chalcogen series,  $\text{XH}_2$ , the HALA effect gives the shielding-type contributions to proton-shielding constant. This is in line with recent findings that in hydrides with formally empty heavy atom valence shells the  $\delta_{\text{SO}}(^1\text{H})$  is of a deshielding-type as in the case of Bi, for instance, while the hydrides with partially filled heavy atom valence shells (i.e., those with partially occupied lone pairs on the heavy atom) exhibit the shielding  $\delta_{\text{SO}}(^1\text{H})$  correction (the case of Po, for example) [37].

Kudo et al. [130] applied the DKH2-CHF and BSS-CHF approaches to calculate hydrogen nuclear magnetic shielding constants of  $H_2X$  ( $X = O, S, Se, Te$ ). Kudo et al. obtained the same values within the both methods, which were in quantitative agreement with the results of Manninen et al. [126,128]. Namely, based on Kudo's results, the relativistic corrections to hydrogen shielding constants in  $H_2X$  series are as follows: 0.1, 0.7, 3.8, and 13 ppm for  $X = O, S, Se,$  and  $Te$ , respectively.

Jaszuński et al. [255] carried out ab initio calculations of nuclear magnetic resonance shielding constants in  $SeH_2$  and  $TeH_2$ . The role of electron correlation effects, relativistic effects, and basis sets was analyzed. The relativistic effects on the isotropic shielding constants of  $SeH_2$  and  $TeH_2$  were calculated within the Dirac–Coulomb Hamiltonian at the RPA, DFT and Spin-Density Functional Theory (SDFT) levels [261] of theory with the KT2 functional. At the non-relativistic level, the convergence of the results with the extension of the basis sets on the heavy chalcogen atom was studied within the RPA, CCSD and CCSD(T) methods. From the presented results, it follows that nonrelativistic hydrogen shielding constants are practically unaffected by the basis set used on the heavy atom, and the electron correlation effects do not exceed 1%. The DFT relativistic corrections to hydrogen shielding constants in  $SeH_2$  and  $TeH_2$  are about  $1.7 \pm 0.1$  and  $4.9 \pm 0.1$  ppm (depending on the basis set used on the heavy atom), respectively. The results obtained within the SDFT approach appeared to be quite different from that obtained within the casual DFT method. To be more precise, the relativistic contributions to the hydrogen shielding constants of  $SeH_2$  and  $TeH_2$  calculated as the difference between the SDFT relativistic values and that obtained within the Lévy–Leblond scheme [262], were  $2.8 \pm 0.1$  and  $8.4 \pm 0.3$  ppm for the  $SeH_2$  and  $TeH_2$ , respectively. This means that the inclusion of the spin magnetization vector in the density and its derivatives significantly affects the magnitude of the relativistic effects on shielding constant of hydrogen nuclei (increasing it by about 1.7 times).

Relativistic heavy atom effect on  $^{13}C$  NMR chemical shifts initiated by adjacent multiple chalcogens was investigated by Rusakov et al. [263] at the four-component GIAO-DFT(KT1)/dyall.av3z level. The dependences of the total relativistic HALA corrections to carbon-shielding constants on the total atomic number of the adjacent chalcogens were investigated in different types of systems with  $sp$ - and  $sp^3$ -hybridized spectator carbons, namely, in  $X=^{13}C=Y$  ( $X, Y = O, S, Se, Te$ ) and  $C(XH)_m(YH)_n(ZH)_p(QH)_sH_{1-m}H_{1-n}H_{1-p}H_{1-s}$  ( $X, Y, Z, Q = S, Se, Te$  and  $m, n, p, s = 0, 1$ ), respectively, see Figure 17. As can be seen from these graphs, the growth of the relativistic correction to carbon-shielding constant is nonlinear with the increase of the total atomic number of adjacent chalcogens. The increase of the HALA effect can be approximated by the polynomials of the third degree,  $\Delta_{rel} = aZ^3 + bZ^2 + cZ + d$ , with  $a = -1 \cdot 10^{-5}$  ( $6 \cdot 10^{-6}$ ),  $b = 9 \cdot 10^{-3}$  ( $5.3 \cdot 10^{-3}$ ),  $c = -3.91 \cdot 10^{-2}$  ( $-5.59 \cdot 10^{-2}$ ),  $d = -1.255$  (1.9703) for the series with  $sp$ - ( $sp^3$ -hybridized spectator carbons) and  $Z$  being the sum of the atomic numbers of the chalcogens attached to the central carbon atom in the model series.

It is also interesting to note that the slope of the curve for the “ $sp$ -series” is steeper than that for the “ $sp^3$ -series” (this follows from the first coefficient  $a$  in the approximative polynomials). This is in line with the fact that the magnitude of the SO-HALA effect is determined by the rate of involvement of the valence  $s$ -orbitals of light atom into the heavy atom-light atom bond [36]. Indeed,  $s$ -character of the  $sp$ -hybridized carbon is obviously higher than that of the  $sp^3$ -hybridized carbon.

Another interesting finding of Rusakov et al. concerns the relativistic effects on carbon-shielding constants in molecules containing lighter chalcogens. For example, the relativistic effect on  $^{13}C$  shielding constant in  $C(SH)_3H$  ( $\Delta_{rel} = 7.7$  ppm) is very close to the effect in  $C(SeH)_3H$  molecule ( $\Delta_{rel} = 9.6$  ppm). At the same time, two selenium atoms in molecule  $C(SeH)_2H_2$  ( $\Delta_{rel} = 24.0$  ppm) provide the relativistic effect, which is practically the same as that in the molecule containing one tellurium atom,  $C(TeH)_3H$  ( $\Delta_{rel} = 22.0$  ppm). This means that in the case of some “not very heavy” chalcogen-containing molecules, the relativistic effect can be unexpectedly large. In this respect, Rusakov et al. suggested that before choosing the general formalism (relativistic or nonrelativistic) to be applied to the cal-

culations of NMR carbon-shielding constants it is pertinent to estimate possible magnitude of the relativistic correction by means of the dependences, presented in Figure 17.

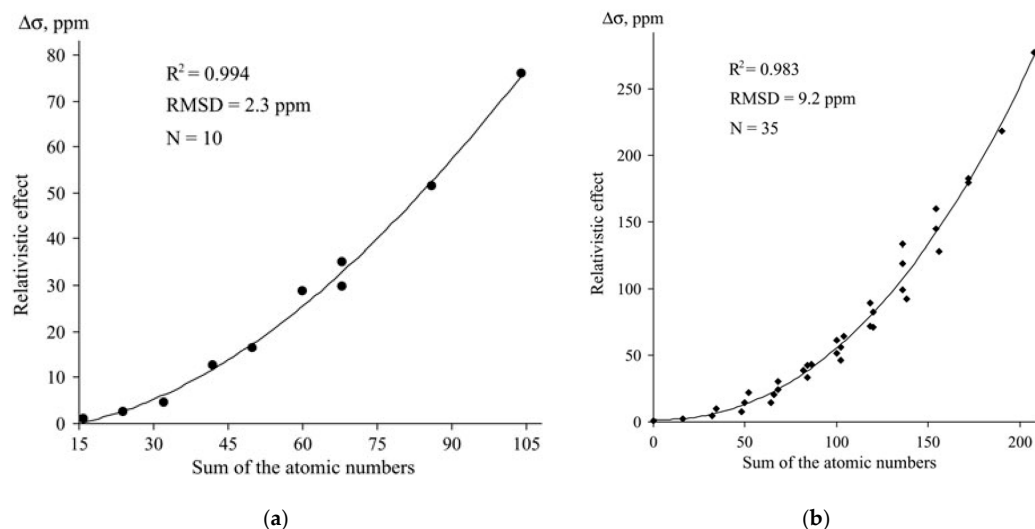


**Figure 17.** The dependence of the total relativistic corrections (HALA effect) to carbon-shielding constants on the total atomic number of the adjacent chalcogens calculated at the GIAO-4DFT(KT1) method: (a) in the series of carbon dichalcogenides  $X=C=Y$  ( $X, Y = O, S, Se, Te$ ); (b)  $C(XH)_m(YH)_n(ZH)_p(QH)_sH_{1-m}H_{1-n}H_{1-p}H_{1-s}$  ( $X, Y, Z, Q = S, Se, Te$  and  $m, n, p, s = 0, 1$ ). Reproduced from Rusakov et al. [263] with the permission of John Wiley and Sons.

Another valuable work of Rusakov et al. [264] was devoted to the computational investigation of the HALA effect on the NMR isotropic carbon-shielding constants in the series of model ethanes, ethylenes, and acetylenes,  $C_\beta H_3-C_\alpha H_2-XH_n$ ,  $C_\beta H_2=C_\alpha H-XH_n$ ,  $C_\beta H\equiv C_\alpha-XH_n$  ( $n = 0, 1, 2, \text{ or } 3$  depending on  $X$ ), where  $X$  covers p-elements in the 13–17 groups of the 3–6 periods in as many as 60 compounds. These compounds provided diverse bonding situations for the  $\alpha$ - and  $\beta$ -carbons, characterizing by a consecutive increase of the  $s$ -character of the  $C_\beta-C_\alpha$  and  $C_\alpha-X$  bonds, being one of the factors influencing the spin-orbit part of SO-HALA effect. Analogically to NHD trend, the chalcogen, pnictogen, tetrel, and triel dependencies were established for the  $^{13}C$  NMR shielding constants in the mentioned three series of compounds with  $X$  being from 16th, 15th, 14th, and 13th groups, respectively. A well-known NHD trend for the  $^{13}C$  NMR chemical shifts was also reproduced for all three series of compounds. The corresponding graphs are presented in Figure 18.

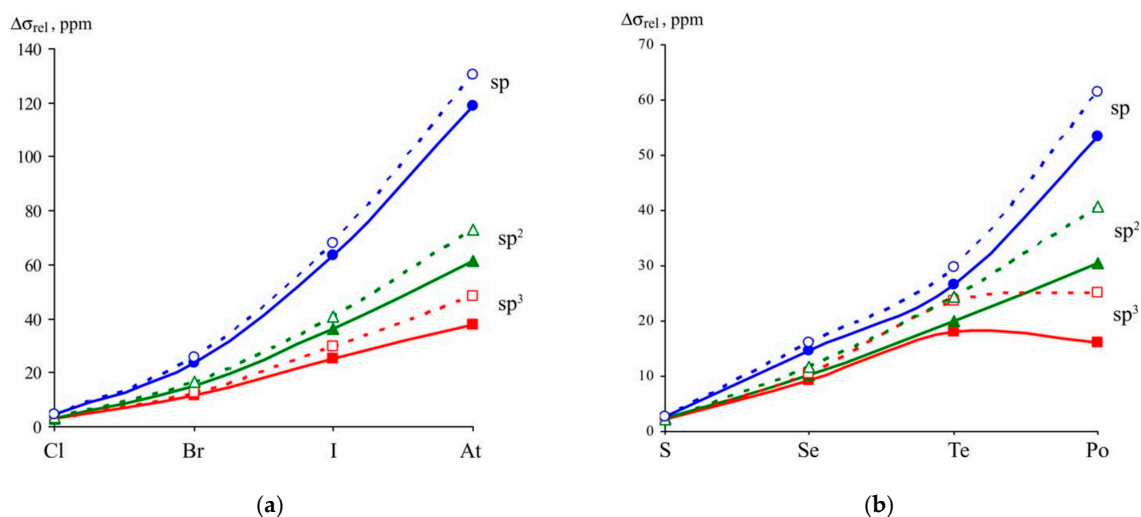


**Figure 18.** Cont.

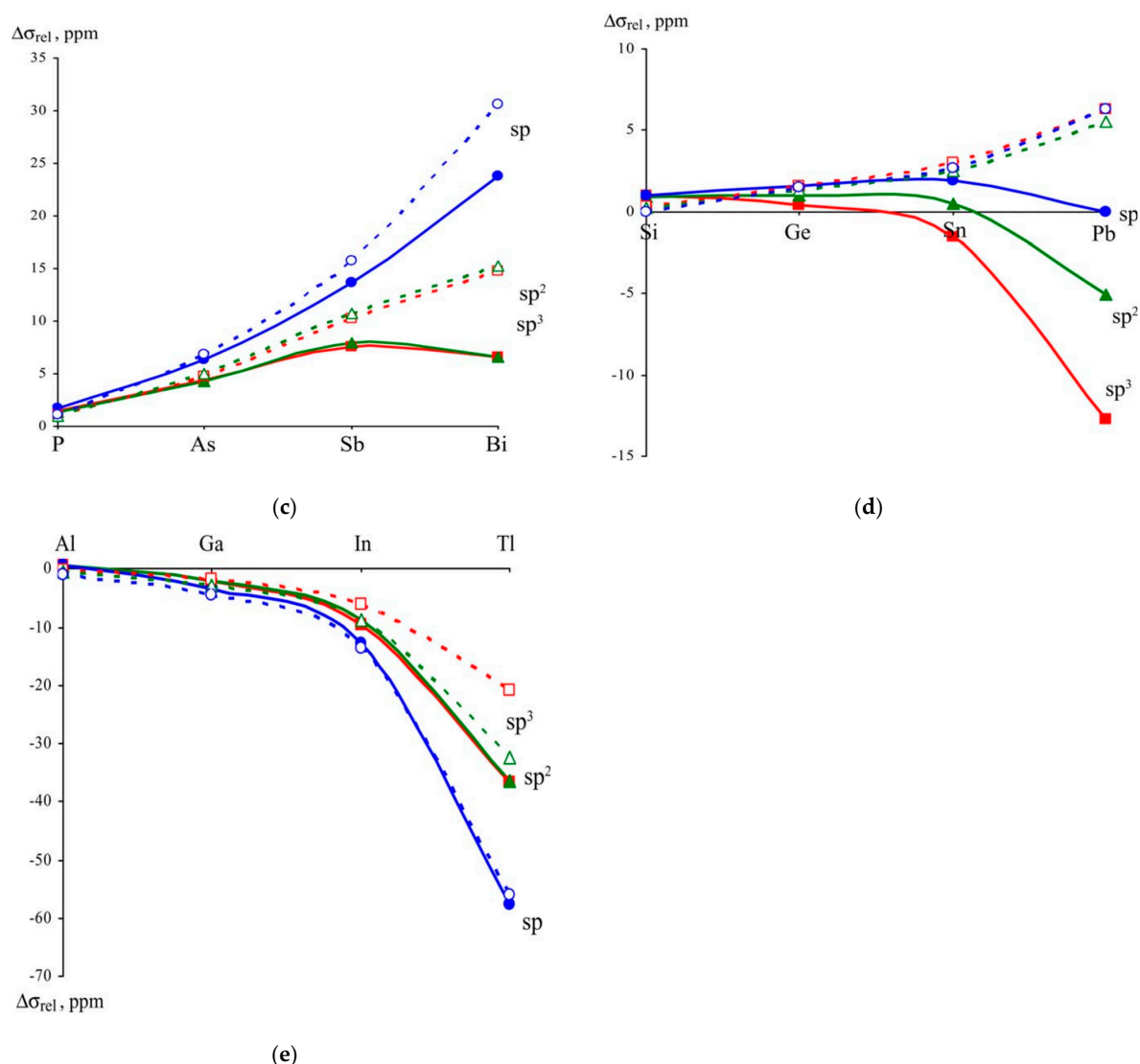


**Figure 18.** Changing of the relativistic corrections to  $^{13}\text{C}$  shielding constants in the series of ethanes, ethylenes, and acetylenes,  $\text{C}_\beta\text{H}_3-\text{C}_\alpha\text{H}_2-\text{XH}_n$ ,  $\text{C}_\beta\text{H}_2=\text{C}_\alpha\text{H}-\text{XH}_n$ ,  $\text{C}_\beta\text{H}\equiv\text{C}_\alpha-\text{XH}_n$  ( $n = 0, 1, 2,$  or  $3$  depending on X), where X covers p-elements in the 13–17 groups: (a) Normal halogen dependences (NHDs); (b) Chalcogen dependences (CDs); (c) Pnictogen dependences (PDs); (d) Tetrel dependences (TetDs); (e) Triel dependences (TriDs). The results obtained at the full four-component DFT(KT2) level are shown with solid lines, while pure spin-orbit corrections obtained at the two-component DFT(KT2)-BSS level are shown with dashed lines. Reproduced from Rusakov et al. [264] with the permission of John Wiley and Sons.

One can see from Figure 18c,d that the SO-HALA trend does not follow the trend of the total four-component relativistic corrections. Out of these two cases, the most pronounced discrepancy in the behaviors of the trends can be observed for the tetrel series (Figure 18d). The SO relativistic corrections to  $\alpha$ -carbons behave themselves as a weak NHD-like trend. At the same time, the total relativistic corrections behave themselves in an opposite way. The total relativistic corrections to the  $sp^3$ -carbon-shielding constants demonstrate the most pronounced inversed behavior (red solid line in Figure 18d). This is hard to explain in simple terms, but it could be speculated that this reflects the lack of the electron lone pairs on heavy atoms in tetrel series that results in significantly diminished or “weak” SO-HALA effect, which is presumably heavily suppressed by the other relativistic contributions. Apparently, the latter are of the scalar origin, because Demissie [265] showed that for the  $^{13}\text{C}$  chemical shifts in  $\text{X}(\text{CCMe})_4$ ,  $\text{Me}_2\text{X}(\text{CCMe})_2$ , and  $\text{Me}_3\text{XCCH}$  ( $\text{X} = \text{Si}, \text{Ge},$

Sn, and Pb) molecules the scalar relativistic corrections, SR-HALA, are very strong giving the contributions which compete with the SO-HALA terms for the lighter tetrels and significantly dominate over the SO-HALA terms for the heavier tetrels, like Sn and Pb. For the pnictogen series (Figure 18c) the discrepancy is noticeably less pronounced which can be due to the presence of one electron pair on heavy pnictogen atom, resulting in more efficient SO-HALA mechanism which is less suppressed by the SR-HALA mechanism in this case.

The dependence of the spin-orbit effects on the number of LEPs on HALA effect has also been investigated by Rusakov et al. [264]. The comparison of theoretical  $^{13}\text{C}$  NMR chemical shifts with experiment was performed for three representative tellurides. The HALA effect in this series is strongly dependent on the number of tellurium LEPs, see Table 3.

**Table 3.** Calculated  $^{13}\text{C}$  isotropic shielding constants and chemical shifts (ppm) in comparison with experiment.

Cmpd.	$\sigma_{\text{nonrel}}$	$\sigma_{\text{rel}}$	$\Delta\sigma$	$\Delta\sigma_{\text{SO}}$	$\delta_{\text{nonrel}}$	$\delta_{\text{rel}}$	$\delta_{\text{exp}}$
$(\text{CH}_3)_2\text{Te}$	184.6	208.7	24.1	27.2	1.8	−21.4	−21.5
$(\text{CH}_3)_4\text{Te}$	157.5	163.3	5.8	7.5	28.9	24.0	20.6
$(\text{CH}_3)_6\text{Te}$	148.8	146.2	−2.6	4.0	37.6	41.1	37.1

As can be seen from Table 3, total relativistic corrections to  $^{13}\text{C}$  shielding constants and their SO parts noticeably diminish with decreasing the number of LEPs on tellurium by about 7 times ongoing from dimethyl telluride to hexamethyl telluride. As a consequence, the authors observed a dramatic disagreement of  $^{13}\text{C}$  nonrelativistic chemical shift of dimethyl telluride with experiment (1.8 ppm against −21.5 ppm), while relativistic  $^{13}\text{C}$  chemical shift exactly reproduced the experimental datum (−21.4 against −21.5 ppm). In tetramethyl telluride and hexamethyl telluride the  $\delta_{\text{nonrel}}$  and  $\delta_{\text{rel}}$  are sufficiently closer to each other than those in dimethyl telluride, indicating the weakening of relativistic effects with decreasing of the number of LEPs on tellurium. From Table 3 it follows that the magnitude and, hence, the importance of the SO-HALA effect for reproducing the carbon chemical shifts depends on the number of p-type LEPs on the adjacent heavy element.

The studies of the HALA effect initiated by the heavy elements of group XIV are very scarce. In particular, the relativistic corrections to proton NMR shielding constants in group XIV hydrides,  $\text{XH}_4$ , were studied by Jaszuński and Ruud [129] in terms of Breit–Pauli theory using the SCF and CASSCF wavefunctions. All types of passive and active relativistic corrections were evaluated for proton-shielding constant in all  $\text{XH}_4$  ( $X = \text{C}, \text{Si}, \text{Ge}, \text{Sn}, \text{Pb}$ ) molecules, though the most part of them appeared to be vanishingly small (smaller than 0.05 ppm in an absolute value). For example, total passive scalar relativistic corrections, representing the sum of  $d/mv$ ,  $d/\text{Dar}$ ,  $p/mv$ ,  $p/\text{Dar}$  contributions, were evaluated as 0.00, −0.02, −0.16, −0.39, and −1.10 ppm for  $\text{CH}_4$ ,  $\text{SiH}_4$ ,  $\text{GeH}_4$ ,  $\text{SnH}_4$ , and  $\text{PbH}_4$ , respectively. The spin-orbit corrections to the same series were 0.01, 0.02, 0.27, 0.38, and 1.45 ppm. Thus, the total relativistic corrections to proton-shielding constant in tetrel series with X varying from C to Sn do not exceed 0.1 ppm (if one takes into consideration the CAS results), while the largest correction was obtained for the  $\text{PbH}_4$  molecule as 0.35 ppm. For the sake of comparison, the relativistic correction to the hydrogen shielding constant in  $\text{XH}_4$  series is an order of magnitude smaller than that in the  $\text{H}_2\text{X}$  series, because of the difference in the FC–I contribution that appeared to be very small in the former case [129]. As was suggested by Jaszuński and Ruud, this is a reflection of the lack of lone electron pairs in the  $\text{XH}_4$  molecules, which leads to a significantly reduced magnitude of the spin-orbit corrections induced by the heavy elements.

Yet, the relativistic HALA effects from heavy group XIV elements can be very substantial. A very interesting example of such case was presented by Vicha et al. [266] recently. The authors investigated the role of relativistic effects on  $^1\text{H}$  NMR chemical shifts of SnII and PbII hydrides with fully relativistic DFT calculations. The stability of possible PbII hydride isomers was studied together with their  $^1\text{H}$  NMR chemical shifts, which were

predicted to be in the high-frequency region, up to 90 ppm. These high-frequency  $^1\text{H}$  signals were attributed to a sizable relativistic spin-orbit contributions initiated by the heavy atom, reaching up to 80 ppm for a hydrogen atom bound to PbII. Approximately seven times smaller but still significant  $\delta_{\text{SO}}(^1\text{H})$  were also found in SnII hydrides. Upon the increasing of the coordination number of the Pb and Sn atoms,  $\delta_{\text{SO}}(^1\text{H})$  were found to drastically decrease. According to canonical MO analysis, it is the vacant  $6p^*$  Pb orbitals that are responsible for large SO magnetic couplings (matrix elements of the SO operator). Thus, the largest values of  $\delta_{\text{SO}}(^1\text{H})$  are obtained for doubly coordinated PbII compounds, where the  $6p^*$  Pb AO does not participate in bonding. The corresponding spin-orbit active MO\* is then composed of 94% of Pb  $6p^*$  AO, which results in  $\delta_{\text{SO}}(^1\text{H}) \approx 80$  ppm. When the coordination number of PbII increases, the  $6p^*$  AO orbital becomes involved in coordination bonding, and its availability for magnetic coupling is reduced. Vicha et al. [267] also have predicted recently that  $^{13}\text{C}$  nuclei in subvalent TII and PbII compounds resonate at very high frequencies (up to 400 ppm), if directly bound to the heavy atom, being outside typical experimental NMR chemical shift ranges for the carbon nuclei. So large  $^{13}\text{C}$  chemical shifts were explained by sizable relativistic spin-orbit effects that can exceed 200 ppm. The origin of such huge spin-orbit contributions was attributed to highly efficient heavy atom  $6p \rightarrow 6p^*$  orbital magnetic couplings in conjunction with low energy gaps between the occupied and virtual orbitals in the subvalent TII and PbII compounds.

### 3.2. Relativistic Effects on $^{19}\text{F}$ , $^{27}\text{Al}$ , $^{29}\text{Si}$ , $^{15}\text{N}$ , and $^{31}\text{P}$ NMR Chemical Shifts

The studies of the relativistic HALA effect from heavy p-elements were carried out not only for the hydrogen and carbon atoms, but also for fluorine, silicon, nitrogen, phosphorus and even for the aluminum atoms. Though, the number of the works on these topics is essentially smaller than that on the HALA effect on the hydrogen and carbon chemical shifts.

In particular, relativistic effects on the fluorine shielding constants were estimated for the FX (X = F, Cl, Br, I, and At) molecular systems [268]. The passive SO contributions to fluorine shielding constants were obtained as the differences between the full four-component RPA calculations and the corresponding spin-free ones. Such approach of extracting the SO effects at the four-component level reproduces well the SO/FC-I corrections obtained by Visscher et al. [167] by means of the quadratic response theory. The fluorine isotropic shielding constants of FX series were estimated as follows:  $-205.8$ ,  $640.4$ ,  $659.8$ ,  $747.3$  and  $547.6$  ppm for  $\text{F}_2$ , FCl, FBr, FI, and FAt, respectively. This trend is neither similar to NHD nor IHD (inverse halogen dependence).

The relativistic corrections to the fluorine isotropic shielding constants were also calculated by Field-Theodore et al. [269] in the  $\text{XF}_3$  (X = N, P, As) systems at the four-component DFT-PBE0 [270–272] and DFT-KT2 [273–276] levels of theory. The relativistic HALA effects on fluorine shielding constants from nitrogen and phosphorus are practically the same, *ca.* 2–4 ppm, while the HALA effect from arsenic is about 0.5–2.5 ppm, depending on the functional/basis set used. It is worth noting that the corresponding total relativistic values of fluorine shielding constant in the series  $\text{XF}_3$  are 34.94, 207.64, and 215.17 (the 4DFT-PBE0/dyall.acv4z level) for X = N, P, and As [269].

Nakatsuji et al. have performed the relativistic quantum chemical calculations of halogen dependencies of  $^{27}\text{Al}$  [195,277] and  $^{29}\text{Si}$  [194] chemical shifts in various halogenated molecules, using the FPT and ab initio UHF wavefunctions (UHF-FPT method). In that way, to study the  $^{27}\text{Al}$  NMR chemical shifts, Nakatsuji et al. [195] considered the systems  $\text{AlX}_4^-$  (X = H, F, Cl, Br and I). The normal halogen dependence was established in going from  $\text{AlCl}_4^-$  to  $\text{AlI}_4^-$  and the inverse halogen dependence was established in going from  $\text{AlF}_4^-$  to  $\text{AlCl}_4^-$ . Thus, the SO corrections to aluminum shielding constants in the  $\text{AlX}_4^-$  (X = H, F, Cl, Br and I) series were calculated as 0.2,  $-0.03$ , 4.96, 48.04 and 99.13 ppm with the total shielding values being about 516.27, 580.21, 494.66, 532.59, and 661.71 ppm, respectively. At that, the SO effect is determined mostly by the contribution from Al s atomic orbital (AO), which increases monotonically from  $\text{AlCl}_4^-$  to  $\text{AlI}_4^-$ , causing the NHD, while the IHD part the authors explained by the Al p-orbital contribution to the paramagnetic term.

The  $^{29}\text{Si}$  NMR chemical shifts of silane,  $\text{SiH}_4$ , silicon tetrahalides,  $\text{SiX}_4$  ( $X = \text{F}, \text{Cl}, \text{Br}$  and  $\text{I}$ ) and  $\text{SiXI}_3$  ( $X = \text{Cl}$  and  $\text{Br}$ ) were calculated by Nakatsuji et al. [194] with the UHF-FPT method including the spin-orbit interaction within the ECP. The  $^{29}\text{Si}$  chemical shifts of the  $\text{SiX}_4$  series were found to follow the same trend as the  $^{27}\text{Al}$  chemical shifts [195], namely the substitution F with Cl causes deshielding-type effect, while the substitution of Cl with Br, and then with I causes the shielding-type effect, shifting the silicon chemical shift to a higher magnetic field. In general, Nakatsuji et al. reached at the conclusion that silicon chemical shifts calculated without the SO effect cannot reproduce the experimental trends for the cases of heavier halogen ligands, bromine and iodine.

Core-dependent and ligand-dependent relativistic corrections to the silicon nuclear magnetic shielding constants of  $\text{SiH}_{4-n}\text{Y}_n$  ( $n = 0-4$ ;  $\text{Y} = \text{H}, \text{F}, \text{Cl}, \text{Br}, \text{I}$ ) model compounds were investigated by Maldonado et al. [85] using the LRESC formalism. From the obtained dependences of  $\sigma(\text{Si})$  on the number of heavy substituents, it follows that only for the iodine series the silicon magnetic shielding increases as the number of iodine atoms is increased, following the classical NHD trend. For bromine series, for instance, the behavior of  $\sigma(\text{Si})$  can be said to be drastically different from that for the iodine series. Namely, the quantity decreases from  $\text{SiH}_4$  to  $\text{SiH}_2\text{Br}_2$  (the deshielding-type effect), then it stays practically unchanged when going to the  $\text{SiHBr}_3$ , and, finally, it increases (shielding-type effect) from  $\text{SiHBr}_3$  to  $\text{SiBr}_4$ . Moreover, Maldonado et al. also has found that when the number of halogen atoms is fixed and, at the same time, the nuclear charge of each halogen is increased,  $\sigma(\text{Si})$  does not show the NHD behavior. These trends were studied in terms of LRESC formalism, where the relativistic corrections can be clustered according to whether they are first- or third-order in response theory and also depending on their spin character, that is, either singlet or triplet. The ligand-dependent relativistic corrections appeared to be the main relativistic corrections to the  $\sigma(\text{Si})$ , with the SO term giving the main contribution.

Relativistic corrections to  $^{29}\text{Si}$  NMR shielding constants in the series of halosilanes  $\text{SiX}_n\text{H}_{4-n}$  ( $X = \text{F}, \text{Cl}, \text{Br}$  and  $\text{I}$ ) were calculated by Fedorov et al. [278] within the full four-component relativistic GIAO-DFT-KT3 [274] and GIAO-RPA schemes using relativistic Dyall's basis sets [279,280]. The performances of these two relativistic schemes along with that of the hybrid computational scheme based on the nonrelativistic GIAO-MP2 [215,216] method with GIAO-RPA relativistic corrections were tested by the comparison of the theoretical results for seventeen silicon compounds with the experimental data. The relativistic effects on  $^{29}\text{Si}$  NMR shielding constants rapidly increase with the total number of halogens attached to silicon (see Figure 19), in line with earlier results by Maldonado and co-workers [85].

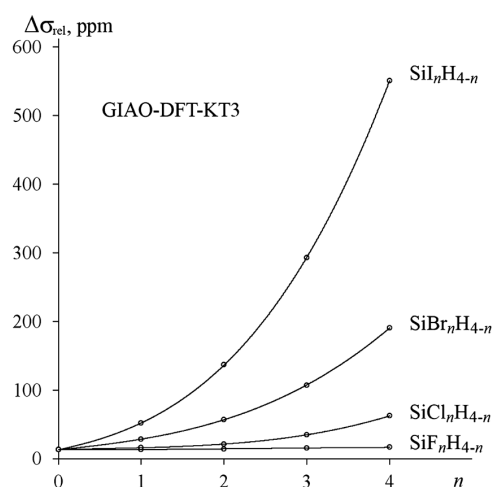


**Figure 19.** Relativistic contribution to  $^{29}\text{Si}$  NMR shielding constant as a function of the number of halogen atoms attached to silicon in  $\text{SiX}_n\text{H}_{4-n}$  ( $X = \text{F}, \text{Cl}, \text{Br}, \text{I}$ ) series calculated at the full four-component GIAO-DFT-KT3/dyall.av3z level. Reproduced from Fedorov et al. [278] with the permission of American Chemical Society.

As exemplified by the curves in Figure 19, the relativistic effects on  $^{29}\text{Si}$  NMR shielding constants of fluorosilanes are next to negligible (up to several ppm), noticeably larger (up to several dozens of ppm) in chlorosilanes, much larger (up to 200 ppm) in bromosilanes and excessively large (several hundreds of ppm) in iodasilanes. The experimental  $^{29}\text{Si}$  NMR chemical shifts were used as a rigorous benchmark for the computational protocols applied. In that way, taking into account the relativistic effects resulted in a dramatic decrease of the MAE of calculated silicon NMR chemical shifts *versus* experiment. Moreover, the four-component relativistic GIAO-RPA scheme combined with the solvent corrections evaluated within the supermolecule solvation model (SSM) demonstrated a better accuracy as compared to both the GIAO-4DFT-KT3 and hybrid MP2-based schemes, providing the MAE of about 7 ppm.

Vícha et al. [267] have predicted  $^{29}\text{Si}$  NMR chemical shifts of subvalent TlI and PbII and found that silicon nuclei in such compounds resonate at very high frequencies in the case if they are directly bound to the heavy atom. Silicon chemical shifts were found to be in the diapason of around 1000 ppm that is outside typical experimental NMR chemical shift ranges for a given type of nucleus. Such large  $^{29}\text{Si}$  NMR chemical shifts were explained by sizable relativistic spin-orbit effects originating from highly efficient  $6p \rightarrow 6p^*$  heavy atom-based orbital magnetic couplings in conjunction with low energy gaps between the occupied and virtual orbital subspaces in the subvalent TlI and PbII compounds.

The manifestation of the SO-HALA effect on phosphorus CSs is very important field of research for today. In particular, Bühl et al. [281] demonstrated the important role of the SO-HALA effect on the phosphorus shielding constant initiated by adjacent multiple halogens. The authors plotted interesting graphs showing the halogen dependence of  $\sigma(^{31}\text{P})$  in two series of phosphorus compounds, namely in  $\text{POX}_3$  and  $\text{PX}_3$  ( $X = \text{F}, \text{Cl}, \text{Br}$ ), see Figure 20.

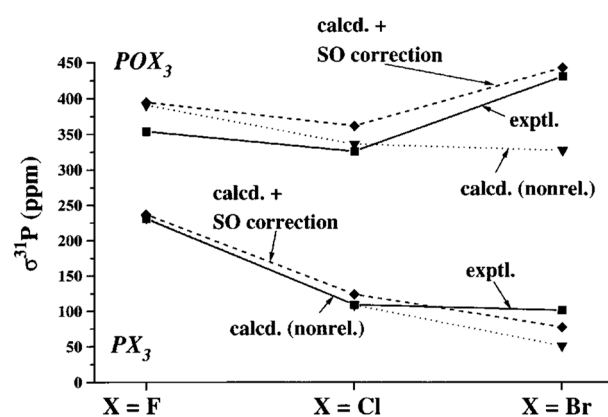


**Figure 20.** Absolute  $^{31}\text{P}$  shielding constants for  $\text{POX}_3$  and  $\text{PX}_3$  molecules ( $X = \text{F}, \text{Cl}, \text{Br}$ ). Calculations were performed at the IGLO-SOS-DFPT level, using IGLO-II basis sets on all atoms. Dotted lines refer to nonrelativistic calculations, dashed lines include one-electron SO corrections, solid lines represent the experimental data. Reproduced from Bühl et al. [281] with permission from John Wiley and Sons.

As can be seen from Figure 20, the  $^{31}\text{P}$  shielding constants of phosphorus(V)oxytrihalides,  $\text{POX}_3$ , demonstrate a typical U-shaped curve due to the onset of significant SO effects. At that, a very different behavior is exhibited by the  $^{31}\text{P}$  shielding constants of the phosphorus(III)trihalides,  $\text{PX}_3$ . In this case, the SO shifts are much smaller, in spite of the fact that the phosphorus centers in both the  $\text{PX}_3$  and  $\text{POX}_3$  species bear three halogen substituents. According to Bühl et al., the reason is that the phosphorus  $3s$ -character in  $\text{PX}_3$  is largely concentrated in the nonbonding electron pair, whereas the P-X bonds are dominated essentially by the phosphorus  $3p$  orbitals. As a result, the computed SO-corrected  $^{31}\text{P}$  shielding constants of  $\text{PCl}_3$  and  $\text{PBr}_3$  are quite similar, as can be seen from Figure 20. This supports the idea proposed by Kaupp for main group elements [185]: “halogen-substituted main group compounds experience particularly large SO effects, provided that the NMR atom

is in its maximum formal oxidation state ( $B^{III}$ ,  $C^{IV}$ ,  $P^V$ ,  $Sb^V$ , etc.).” Only then the valence  $s$ -orbitals of the NMR atom fully participate in bonding to the heavy substituent atom.

Kaupp et al. [207] also presented the IGLO-SOS-DFPT calculations of  $^{31}P$  chemical shifts of the tetrahalophosphonium cations  $PX_4^+$  ( $X = F-I$ ) with and without taking into account the SO corrections (with both one- and two-electron contributions). For these  $P^V$  cations, the authors showed that the SO/FC mechanism is very efficient, causing large SO shifts. To be more precise, the relativistic phosphorus chemical shifts follow the trend:  $-34$ ,  $94$ ,  $-26$ , and  $-523$  ppm for the  $PX_4^+$  series with  $X$  varying from F to I, see Figure 21.

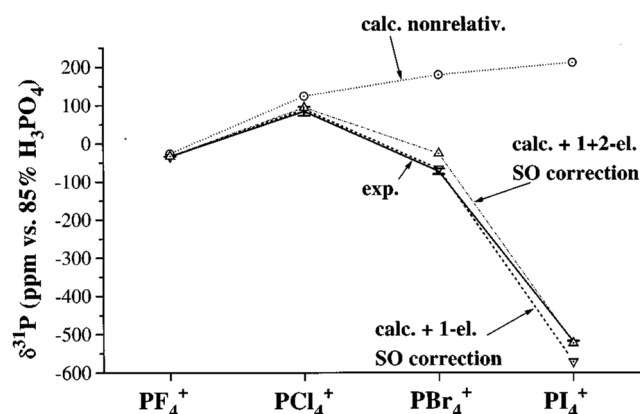


**Figure 21.** Comparison of computed and experimental isotropic  $^{31}P$  chemical shifts. Dotted line: Non-relativistic calculations; dashed line: Results including one-electron SO corrections only; dash-dotted line: Results with one- and two-electron SO corrections; solid line: Experimental data, horizontal bars indicate the largest and smallest known values. Reproduced from Kaupp et al. [207] with the permission of AIP Publishing.

At that, the total SO-HALA corrections to phosphorus CSs were estimated as  $-6$ ,  $-30$ ,  $-205$ , and  $-734$  ppm, respectively. These are indeed very significant corrections shaping the NHD trend, though, the total  $^{31}P$  CSs start to follow the NHD trend only from the chlorine substituent. Apparently, there are some other suppressing electronic mechanisms in the beginning of the series. The authors also noticed that the observed behavior of the spin-orbit corrections is in line with previously established rule for the other tetrahedral main group halides, which consists in following. In the case of p-block main-group central atoms considered as the light NMR spectator atoms, the valence  $s$ -orbitals are fully involved in bonding when these atoms are in their highest oxidation states, therefore, large shielding-type SO effects should be expected for them. This explains, why the NHD is a general behavior for main-group p-elements in high oxidation states: the bonds have generally high  $s$ -character. In contrast, a low  $s$ -character of the bond leads to an inefficient SO/FC mechanism for the p-block main-group elements in low oxidation states, and this may cause the “inverse halogen dependence” (IHD). It is also interesting to notice that Kaupp et al. [207] have established the role of the two-particle SO contributions to the total SO-HALA effect on  $^{31}P$  CSs in  $PX_4^+$  series. For the light halogen substituents, F and Cl, the two-particle SO term is not significant and is worth neglecting, while for the heavier substituents, Br and I, the two-particle SO term becomes significant resulting in the deshielding-type contributions of about 40–50 ppm.

Several attempts have been made to investigate the relativistic effects initiated by heavy chalcogenides on phosphorous chemical shifts. In particular, Chernyshev et al. [282] carried out the ZORA/GIAO-DFT(B3LYP)/Basis (Basis = DZ, DZP and TZP) calculations of phosphorous chemical shifts of  $Me_3P$  and  $Me_3P=X$  ( $X=O, S, Se$ ). The spin-orbit relativistic corrections to phosphorous chemical shifts in the heaviest selenium-containing phosphine appeared to be as much as practically equal to the non-relativistic value in an absolute value. Chernyshev et al. [283] also evaluated the relativistic effects on the  $^{31}P$  chemical shifts in a series of diphenyl- and bis-(2-phenylethyl)phosphine selenides at the ZORA-

GIAO-B1PW91/TZP level. It was found that the spin–orbit contribution to  $\delta(^{31}\text{P})$  from the neighboring selenium atom reaches up to  $-40$  ppm.

Fedorov et al. [284] also have performed the calculations of  $^{31}\text{P}$  NMR chemical shifts in wide representative series of organophosphorous compounds at the GIAO-MP2 and GIAO-4DFT-KT2 levels of theory. The magnitudes of the relativistic corrections reached as much as 20–30 ppm (*ca.* 7% of the total values), thus providing the MAE of the total calculated values against the experimental data of about 9 ppm in the range of about 550 ppm.

Four-component GIAO-DFT(KT2)/dyall.av3z calculations of relativistic corrections to  $^{31}\text{P}$  NMR chemical shifts have been performed by Rusakov et al. [257] for a representative series of 56 tertiary phosphine chalcogenides,  $\text{R}_3\text{P}=\text{X}$  ( $\text{X} = \text{O}, \text{S}, \text{Se}, \text{Te}$ ), in order to investigate the influence of different functional groups at the heavy chalcogen atom on the relativistic HALA effect on the NMR chemical shifts of phosphorous atom. The relativistic effects were found to be next to negligible ( $<1$  ppm in absolute value) only for trimethylphosphine oxide. Already for trimethylphosphine sulfide the HALA effect is about  $-6$  ppm, and for the trimethylphosphine selenide, tri-*t*-butylphosphine selenide and tri-*t*-butylphosphine telluride it is essentially large (of up to almost  $-45$  ppm). In particular, for the trimethylphosphine selenide, the contribution of the relativistic effects is  $-44.6$  ppm, which is about five times larger than its experimental value of about 8.8 ppm. In general, typical relativistic corrections to  $^{31}\text{P}$  NMR chemical shifts of phosphine oxides, sulfides, selenides and tellurides are illustrated in Figure 22.

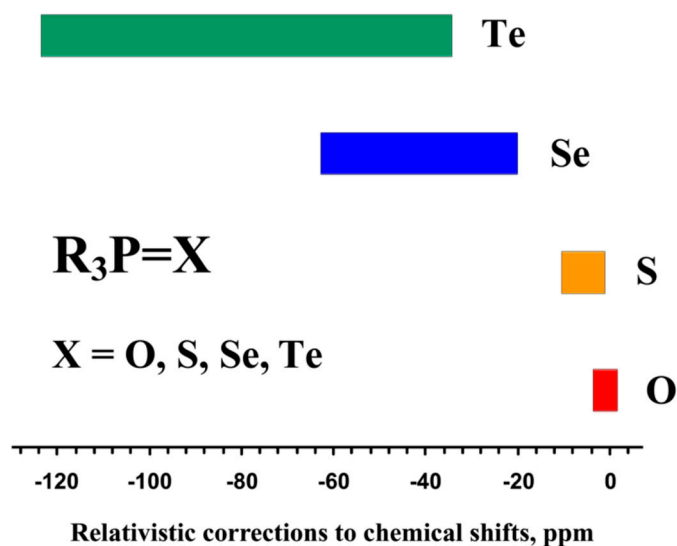


**Figure 22.** The ranges of relativistic corrections to  $^{31}\text{P}$  NMR chemical shifts of phosphine oxides, sulfides, selenides and tellurides. Reproduced from Rusakov et al. [257] with the permission of John Wiley and Sons.

Rusakov et al. [257] have made a very important observation that the branching of alkyl substituents from methyl to tertiary butyl groups at phosphorous results in an increasing (or decreasing in magnitude if one does not take into account their negative sign) of the relativistic corrections to  $^{31}\text{P}$  NMR chemical shifts. Indeed, for phosphorus chemical shifts, the HALA effect in trimethylphosphine selenide is about  $-45$  ppm, while in the tri-*t*-butylphosphine selenide it amounts to only  $-23$  ppm. For the tellurium compounds the difference appeared to be rather pronounced. For example, in the shielding scale, the relativistic correction to phosphorus shielding constant in  $\text{Me}_3\text{PTe}$  was found to be 115 ppm, whereas in tertiary phosphine tellurides with branched alkyl substituents, such as *iso*-propyl and *tert*-butyl, it was found to be equal to 55 ppm. Thus, the difference between the relativistic corrections to phosphorus shielding constants in related phosphine tellurides amounted to as much as 60 ppm!

This strange peculiarity has been thoroughly investigated theoretically in the following paper by Rusakova et al. [184]. The established trend was assumed to be connected with the spatial deformation of the chalcogens' lone electron pairs. To prove this hypothesis, Rusakova et al. considered a series of phosphine tellurides  $X_nY_{3-n}P=Te$  ( $X = Me, Y = Et,$  or  $Vin, n = 0-3$ ), for which total HALA effect (almost totally determined by the SO-HALA effect) was shown to be governed by the frontier MOs, which, in their turn, involve the tellurium  $p$ -type LEPs, being very sensitive to any changes in their close vicinity. The example of striking changes in the relativistic HALA effect on  $^{31}P$  NMR shielding constant for  $Et(Me)_2P=Te$  molecule when varying the dihedral angle  $\varphi = Te-P-C-C$  is shown in Figure 23.

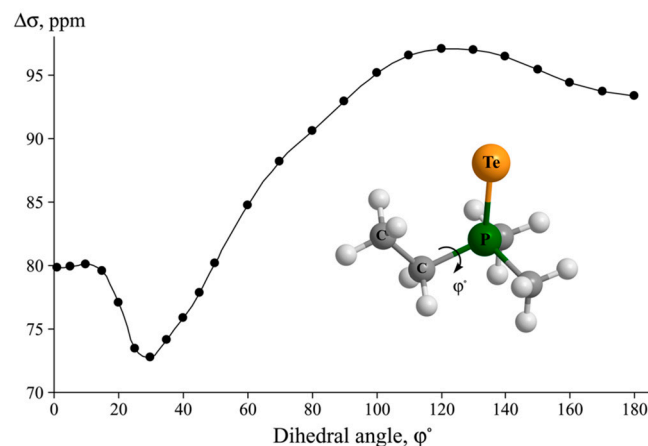


**Figure 23.** The dependence of the relativistic HALA effect on  $^{31}P$  nuclear magnetic resonance shielding constant in  $Et(Me)_2P=Te$  molecule on the dihedral angle  $\varphi = Te-P-C-C$ , obtained at the four-component density functional theory (KT1)/dyall.av3z level. Reproduced from Rusakova et al. [184] with the permission of John Wiley and Sons.

Another vivid example of dramatic changes of the HALA effect on phosphorus shielding constant was modelled by approaching of the Ar atom toward tellurium in  $(Me)_3P=Te$  along the axis, which is perpendicular to the  $P-Te$  bond in  $(Me)_3P=Te$  and traverses the position of tellurium atom. Its linear trajectory starts from the tellurium–argon distance of 3.5 Å and then gradually reduces to 2.2 Å. At that, the relativistic HALA effect on phosphorus shielding constant was found to decrease from 100 to 70 ppm.

Based on the canonical molecular orbital (CMO) analysis, which revealed the leading contributions due to a certain MOs for the particular cases, Rusakova et al. deduced a simplified formulae that allowed to confirm the initially proposed hypothesis about the responsibility of the spatial deformation of the halogens' LEPs for the observed trends. Figure 24 shows a pronounced steric squashing of the  $LEP_3(Te)$  induced by the argon  $p$ -type LEP, resulting in a drastic decrease of the SO-HALA correction to the phosphorous shielding constant in  $(Me)_3P=Te$  molecule on approaching the argon towards the tellurium atom.

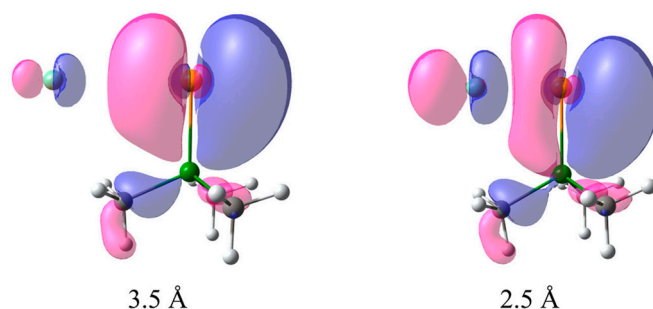


**Figure 24.** The deformation of the HOMO with the decreasing of the  $Te-Ar$  distance in the  $Ar \cdots (Me)_3P=Te$  system. Reproduced from Rusakova et al. [184] with the permission of John Wiley and Sons.

The relativistic effects on nitrogen chemical shifts initiated by heavy p-elements are also of paramount importance, but the works on this topic are very scarce. In particular, nitrogen chemical shifts were investigated in a series of 6-halopurines (see Figure 13) containing heavy halogen atoms [247] using BPPT with common gauge origin (CGO) placed at the nucleus of the halogen atom. For the NMR signals of halogenated purines, there were many misassignments, especially for the iodopurines [285], and an accurate prediction of the NMR chemical shifts of these compounds by taking into account relativistic effects is of paramount importance. For the nitrogen chemical shifts, the most pronounced relativistic effects were found for the nitrogen N-1 atom in the six-membered pyrimidine ring of the purine molecule. For example, for 6-X-7-methyl-7H-purine with X = Cl, Br, I (see Figure 25), the relativistic BPPT correction to N-1 CSs rapidly increases from 0.84 to 2.25 to 4.32 ppm in going from Cl to Br to I, respectively. This indicates an increasing deshielding-type two-bond HALA effect that superimposes on the overall deshielding-type electronic effect from the halogen atom ongoing from Cl to I. The N-1 chemical shift of 6-X-7-methyl-7H-purine with X = Cl, Br, I calculated within the DFT-BLYP method using different methodologies (with the reference to either primary or secondary standards, with or without taking into account relativistic corrections) is illustrated in Figure 25. It can be seen from this figure that the graph (NR + R) that corresponds to the total calculated N-1 chemical shifts with PCM(DMSO) and BPPT corrections is in very good agreement with the graph (EXP), representing the experimental values. It also can be seen that the solvent corrections are much more important for the N-1 chemical shifts of 6-X-7-methyl-7H-purine with X = Cl, Br, I than the relativistic corrections.

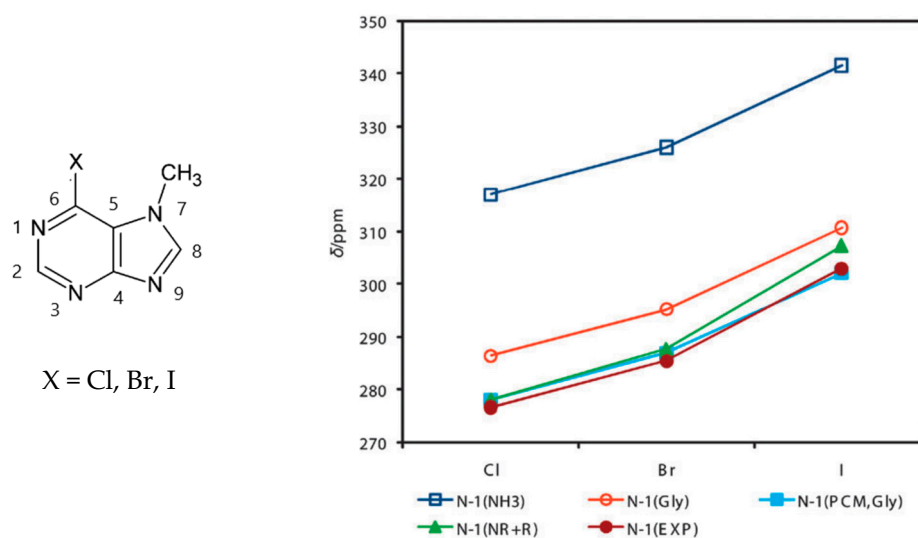


**Figure 25.** Calculated [BLYP/HIII(FIII)] and experimental chemical shifts of N-1 for -X-7-methyl-7H-purine with X = Cl, Br, I. (NH<sub>3</sub>)—calculated CSs referenced to NH<sub>3</sub>, (Gly)—calculated CSs referenced to  $\alpha$ -glycine secondary standard, (PCM, Gly)—CSs calculated with the PCM(DMSO) and referenced to  $\alpha$ -glycine, (NR + R)—total chemical shifts calculated with the PCM(DMSO) and BPPT corrections, (EXP)—experimental values. Reproduced from Standara et al. [247] with the permission of Royal Chemical Society.

It is also worth noting that for the nitrogen shielding constants, the relativistic  $\alpha$ -HALA effect is cumulative. Namely, Samultsev et al. [286] reported on the nonlinear increase of the nitrogen shielding constant from 3.6 to 6.6 to 8.3 ppm in the series of chlorine compounds, Me<sub>2</sub>NCl, MeNCl<sub>2</sub>, and NCl<sub>3</sub>, respectively. Samultsev et al. [287] also investigated the long-range  $\beta$ - and  $\gamma$ -relativistic HALA effects of halogens on <sup>15</sup>N NMR chemical shifts of 20 halogenated azines (pyridines, pyrimidines, pyrazines, and 1,3,5-triazines) at the four-component DFT(KT3)/pcS-3 [288] level. The authors found that for the fluoro-, chloro-, and bromo-derivatives, the long-range relativistic corrections to nitrogen chemical shifts due to  $\beta$ - and  $\gamma$ -HALA effects are insignificant, varying in the range of 1–2 ppm, while,

for the iodocontaining compounds, the relativistic  $\beta$ -HALA effect provides noticeable contributions, varying from *ca.* 4 to 11 ppm.

#### 4. Stereochemistry of the Relativistic Effects on the NMR Shielding Constants of Light Nuclei Initiated by Heavy Main Group p-Elements

As was noticed by Kaupp et al. [186], for the light atoms that are separated from the heavy atom by several bonds, one can expect the rules known for the corresponding spin–spin coupling constants to hold. Thus, for example, one can expect a Karplus-type relationship [289,290] for the spin–orbit contribution of a light atom three bonds away from heavy atom as a function of the corresponding dihedral angle. In this sense, relativistic HALA effect is of potential interest for the stereochemical studies of organic and bioorganic molecules.

Kaupp et al. [186] calculated the dihedral angle dependence of the reduced three-bond spin–spin coupling constant  ${}^3K_{\text{FC}}(\text{I,H})$  in iodoethane and plotted it against the corresponding graph for the relativistic SO-HALA correction, see Figure 26.

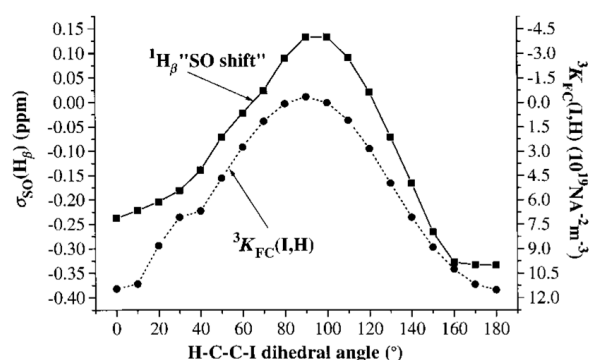


**Figure 26.** Karplus-type relationship:  ${}^1\text{H}$  spin–orbit shifts  $\sigma_{\text{SO}}(\text{H}_\beta)$  and reduced spin–spin coupling constants  ${}^3K_{\text{FC}}(\text{I,H})$  as a function of the H–C–C–I dihedral angle in iodoethane. Reproduced from Kaupp et al. [186] with the permissions of John Wiley and Sons.

As it can be seen in Figure 26, the  $\sigma_{\text{SO}}(\text{H}_\beta)$  of iodoethane approximately follows the Karplus-type behavior of the  ${}^3K_{\text{FC}}(\text{I,H})$  within numerical accuracy with almost coinciding angles for maxima and minima of the two curves. The overall behavior does relate increasingly shielding-type  $\sigma_{\text{SO}}(\text{H}_\beta)$  correction to increasingly negative  ${}^3K_{\text{FC}}(\text{I,H})$ , and increasingly deshielding-type  $\sigma_{\text{SO}}(\text{H}_\beta)$  correction to increasingly positive  ${}^3K_{\text{FC}}(\text{I,H})$ . Thus, Figure 26 indicates that the analogy between the spin–orbit shift and spin–spin coupling does hold even for such small interactions across three single bonds. However, it is pertinent to bear in mind that such an analogy does not appear in all cases. For example, when there are *p*-type lone electron pairs at the heavy atom, the analogy ceases to be [186].

Another example of stereospecificity of the HALA effect was presented by Viesser et al. [230]. The authors carried out a stereoelectronic study of *cis*- and *trans*-1,2-dihaloethene isomers (halo = F, Cl, Br or I) to explain the experimental difference [291–293] in the magnitude of  ${}^{13}\text{C}$  NMR chemical shifts in these two isomers. Namely,  ${}^{13}\text{C}$  chemical shift of *trans* isomer appeared to be more shielded than that of *cis* isomer, especially for iodine, where the difference was found to be approximately 17 ppm. From the beginning of that work, the experimental values were compared to the calculated values with various DFT functionals using both the nonrelativistic approach and the relativistic approximations SR-ZORA and SO-ZORA. The analysis of basis set (QZ4P, TZ2P) and inclusion of the solvent effects via the conductor-like screening model for the realistic solvent (COSMO-RS) was also performed to carefully approach to the problem under consideration. As a result, the authors chose the SO-ZORA-DFT(KT2)/TZ2P level without taking into account solvent corrections, because, as strange as it may be, the use of COSMO-RS model worsened the accuracy in comparison with experiment. This result was explained either by the error cancellation at the TZ2P/gas-phase level or by the poor performance of the COSMO-RS model. The analysis of the HOMO–LUMO energy gap also did not give any strong arguments

to explain the observed differences in two isomers of bromine and iodine compounds. Only taking into consideration the SO-HALA effect within the SO-ZORA-DFT(KT2)/TZ2P approach resulted in a coherent explanation. The SO-HALA shift provided the largest difference between the *cis* and *trans* isomers of the bromine and iodine derivatives. The difference of 17 ppm in the  $^{13}\text{C}$  NMR chemical shifts of *cis*- and *trans*-diiodoethene isomers was explained by the steric repulsion of two iodine lone pairs in the *cis* isomer, which affects in much extent both the SO-HALA effect and the paramagnetic contribution to carbon-shielding constant.

Unexpectedly large HALA effects have been found by Rusakov et al. [256] in  $^{13}\text{C}$  NMR chemical shifts of  $\beta$ - and  $\gamma$ -carbons of seleno- and telluroketones as was exemplified by three representative real-life compounds, 2,2,5,5-tetramethyl-3-cyclopentene-1-selone, selenofenchone and 1,1,3,3-tetramethyl-1,3-dihydro-2H-indene-2-tellurone. The relativistic corrections (calculated at the 4DFT-KT2/dyall.av3z level) to chemical shifts of  $\beta$ -carbons in selenoketones gave the deshielding-type contributions of as much as 5–6 ppm, while that for the telluroketones reached as much as 18 ppm. The magnitude of the shielding-type HALA effect on chemical shifts of  $\gamma$ -carbons was calculated as approximately  $-6$  ppm in selenoketones and  $-13$  ppm in telluroketones. Considering 2,2,5,5-tetramethyl-3-cyclopentene-1-selone, selenofenchone and 1,1,3,3-tetramethyl-1,3-dihydro-2H-indene-2-tellurone, Rusakov et al. established that the relativistic corrections to chemical shifts of  $\beta$ - and  $\gamma$ -carbons vary substantially depending on the geometry of the pathway between the heavy chalcogen and the resonance carbon itself. Impelled by this finding, the authors investigated the stereochemical dependence of the long-range relativistic HALA effect on  $\gamma$ -carbons in conformationally labile systems. In particular, the authors obtained the bell-like dihedral angle dependence of both total HALA effect and the SO-HALA part on the shielding constant of  $\gamma$ -carbons in butane-2-selone and butane-2-tellurone. The MO analysis revealed that the most part of the change of the SO contributions to carbon-shielding constant in going from  $\phi = 0^\circ$  to  $\phi = 90^\circ$  is mostly determined by the HOMO $\rightarrow$ LUMO and HOMO-1 $\rightarrow$ LUMO magnetic couplings.

Moreover, it was noted that the  $\alpha$ -,  $\beta$ - and  $\gamma$ -HALA effects on  $^{13}\text{C}$  NMR chemical shifts alternate in sign being negative for the  $\alpha$ - and  $\gamma$ -carbons (shielding-type effect) and positive for the  $\beta$ -carbons (deshielding-type effect).

The study of the  $\beta$ - and  $\gamma$ -SO-HALA effects on  $^{13}\text{C}$  NMR chemical shifts in selenoketones and telluroketones conducted in the Ref. [256] has been continued for the long-range SO-HALA effects on  $^1\text{H}$  NMR chemical shifts in selenium- and tellurium containing compounds [187]. Chemical shifts of  $\beta$ - and  $\gamma$ -protons in series of eleven selenium- and tellurium-containing compounds have been calculated via the CCSD method taking into account solvent, vibrational and relativistic corrections. Relativistic corrections were calculated at the GIAO-4DFT(KT1)/dyall.av3z level. Taking into account the relativistic effects considerably improved the agreement of theoretical results with the experimental data, reducing the MAE (evaluated in relation to experiment) from 1.1 to 0.26 ppm. The GIAO-DFT(KT1)/dyall.av3z computational scheme has been proven to provide reliable relativistic corrections and was used further in the mentioned work to investigate the stereochemical behavior of long-range  $\beta$ - and  $\gamma$ -HALA effects in different structures. The BSS calculations for the benchmark compounds were also performed and the SO contributions were found to almost totally determine the HALA corrections. The  $\beta$ -HALA effect on hydrogen chemical shifts has been found to give a deshielding-type contribution varying from 0.1 to as much as 14.5 ppm, while  $\gamma$ -HALA effect was found to give a shielding-type contribution of lesser magnitude, though, reaching a noticeable value of *ca.*  $-3$  ppm for ethanetellural.

Taking into account that SO-HALA effect is analogous, to some extent, to the well-established mechanism of the indirect Fermi-contact nuclear spin–spin coupling constant (SSCC), the authors expected a degree of correlation in behaviors of these two quantities. The correlation with the spin–spin coupling constant has been found only for a certain type of tellurium compounds, namely for the  $\gamma$ -HALA effect in telluroketone, see Figure 27.

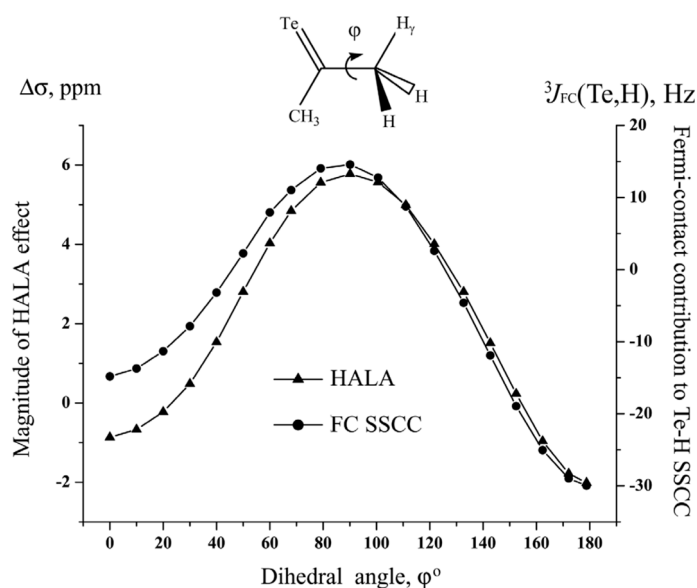


**Figure 27.** The dependencies of the HALA contribution to  $\gamma$ -proton NMR shielding constant and Fermi-contact contribution to vicinal tellurium-hydrogen spin–spin coupling constant  ${}^3J({}^{125}\text{Te}, {}^1\text{H}_\gamma)$  in telluroketone on the dihedral angle  $\angle \text{Te-C-C-H}_\gamma$ , obtained at four-component GIAO(KT1)/dyall.av3z and nonrelativistic DFT(KT1)/ATZP levels, respectively. Reproduced from Rusakov et al. [187] with permission from John Wiley and Sons.

In the other cases the correlation either did not manifest itself at all or did it only partially. For example, Figure 28 shows the graphs of  $\beta$ -HALA effect on proton and FC two-bond Te-H SSCC in dimethyltelluride on the left and  $\gamma$ -HALA effect on proton and FC three-bond Te-H SSCC in ethyl(methyl)telluride on the right.

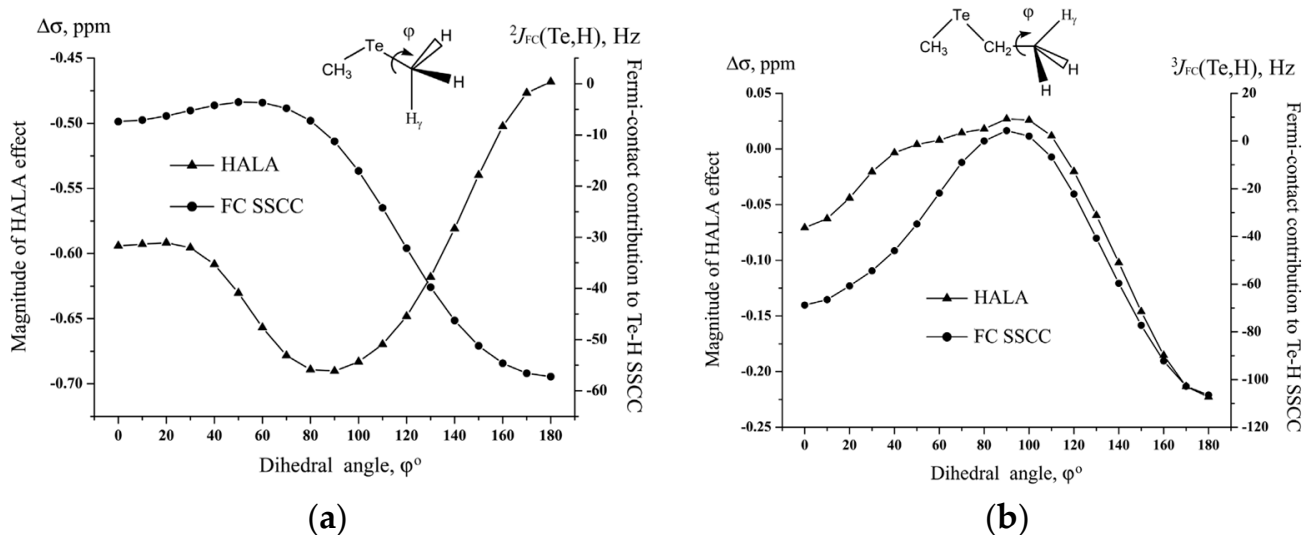


**Figure 28.** Stereochemical dependencies of long-range relativistic HALA effects on proton and that of the corresponding FC-contributions to Te-H SSCCs in: (a) dimethyltelluride; (b) ethyl(methyl)telluride. Reproduced from Rusakov et al. [187] with permission from John Wiley and Sons.

Based on the CMO analysis, the authors established that coincidental stereochemical behaviors of  $\gamma$ -HALA effect and  ${}^3J({}^{125}\text{Te}, {}^1\text{H}_\gamma)$  in telluroketone is due to the contributions from pairs HOMO-1—LUMO and HOMO—LUMO, where HOMO consist of 94% of the  $p$ -type tellurium lone pair, HOMO-1 represents 86% of  $\pi_{\text{Te-C}}$ , and LUMO is 82% of  $\pi_{\text{Te-C}}^*$ . For the other compounds, there were no leading contributions found which could be responsible for the observed stereochemical behaviors. Thus, Rusakov et al. have come

to a conclusion that the correlation between the stereochemical behaviors of the HALA effect on the proton-shielding constant and the corresponding nonrelativistic FC SSCC, involving the proton under consideration and the heavy chalcogen, can be observed in the case when there is no significant distortion of the molecular orbital structure connected to the heavy chalcogen, and, especially, to its lone electron pairs. Indeed, apart from the MO matrix elements of the FC operator, the leading term of the SO-HALA effect also includes the matrix elements of the spin-orbit operator, centered on the heavy atom, which depends at the most part on the orbitals with nonzero angular momentum. Hence, in the case when inner rotations do not change the SOC on the heavy atom significantly, one could expect the behavior of the FC matrix elements in the SO expression to be less suppressed, resulting in some degree of correlation between the SO shielding and the FC SSCC.

### 5. Influence of the Relativistic Effects Initiated by Heavy p-Elements on the Vibrational Contributions to the Shielding Constants of Light Nuclei

The internuclear distance dependence of the relativistic effects on the nuclear magnetic resonance shielding constants is practically unexplored field of research. At the same time, leaning on the contemporary experience, one can conclude that the geometrical factor may play a very substantial role in the shielding constants calculated both at the nonrelativistic and relativistic levels of theory. This rises many important questions. We know that the vibrational corrections to CSs calculated at the nonrelativistic level of theory give sometimes a substantial contribution. What can we say about these corrections calculated at the relativistic level of electronic theory in the case of the presence of heavy elements in the system? Or, what is the role of the SO-HALA effect in the vibrationally averaged values of the chemical shifts of light atoms directly bonded to a heavy atom? These issues are still open, and there are only a few works that were destined to shed some light on this matter.

Internuclear distance dependence of the spin-orbit coupling contributions to the proton NMR chemical shift of HI molecule was investigated by Minaev et al. [294]. The calculations were carried out using the complete active space self-consistent field (CASSCF) wavefunction on hydrogen iodide at different internuclear distances. This is an important issue for many reasons. For example, semi-empirical calculations by taking into account the SOC illustrated that there is a strong dependence of the  $T_1 \leftarrow S_0$  transition matrix elements on the H-I internuclear distance [295]. This was assumed to cause a substantial effect on the  $^1\text{H}$  LS shift of the HI molecule. Indeed, the SOC contribution was shown to increase monotonically, becoming about eight times larger when the internuclear distance increases from 1.4 to 2.0 Å. At the internuclear distance of 2.0 Å, the SOC contribution was found to be twice as large as the non-relativistic shielding constant. The non-relativistic diamagnetic contribution also showed a strong dependence on the bond length, decreasing with an increase in the bond length in the vicinity of the equilibrium value. Actually, this suggests that the relativistic spin-orbit effect might be very important when calculating the vibrational corrections to the shielding constants of light nuclei located in the vicinity of the heavy nuclei. Indeed, for the HI molecule, the total vibrationally averaged  $^1\text{H}$  shielding constant was found to be slightly increased compared to the value calculated at the equilibrium distance  $r = 1.605$  Å, while taking into account the SOC induced contribution reversed the sign of the total vibrational contribution to the  $^1\text{H}$  shielding constant. The dependences of the nonrelativistic terms, diamagnetic  $\sigma^D$  and paramagnetic  $\sigma^P$ , and the relativistic SOC-induced contributions ( $\sigma^{\text{SO/FC-1/II}}$ ,  $\sigma^{\text{SO/SD-1/II}}$ , and total  $\sigma^{\text{SO}}$ ) to the proton-shielding constant of HI molecule ( $\sigma^{\text{tot}}$ ) on the internuclear distance are presented in Figure 29.

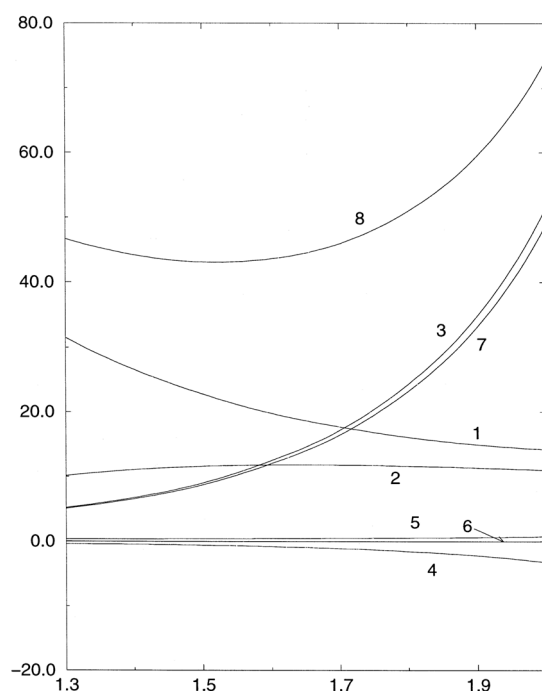


**Figure 29.** Calculated internuclear distance dependence of different contributions to the  $^1\text{H}$  NMR shielding constants of HI molecule (in ppm): (1)  $\sigma^D$ ; (2)  $\sigma^P$ ; (3)  $\sigma^{\text{SO/FC-I}}$ ; (4)  $\sigma^{\text{SO/FC-II}}$ ; (5)  $\sigma^{\text{SO/SD-I}}$ ; (6)  $\sigma^{\text{SO/SD-II}}$ ; (7)  $\sigma^{\text{SO}}$ ; (8)  $\sigma^{\text{tot}}$ . Reproduced from Minaev et al. [294] with the permission of Elsevier.

As was mentioned by Minaev et al., the phenomenon that is responsible for the observed strong dependence of the  $\sigma^{\text{SO}}$  correction to the  $^1\text{H}$  NMR shielding constant is similar to that which causes significant changes in the spin–spin coupling constant of the HD molecule when varying the internuclear distance [296]. Both effects were explained by the decreasing of triplet excitation energy with bond length extension [294].

Another comprehensive work confirming the presence of a pronounced sensitivity of the rovibrational corrections to the  $^1\text{H}$  chemical shifts calculated by taking into account the SO effects was carried out by Crompton et al. [297]. The influence of the spin–orbit effects on the rovibrational corrections to  $^1\text{H}$  shielding constants was investigated for the HBr molecule. For this purpose, the SO correction to the shielding was calculated as a function of the interatomic distance in HBr. Without the SO correction, the  $\sigma(^1\text{H})$  would have had a typical form (shielding constants usually decrease as the interatomic distance is increased), whereas the inclusion of the SO correction resulted in a different behavior. Namely, the total shielding constant obtained with the SO correction as a function of the internuclear distance had a non-monotonic U-shape form and the corresponding rovibrational correction to  $^1\text{H}$  shielding constant of HBr appeared to be small, about 0.34 ppm, with an unusual positive sign. This was in contrast to the significant nonrelativistic negative rotational-vibrational correction of  $-7.11$  ppm given by Jameson et al. [298]. Crompton et al. tried to explain the discrepancy by neglecting the two-electron SO terms. Namely, the authors assumed that notwithstanding the two-electron SO corrections are quite small at the equilibrium bond lengths for hydrogen halides, they could have had a strong dependence on the interatomic distance and therefore might contribute noticeably to the temperature dependence and rovibrational corrections to the  $^1\text{H}$  chemical shift. Another plausible explanation given by Crompton et al. consisted in that the experimental data presented for HBr molecule in the Ref. [298] requires further clarification.

The fact that the SO interaction produces qualitative changes in the effects of rovibrational motion on the proton NMR chemical shifts of hydrogen halides [294,297] motivated the researches to investigate the issue in application to the  $^{13}\text{C}$  nuclear shielding constants of carbon dichalcogenides,  $\text{CX}_2$  ( $X = \text{O}, \text{S}, \text{Se}, \text{Te}$ ) [258,299]. One of the main purposes of these studies consisted in the investigation of the influence of the SO interaction on the

one-bond secondary isotope effects of the  $^{13}\text{C}$  nuclear shielding constants of  $\text{CX}_2$  molecules. The SO corrections were calculated with the Breit-Pauli one-electron one-center mean-field approximation [206,300] for the one- and two-electron SO operators. The SO effects on the rovibrational corrections to  $^{13}\text{C}$  nuclear shielding constants and thereby on the secondary isotope effects appeared to be significant. In general, the SO interaction was shown to provide a contribution that diminishes the effects calculated at the nonrelativistic level. In the  $\text{CTe}_2$  molecule, the magnitude of the SO contribution occurred to constitute as much as 65% of the magnitude of the nonrelativistic contribution in the  $^{13}\text{C}$  isotope shift and 55% in the temperature dependence of this shift. Hence, it is advisable to take into account the SO coupling into account in calculations of the isotope shifts, their temperature dependence, and, overall, in the rovibrational averaging of shielding constants when dealing with the molecules containing heavy chalcogens such as  $\text{CSe}_2$  and  $\text{CTe}_2$ . For example, the comparison of the calculated and experimental secondary one-bond isotope shifts on the  $^{13}\text{C}$  shielding for  $\text{CSe}_2$  at 300 K is presented in Figure 30. This figure demonstrates the importance of the SO relativistic corrections in the calculation of the secondary one-bond isotope shifts on the example of carbon-shielding constant of the  $\text{CSe}_2$  molecule.

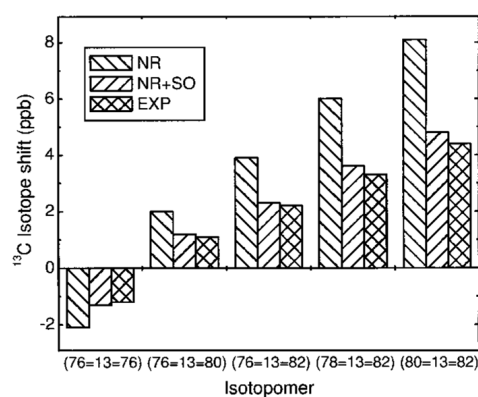


**Figure 30.** Comparison of the calculated and experimental secondary one-bond isotope shifts on  $^{13}\text{C}$  shielding for  $\text{CSe}_2$  at 300 K. The reference is the  $^{76}\text{Se}=^{13}\text{C}=^{78}\text{Se}$  isotopomer. The calculated shifts are presented both at the nonrelativistic (NR) level and by taking into account the spin-orbit corrections (NR + SO). Reproduced from Lantto et al. [299] with permission from the American Chemical Society.

It is also worth noting that the relativistic effects turned out to be of crucial importance for the zero-point vibrational (ZPV) corrections to the NMR spin-spin coupling constants that involve heavy atoms [301]. This indeed compels one to make an assumption that large SO corrections should be expected for vibrationally averaged shielding constants of light atoms located in the vicinity of heavy elements.

## 6. Conclusions

To conclude, it is helpful to briefly mention the main findings that have been established for the HALA effect from heavy p-elements in the papers covered in this review:

1. The total relativistic HALA effect initiated by the heavy p-elements on the chemical shifts of the light p-block main group nuclei is actually determined by the efficiency of the spin-orbit/Fermi-contact (SO/FC) mechanism that plays a predominant role in the total SO-HALA effect.
2. The scalar relativistic HALA corrections to the chemical shifts of light atoms due to the mass-velocity and Darwin relativistic effects are negligible in most cases when the heavy atom belongs to the 16th and 17th groups of PTE. For the 14th group's heavy atoms, the scalar-HALA can reach significant magnitudes effectively suppressing the SO-HALA mechanism.
3. The NHD trends for NMR chemical shifts of light nuclei are due to the relativistic SO-HALA effects.

4. The efficiency of the SO/FC (SO-HALA) mechanism was found to depend on the rate of involvement of the valence *s* orbitals of the light atom in the heavy atom—light atom bond. This is important for the SO/FC mechanism to be efficient, because *ns* orbitals are responsible for bringing the heavy-atom SOC-induced spin-polarization into contact with the light atom nucleus.
5. The most pronounced SO-HALA effect is expected to manifest itself in the  $^1\text{H}$  NMR chemical shifts of protons directly bound to a heavy atom, because in this case the hydrogen 1*s*-orbital predominates in bonding.
6. The  $^{13}\text{C}$  SO-HALA effects increase from  $sp^3$  to  $sp^2$  to  $sp$  hybridization of the carbon atom.
7. In the case of p-block main-group central atoms considered as the light NMR spectator atoms, the valence *s*-orbitals are fully involved in bonding when these atoms are in their highest oxidation states; therefore, large shielding-type SO effects should be expected for them. This explains why the NHD trend is the general behavior for the chemical shifts of the main-group p-elements being in high oxidation states: the bonds have a generally high *s*-character. In contrast, a low *s*-character of the bond leads to an inefficient SO/FC mechanism for the p-block main-group elements in low oxidation states, and this may cause the “inverse halogen dependence” (IHD).
8. The magnitudes of the energy gaps between the frontier occupied and vacant molecular orbitals (MOs) involved in the SO-HALA mechanism are important for the SO-HALA correction: the less the energy gaps, the larger the magnitude of the SO-HALA effect.
9. The magnitude of the spin–orbit coupling (SOC) at heavy atoms is responsible for the efficiency of the SO-HALA mechanism. In particular, the occupation of orbitals with  $l \geq 1$  and the partial charge on the heavy atom play a decisive role in the magnitude of the spin–orbit splitting. This results in the fact that  $\pi$ -type lone electron pairs (LEPs) on the heavy atom can provide significant contributions to the SO-HALA effect.
10. The overlap of the  $90^\circ$ -rotated frontier occupied molecular orbitals (for example, the lone electron pairs of a heavy atom) with lowest unoccupied frontier molecular orbitals (for example, the frontier antibonding molecular orbitals) must be significant to provide considerable MO matrix elements of the spin–orbit and orbital Zeeman (OZ) operators that are included in the main SO/FC–I term.
11. Spatial deformation of the chalcogen’s lone electron pairs (LEPs) influences the magnitude of the one-bond SO-HALA effect: the squashing of LEPs at a heavy atom diminishes the magnitude of the SO-HALA effect.
12. In the case when inner rotations do not change the SOC on the heavy atom significantly, one can expect a degree of correlation between the stereochemical behaviors of the SO-HALA effect on the shielding constant of a light nuclei and the FC contribution to the corresponding spin–spin coupling constant.
13. Like in the case of NHD, the chalcogen and triel dependencies established for the  $^{13}\text{C}$  NMR shielding constants were explained by the SO-HALA effect, though, the pnictogen and tetrel dependences appeared to reflect some additional relativistic mechanisms that interfered with the SO-HALA effect.
14. The SO-HALA effect on shielding constants of light atoms, such as  $^1\text{H}$ ,  $^{13}\text{C}$  or  $^{15}\text{N}$ , is cumulative and it increases nonlinearly with the total atomic number of adjacent halogens or chalcogens.
15. The deshielding-type SO effect is associated with the occupied  $\sigma$ -type heavy atom—light atom bonding MOs, while the  $\pi$ -type MOs leads to a shielding-type SO effect.
16. The  $\alpha$ -,  $\beta$ - and  $\gamma$ -HALA effects on  $^{13}\text{C}$  NMR chemical shifts alternate in sign, being negative for the  $\alpha$ - and  $\gamma$ -carbons (shielding-type effect) and positive for the  $\beta$ -carbons (deshielding-type effect).
17. Relativistic SO-HALA effect on the NMR chemical shifts is not restricted to a covalently heavy atom—light atom-bound systems. It manifests itself, in particular, in ion pairs and is known as the “through-space” HALA effect.
18. The relativistic rovibrational corrections to the light atom chemical shifts may substantially differ from that calculated at the nonrelativistic level of electronic theory, if

there are heavy atoms in the system (especially in the case when the light spectator atom is directly bound to the heavy atom).

**Author Contributions:** Conceptualization, data curation, writing—original draft preparation, writing—review and editing, visualization, I.L.R. and Y.Y.R. All authors have read and agreed to the published version of the manuscript.

**Funding:** This research received no external funding.

**Institutional Review Board Statement:** Not applicable.

**Informed Consent Statement:** Not applicable.

**Data Availability Statement:** Not applicable.

**Acknowledgments:** This work was carried out within the framework of the research project of Russian Academy of Sciences # 121021000264-1.

**Conflicts of Interest:** The authors declare no conflict of interest.

## References

1. Gauss, J.; Stanton, J.F. Electron-correlated methods for the calculation of NMR chemical shifts. In *Calculation of NMR and EPR Parameters, Theory and Applications*, 1st ed.; Kaupp, M., Bühl, M., Malkin, V.G., Eds.; WILEY-VCH Verlag GmbH & Co. KGaA: Weinheim, Germany, 2004; Chapter 8, pp. 123–139.
2. Fukui, H. Theory and calculation of nuclear shielding constants. *Prog. Nucl. Magn. Reson. Spectrosc.* **1997**, *31*, 317–342. [[CrossRef](#)]
3. Fukui, H. Theoretical aspects of spin–spin couplings. *Nucl. Magn. Reson.* **2007**, *36*, 113–130. [[CrossRef](#)]
4. Webb, G.A.; Fukui, H.; Baba, T. Theoretical Aspects of Spin-spin coupling constants. In *Nuclear Magnetic Resonance*, 1st ed.; Webb, G.A., Ed.; Royal Society of Chemistry: London, UK, 2003; Volume 32, pp. 126–145. [[CrossRef](#)]
5. Helgaker, T.; Coriani, S.; Jørgensen, P.; Kristensen, K.; Olsen, J.; Ruud, K. Recent advances in wave function-based methods of molecular-property calculations. *Chem. Rev.* **2012**, *112*, 543–631. [[CrossRef](#)]
6. Helgaker, T.; Jaszuński, M.; Pecul, M. The quantum-chemical calculation of NMR indirect spin-spin coupling constants. *Prog. Nucl. Magn. Reson. Spectrosc.* **2008**, *53*, 249–268. [[CrossRef](#)]
7. Helgaker, T.; Jaszuński, M.; Ruud, K. Ab initio methods for the calculation of NMR shielding and indirect spin-spin coupling constants. *Chem. Rev.* **1999**, *99*, 293–352. [[CrossRef](#)]
8. Helgaker, T.; Pecul, M. Spin-Spin Coupling Constants with HF and DFT Methods. In *Calculation of NMR and EPR Parameters: Theory and Applications*, 1st ed.; Kaupp, M., Bühl, M., Malkin, V.G., Eds.; WILEY-VCH Verlag GmbH & Co. KGaA: Weinheim, Germany, 2004; Chapter 7, pp. 101–121.
9. Contreras, R.H.; Ferraro, M.B.; de Azúa, M.C.R.; Aucar, G.A. Brief account of nonrelativistic theory of NMR parameters. In *High Resolution NMR Spectroscopy. Understanding Molecules and Their Electronic Structures*, 1st ed.; Contreras, R.H., Ed.; Elsevier B.V.: London, UK, 2013; Volume 3, Chapter 2, pp. 9–39.
10. Contreras, R.H.; Tormena, C.F.; Ducati, L.C. Transmission mechanisms of the Fermi-contact term of spin-spin couplings. In *High Resolution NMR Spectroscopy. Understanding Molecules and Their Electronic Structures*, 1st ed.; Contreras, R.H., Ed.; Elsevier B.V.: London, UK, 2013; Volume 3, Chapter 8, pp. 245–284.
11. Aucar, G.A.; Romero, R.H.; Maldonado, A.F. Polarization propagators: A powerful theoretical tool for a deeper understanding of NMR spectroscopic parameters. *Int. Rev. Phys. Chem.* **2010**, *29*, 1–64. [[CrossRef](#)]
12. Aucar, G.A.; de Azúa, M.C.R.; Giribet, C.G. The polarization propagator approach as a tool to study electronic molecular structures from high-resolution NMR parameters. In *High Resolution NMR Spectroscopy. Understanding Molecules and Their Electronic Structures*, 1st ed.; Contreras, R.H., Ed.; Elsevier B.V.: London, UK, 2013; Volume 3, Chapter 5, pp. 119–159.
13. Autschbach, J.; Le Guennic, B. Analyzing and Interpreting NMR Spin–Spin Coupling Constants Using Molecular Orbital Calculations. *J. Chem. Educ.* **2007**, *84*, 156–171. [[CrossRef](#)]
14. Autschbach, J. The Calculation of NMR Parameters in Transition Metal Complexes. In *Principles and Applications of Density Functional Theory in Inorganic Chemistry I, Structure and Bonding*, 1st ed.; Kaltsoyannis, N., McGrady, J.E., Eds.; Springer: Berlin/Heidelberg, Germany, 2004; Volume 112, pp. 1–48. [[CrossRef](#)]
15. Xiao, Y.; Liu, W.; Autschbach, J. Relativistic Theories of NMR Shielding. In *Handbook of Relativistic Quantum Chemistry*, 1st ed.; Liu, W., Ed.; Springer: Berlin/Heidelberg, Germany, 2015; pp. 1–33. [[CrossRef](#)]
16. Autschbach, J. Calculating NMR Chemical Shifts and J-Couplings for Heavy Element Compounds. In *Encyclopedia of Analytical Chemistry: Applications, Theory and Instrumentation, Nuclear Magnetic Resonance and Electron Spin Resonance Spectroscopy*, 1st ed.; John Wiley & Sons, Ltd.: Hoboken, NJ, USA, 2014; pp. 1–14. [[CrossRef](#)]
17. Faber, R.; Kaminsky, J.; Sauer, S.P.A. Rovibrational and Temperature Effects in Theoretical Studies of NMR Parameters. In *Gas Phase NMR*, 1st ed.; Jackowski, K., Jaszuński, M., Eds.; Royal Society of Chemistry: London, UK, 2016; Volume 6, Chapter 7, pp. 218–266. [[CrossRef](#)]

18. Lazzeretti, P. Electronic current densities induced by magnetic fields and nuclear magnetic dipoles: Theory and computation of NMR spectral parameters. In *High Resolution NMR Spectroscopy. Understanding Molecules and Their Electronic Structures*, 1st ed.; Contreras, R.H., Ed.; Elsevier B. V.: London, UK, 2013; Volume 3, Chapter 7, pp. 209–243.
19. Cremer, D.; Gräfenstein, J. Calculation and analysis of NMR spin-spin coupling constants. *Phys. Chem. Chem. Phys.* **2007**, *9*, 2791–2816. [[CrossRef](#)] [[PubMed](#)]
20. De la Vega, J.M.G.; Fabián, J.S. Analysis of Contributions to Spin-Spin Coupling Constants by the Natural J-Coupling Method. In *High Resolution NMR Spectroscopy. Understanding Molecules and Their Electronic Structures*, 1st ed.; Contreras, R.H., Ed.; Elsevier B. V.: London, UK, 2013; Volume 3, Chapter 6, pp. 161–207.
21. Rusakova, I.L. Quantum Chemical Approaches to the Calculation of NMR Parameters: From Fundamentals to Recent Advances. *Magnetochemistry* **2022**, *8*, 50. [[CrossRef](#)]
22. Rusakova, I.L.; Rusakov, Y.Y. Quantum chemical calculations of <sup>77</sup>Se and <sup>125</sup>Te nuclear magnetic resonance spectral parameters and their structural applications. *Magn. Reson. Chem.* **2021**, *59*, 359–407. [[CrossRef](#)] [[PubMed](#)]
23. Rusakova, I.L.; Rusakov, Y.Y.; Krivdin, L.B. Theoretical grounds of relativistic methods for calculation of spin–spin coupling constants in nuclear magnetic resonance spectra. *Russ. Chem. Rev.* **2016**, *85*, 356–426. [[CrossRef](#)]
24. Rusakov, Y.Y.; Krivdin, L.B. Modern quantum chemical methods for calculating spin–spin coupling constants: Theoretical basis and structural applications in chemistry. *Russ. Chem. Rev.* **2013**, *82*, 99–130. [[CrossRef](#)]
25. Mulder, F.A.A.; Filatov, M. NMR chemical shift data and ab initio shielding calculations: Emerging tools for protein structure determination. *Chem. Soc. Rev.* **2010**, *39*, 578–590. [[CrossRef](#)]
26. Pyykkö, P. Theory of NMR parameters. From Ramsey to Relativity, 1953 to 1983. In *Calculation of NMR and EPR Parameters. Theory and Applications*, 1st ed.; Kaupp, M., Bühl, M., Malkin, V.G., Eds.; WILEY-VCH Verlag GmbH & Co. KGaA: Weinheim, Germany, 2004; Chapter 2, pp. 7–19.
27. Facelli, J.C. Chemical shift tensors: Theory and application to molecular structural problems. *Prog. Nucl. Magn. Reson.* **2011**, *58*, 176–201. [[CrossRef](#)]
28. Webb, G.A.; Jameson, C.J.; De Dios, A.C. Theoretical and physical aspects of nuclear shielding. In *Nuclear Magnetic Resonance*, 1st ed.; Webb, G.A., Ed.; Royal Society of Chemistry: London, UK, 2003; Volume 32, pp. 43–74. [[CrossRef](#)]
29. Ebraheem, K.A.K.; Webb, G.A. Semi-empirical calculations of the chemical shifts of nuclei other than protons. *Prog. Nucl. Magn. Reson.* **1977**, *11*, 149–181. [[CrossRef](#)]
30. O'Reilly, D.E. Chapter 1 Chemical shift calculations. *Prog. Nucl. Magn. Reson.* **1967**, *2*, 1–61. [[CrossRef](#)]
31. Vaara, J.; Jokisaari, J.; Wasylishen, R.E.; Bryce, D.L. Spin–spin coupling tensors as determined by experiment and computational chemistry. *Prog. Nucl. Magn. Reson.* **2002**, *41*, 233–304. [[CrossRef](#)]
32. Murrell, J.N. Chapter 1 The theory of nuclear spin-spin coupling in high resolution NMR spectroscopy. *Prog. Nucl. Magn. Reson.* **1970**, *6*, 1–60. [[CrossRef](#)]
33. Jameson, C.J. Parameters, Calculation of Nuclear Magnetic Resonance. In *Encyclopedia of Analytical Chemistry: Applications, Theory and Instrumentation, Nuclear Magnetic Resonance and Electron Spin Resonance Spectroscopy*, 1st ed.; John Wiley & Sons, Ltd.: Hoboken, NJ, USA, 2014; pp. 1–38. [[CrossRef](#)]
34. Pyykkö, P. Relativistic effects in structural chemistry. *Chem. Rev.* **1988**, *88*, 563–594. [[CrossRef](#)]
35. Nomura, Y.; Takeuchi, Y.; Nakagawa, N. Substituent effects in aromatic proton NMR spectra. III substituent effects caused by halogens. *Tetrahedron Lett.* **1969**, *10*, 639–642. [[CrossRef](#)]
36. Vicha, J.; Novotný, J.; Komorovsky, S.; Straka, M.; Kaupp, M.; Marek, R. Relativistic Heavy-Neighbor-Atom Effects on NMR Shifts: Concepts and Trends Across the Periodic Table. *Chem. Rev.* **2020**, *120*, 7065–7103. [[CrossRef](#)] [[PubMed](#)]
37. Vicha, J.; Komorovsky, S.; Repisky, M.; Marek, R.; Straka, M. Relativistic Spin–Orbit Heavy Atom on the Light Atom NMR Chemical Shifts: General Trends Across the Periodic Table Explained. *J. Chem. Theory Comput.* **2018**, *14*, 3025–3039. [[CrossRef](#)] [[PubMed](#)]
38. Xue, Z.-L.; Cook, T.M.; Lamb, A.C. Trends in NMR chemical shifts of d0 transition metal compounds. *J. Organomet. Chem.* **2017**, *852*, 74–93. [[CrossRef](#)]
39. Ehlers, A.W.; Ruiz-Morales, Y.; Baerends, E.J.; Ziegler, T. Dissociation Energies, Vibrational Frequencies, and <sup>13</sup>C NMR Chemical Shifts of the 18-Electron Species [M(CO)<sub>6</sub>]<sub>n</sub> (M = Hf–Ir, Mo, Tc, Ru, Cr, Mn, Fe). A Density Functional Study. *Inorg. Chem.* **1997**, *36*, 5031–5036. [[CrossRef](#)]
40. Kaupp, M.; Malkin, V.G.; Makina, O.L.; Salahub, D.R. Scalar Relativistic Effects on <sup>17</sup>O NMR Chemical Shifts in Transition-Metal Oxo Complexes. An ab Initio ECP/DFT Study. *J. Am. Chem. Soc.* **1995**, *117*, 1851–1852. [[CrossRef](#)]
41. Novotny, J.; Vicha, J.; Bora, P.L.; Repisky, M.; Straka, M.; Komorovsky, S.; Marek, R. Linking the Character of Metal-Ligand Bond to the Ligand NMR Shielding in Transition-Metal Complexes: NMR Contributions from Spin-Orbit Coupling. *J. Chem. Theory Comput.* **2017**, *13*, 3586–3601. [[CrossRef](#)] [[PubMed](#)]
42. Samultsev, D.O.; Semenov, V.A.; Rusakova, I.L.; Krivdin, L.B. Four-Component Relativistic Calculations of NMR Shielding Constants of the Transition Metal Complexes—Part 2: Nitrogen-Coordinated Complexes of Cobalt. *Int. J. Mol. Sci.* **2022**, *23*, 13178. [[CrossRef](#)]
43. Bora, P.L.; Novotny, J.; Ruud, K.; Komorovsky, S.; Marek, R. Electron-Spin Structure and Metal-Ligand Bonding in Open-Shell Systems from Relativistic EPR and NMR: A Case Study of Square-Planar Iridium Catalysts. *J. Chem. Theory Comput.* **2019**, *15*, 201–214. [[CrossRef](#)]

44. Kaupp, M.; Malkina, O.L. Density functional analysis of  $^{13}\text{C}$  and  $^1\text{H}$  chemical shifts and bonding in mercurimethanes and organomercury hydrides: The role of scalar relativistic, spinorbit, and substituent effects. *J. Chem. Phys.* **1998**, *108*, 3648–3659. [[CrossRef](#)]
45. Wodyński, A.; Gryff-Keller, A.; Pecul, M. The Influence of a Presence of a Heavy Atom on  $^{13}\text{C}$  Shielding Constants in Organomercury Compounds and Halogen Derivatives. *J. Chem. Theory Comput.* **2013**, *9*, 1909–1917. [[CrossRef](#)]
46. Hrobárik, P.; Hrobáriková, V.; Meier, F.; Repiský, M.; Komorovský, S.; Kaupp, M. Relativistic Four-Component DFT Calculations of  $^1\text{H}$  NMR Chemical Shifts in Transition-Metal Hydride Complexes: Unusual High-Field Shifts Beyond the Buckingham–Stephens Model. *Phys. Chem. A* **2011**, *115*, 5654–5659. [[CrossRef](#)] [[PubMed](#)]
47. Greif, A.H.; Hrobárik, P.; Hrobáriková, V.; Arbuznikov, A.V.; Autschbach, J.; Kaupp, M. A Relativistic Quantum-Chemical Analysis of the trans Influence on  $^1\text{H}$  NMR Hydride Shifts in Square-Planar Platinum(II) Complexes. *Inorg. Chem.* **2015**, *54*, 15. [[CrossRef](#)] [[PubMed](#)]
48. Rocchigiani, L.; Fernandez-Cestau, J.; Chambrier, I.; Hrobárik, P.; Bochmann, M. Unlocking Structural Diversity in Gold(III) Hydrides: Unexpected Interplay of cis/trans-Influence on Stability, Insertion Chemistry, and NMR Chemical Shifts. *J. Am. Chem. Soc.* **2018**, *140*, 8287–8302. [[CrossRef](#)] [[PubMed](#)]
49. Bagno, A.; Saielli, G. Relativistic DFT Calculations of the NMR Properties and Reactivity of Transition Metal Methane Sigma-Complexes: Insights on C-H Bond Activation. *Phys. Chem. Chem. Phys.* **2011**, *13*, 4285–4291. [[CrossRef](#)]
50. Vícha, J.; Novotný, J.; Straka, M.; Repisky, M.; Ruud, K.; Komorovsky, S.; Marek, R. Structure, solvent, and relativistic effects on the NMR chemical shifts in square-planar transitionmetal complexes: Assessment of DFT approaches. *Phys. Chem. Chem. Phys.* **2015**, *17*, 24944–24955. [[CrossRef](#)]
51. Vícha, J.; Straka, M.; Munzarová, M.L.; Marek, R. Mechanism of Spin–Orbit Effects on the Ligand NMR Chemical Shift in Transition-Metal Complexes: Linking NMR to EPR. *J. Chem. Theory Comput.* **2014**, *10*, 1489–1499. [[CrossRef](#)]
52. Greif, A.H.; Hrobárik, P.; Kaupp, M. Insights into trans-Ligand and Spin-Orbit Effects on Electronic Structure and Ligand NMR Shifts in Transition-Metal Complexes. *Chem. Eur. J.* **2017**, *23*, 9790–9803. [[CrossRef](#)]
53. Demissie, T.B.; Kostenko, N.; Komorovsky, S.; Repisky, M.; Isaksson, J.; Bayer, A.; Ruud, K. Experimental and Four-Component Relativistic DFT Studies of Tungsten Carbonyl Complexes. *J. Phys. Org. Chem.* **2015**, *28*, 723–731. [[CrossRef](#)]
54. Pawlak, T.; Munzarová, M.; Pazderski, L.; Marek, R. Validation of Relativistic DFT Approaches to the Calculation of NMR Chemical Shifts in Square-Planar  $\text{Pt}^{2+}$  and  $\text{Au}^{3+}$  Complexes. *J. Chem. Theory Comput.* **2011**, *7*, 3909–3923. [[CrossRef](#)]
55. Greif, A.H.; Hrobárik, P.; Autschbach, J.; Kaupp, M. Giant Spin-Orbit Effects on H-1 and C-13 NMR Shifts for Uranium(VI) Complexes Revisited: Role of the Exchange-Correlation Response Kernel, Bonding Analyses, and New Predictions. *Phys. Chem. Chem. Phys.* **2016**, *18*, 30462–30474. [[CrossRef](#)]
56. Hrobárik, P.; Hrobáriková, V.; Greif, A.H.; Kaupp, M. Giant Spin-Orbit Effects on NMRShifts in Diamagnetic Actinide Complexes: Guiding the Search of Uranium(VI) Hydride Complexes in the Correct Spectral Range. *Angew. Chem. Int. Ed.* **2012**, *51*, 10884–10888. [[CrossRef](#)] [[PubMed](#)]
57. Gowda, V.; Laitinen, R.S.; Telkki, V.-V.; Larsson, A.-C.; Antzutkin, O.N.; Lantto, P. DFT Calculations in the Assignment of Solid-State NMR and Crystal Structure Elucidation of a Lanthanum-(III) Complex with Dithiocarbamate and Phenanthroline. *Dalton Trans.* **2016**, *45*, 19473–19484. [[CrossRef](#)] [[PubMed](#)]
58. Kaupp, M.; Schleyer, P.v.R.; Stoll, H.; Preuss, H. Pseudopotential Approaches to Ca, Sr, and Ba Hydrides. Why Are Some Alkaline Earth MX<sub>2</sub> Compounds Bent? *J. Chem. Phys.* **1991**, *94*, 1360–1366. [[CrossRef](#)]
59. Nicol, A.T.; Vaughan, R.W. Proton Chemical Shift Tensors of Alkaline Earth Hydrides. *J. Chem. Phys.* **1978**, *69*, 5211–5213. [[CrossRef](#)]
60. Morishima, I.; Endo, K.; Yonezawa, T. Effect of the heavy atom on the nuclear shielding constant. I. The proton chemical shifts in hydrogen halides. *J. Chem. Phys.* **1973**, *59*, 3356–3364. [[CrossRef](#)]
61. Cheremisin, A.A.; Schastneva, P.V. Effects of spin-orbital interactions on  $^{13}\text{C}$  NMR chemical shifts in halogen-substituted methanes. *J. Magn. Reson.* **1969**, *40*, 459–468. [[CrossRef](#)]
62. Pyper, N.C. The relativistic theory of the chemical shift. *Chem. Phys. Lett.* **1983**, *96*, 204–210. [[CrossRef](#)]
63. Pyper, N.C. Exact relativistic analogues of the non-relativistic hyperfine structure operators. *Mol. Phys.* **1988**, *64*, 933–961. [[CrossRef](#)]
64. Pyper, N.C. Relativistic theory of nuclear shielding in one-electron atoms 1. Theoretical foundations and first-order terms. *Mol. Phys.* **1999**, *97*, 381–390. [[CrossRef](#)]
65. Pyper, N.C.; Zhang, Z.C. Relativistic theory of nuclear shielding in one-electron atoms 2. Analytical and numerical results. *Mol. Phys.* **1999**, *97*, 391–413. [[CrossRef](#)]
66. Zhang, Z.C.; Webb, G.A. On the relativistic molecular orbital theory of diamagnetism and NMR chemical shifts. *J. Mol. Struct. Theochem.* **1983**, *104*, 439–444. [[CrossRef](#)]
67. Pyykkö, P. On the relativistic theory of NMR chemical shifts. *Chem. Phys.* **1983**, *74*, 1–7. [[CrossRef](#)]
68. Pyykkö, P.; Görling, A.; Rösch, N. A transparent interpretation of the relativistic contribution to the N.M.R. ‘heavy atom chemical shift’. *Mol. Phys.* **1987**, *61*, 195–205. [[CrossRef](#)]
69. Nakatsuji, H.; Takashima, H.; Hada, M. Spin-orbit effect on the magnetic shielding constant using the ab initio UHF method. *Chem. Phys. Lett.* **1995**, *233*, 95–101. [[CrossRef](#)]

70. Kazunaka, E.; Kyonosuke, Y.; Hiroaki, O. Heavy Atom Effect on 14 Group Nuclear Shielding Constant of  $\text{SiX}_4$  and  $\text{CH}_4-n\text{X}_n$  ( $X = \text{Cl, Br, I; } n = 1, 2, 3, 4$ ). *Bull. Chem. Soc. Jpn.* **1995**, *68*, 3341–3345. [[CrossRef](#)]
71. Breit, G. The Effect of Retardation on the Interaction of Two Electrons. *Phys. Rev.* **1929**, *34*, 553–573. [[CrossRef](#)]
72. Mittleman, M.H. Configuration-Space Hamiltonian for Heavy Atoms and Correction to the Breit Interaction. *Phys. Rev. A* **1972**, *5*, 2395–2401. [[CrossRef](#)]
73. Sakurai, J.J. *Advanced Quantum Mechanics*, 1st ed.; Addison-Wesley Publishing Company, Reading: Chicago, IL, USA, 1967; pp. 108–109.
74. Ramsey, N.F. Magnetic shielding of nuclei in molecules. *Phys. Rev.* **1950**, *78*, 699–703. [[CrossRef](#)]
75. London, F. Théorie quantique des courants interatomiques dans les combinaisons aromatiques. *J. Phys. Radium* **1937**, *8*, 397–409. [[CrossRef](#)]
76. Ditchfield, R. Self-consistent perturbation theory of diamagnetism I. A gauge-invariant LCAO method for N.M.R. chemical shifts. *Mol. Phys.* **1974**, *27*, 789–807. [[CrossRef](#)]
77. Quiney, H.M.; Skaane, H.; Grant, I.P. Relativistic, quantum electrodynamic and many-body effects in the water molecule. *Chem. Phys. Lett.* **1998**, *290*, 473–480. [[CrossRef](#)]
78. Quiney, H.M.; Skaane, H.; Grant, I.P. Ab initio relativistic quantum chemistry: Four-components good, two-components bad! *Adv. Quantum Chem.* **1998**, *32*, 1–49. [[CrossRef](#)]
79. Grant, I.P.; Quiney, H.M. Application of relativistic theories and quantum electrodynamics to chemical problems. *Int. J. Quantum Chem.* **2000**, *80*, 283–297. [[CrossRef](#)]
80. Aucar, G.A.; Oddershede, J. Relativistic theory for indirect nuclear spin–spin couplings within the polarization propagator approach. *Int. J. Quantum Chem.* **1993**, *47*, 425–435. [[CrossRef](#)]
81. Aucar, G.A.; Aucar, I.A. Recent developments in absolute shielding scales for NMR spectroscopy. In *Annual Reports on NMR Spectroscopy*, 1st ed.; Webb, G., Ed.; Academic Press: London, UK, 2019; Volume 96, Chapter 3, pp. 77–141.
82. Aucar, G.A.; Maldonado, A.F.; Montero, M.D.A.; Cruz, T.S. Theoretical developments and applications of polarization propagators. *Int. J. Quantum Chem.* **2019**, *119*, e25722. [[CrossRef](#)]
83. Melo, J.I.; de Azua, M.C.R.; Giribet, C.G.; Aucar, G.A.; Provasi, P.F. Relativistic effects on nuclear magnetic shielding constants in  $\text{HX}$  and  $\text{CH}_3\text{X}$  ( $X = \text{Br, I}$ ) based on the linear response within the elimination of small component approach. *J. Chem. Phys.* **2004**, *121*, 6798–6808. [[CrossRef](#)]
84. Gomez, S.S.; Romero, R.H.; Aucar, G.A. Fully relativistic calculation of nuclear magnetic shieldings and indirect nuclear spin-spin couplings in group-15 and -16 hydrides. *J. Chem. Phys.* **2002**, *117*, 7942–7946. [[CrossRef](#)]
85. Maldonado, A.F.; Aucar, G.A.; Melo, J.I. Core-dependent and ligand-dependent relativistic corrections to the nuclear magnetic shieldings in  $\text{MH}_4-n\text{Y}_n$  ( $n = 0-4$ ;  $M = \text{Si, Ge, Sn}$ , and  $Y = \text{H, F, Cl, Br, I}$ ) model compounds. *J. Mol. Model.* **2014**, *20*, 2417. [[CrossRef](#)]
86. Aucar, G.A.; Saue, T.; Visscher, L.; Jensen, H.J.A. On the origin and contribution of the diamagnetic term in four-component relativistic calculations of magnetic properties. *J. Chem. Phys.* **1999**, *110*, 6208–6218. [[CrossRef](#)]
87. Maldonado, A.F.; Aucar, G.A. The UKB prescription and the heavy atom effects on the nuclear magnetic shielding of vicinal heavy atoms. *Phys. Chem. Chem. Phys.* **2009**, *11*, 5615–5627. [[CrossRef](#)]
88. Kozioł, K.; Aucar, I.A.; Aucar, G.A. Relativistic and QED effects on NMR magnetic shielding constant of neutral and ionized atoms and diatomic molecules. *J. Chem. Phys.* **2019**, *150*, 184301. [[CrossRef](#)] [[PubMed](#)]
89. Iliáš, M.; Saue, T.; Enevoldsen, T.; Jensen, H.J.A. Gauge origin independent calculations of nuclear magnetic shieldings in relativistic four-component theory. *J. Chem. Phys.* **2009**, *131*, 124119. [[CrossRef](#)]
90. Olejniczak, M.; Bast, R.; Saue, T.; Pecul, M. A simple scheme for magnetic balance in four-component relativistic Kohn-Sham calculations of nuclear magnetic resonance shielding constants in a Gaussian basis. *J. Chem. Phys.* **2012**, *136*, 014108. [[CrossRef](#)] [[PubMed](#)]
91. Cheng, L.; Xiao, Y.; Liu, W. Four-component relativistic theory for nuclear magnetic shielding: Magnetically balanced gauge-including atomic orbitals. *J. Chem. Phys.* **2009**, *131*, 244113. [[CrossRef](#)]
92. Vaara, J.; Pyykkö, P. Relativistic, nearly basis-set-limit nuclear magnetic shielding constants of the rare gases He–Rn: A way to absolute nuclear magnetic resonance shielding scales. *J. Chem. Phys.* **2003**, *118*, 2973–2976. [[CrossRef](#)]
93. Antušek, A.; Pecul, M.; Sadlej, J. Relativistic calculation of NMR properties of  $\text{XeF}_2$ ,  $\text{XeF}_4$  and  $\text{XeF}_6$ . *Chem. Phys. Lett.* **2006**, *427*, 281–288. [[CrossRef](#)]
94. Schnack-Petersen, A.K.; Simmermacher, M.; Fasshauer, E.; Jensen, H.J.A.; Sauer, S.P.A. The second-order-polarization-propagator-approximation (SOPPA) in a four-component spinor basis. *J. Chem. Phys.* **2020**, *152*, 134113. [[CrossRef](#)]
95. Oddershede, J. Response and propagator methods. In *Methods in Computational Molecular Physics*, 1st ed.; Wilson, S., Diercksen, G.H.F., Eds.; Plenum Press: New York, NY, USA, 1992; Chapter 11, pp. 303–324.
96. Enevoldsen, T.; Oddershede, J.; Sauer, S.P.A. Correlated calculations of indirect nuclear spin-spin coupling constants using second-order polarization propagator approximations: SOPPA and SOPPA(CCSD). *Theor. Chem. Acc.* **1998**, *100*, 275–284. [[CrossRef](#)]
97. Malkin, V.G.; Malkina, O.L.; Salahub, D.R. Spin-orbit correction to NMR shielding constants from density functional theory. *Chem. Phys. Lett.* **1996**, *261*, 335–345. [[CrossRef](#)]
98. Kutzelnigg, W.; Fleischer, U.; Schindler, M. The IGLO-Method: Ab-initio Calculation and Interpretation of NMR Chemical Shifts and Magnetic Susceptibilities. In *Deuterium and Shift Calculation. NMR Basic Principles and Progress*, 1st ed.; Diehl, P., Fluck, E., Gunther, H., Kosfeld, R., Seelig, J., Eds.; Springer: Berlin/Heidelberg, Germany, 1990; Volume 23, pp. 165–262. [[CrossRef](#)]

99. Komorovsky, S.; Repisky, M.; Malkina, O.L.; Malkin, V.G. Fully relativistic calculations of NMR shielding tensors using restricted magnetically balanced basis and gauge including atomic orbitals. *J. Chem. Phys.* **2010**, *132*, 154101. [[CrossRef](#)]
100. Komorovsky, S.; Repisky, M.; Malkina, O.L.; Malkin, V.G.; Ondik, I.M.; Kaupp, M. A fully relativistic method for calculation of nuclear magnetic shielding tensors with a restricted magnetically balanced basis in the framework of the matrix Dirac–Kohn–Sham equation. *J. Chem. Phys.* **2008**, *128*, 104101. [[CrossRef](#)] [[PubMed](#)]
101. Xiao, Y.; Peng, D.; Liu, W. Exact two-component relativistic theory for nuclear magnetic resonance parameters. *J. Chem. Phys.* **2007**, *126*, 081101. [[CrossRef](#)] [[PubMed](#)]
102. Xiao, Y.; Liu, W.; Cheng, L.; Peng, D. Four-component relativistic theory for nuclear magnetic shielding constants: Critical assessments of different approaches. *J. Chem. Phys.* **2007**, *126*, 214101. [[CrossRef](#)] [[PubMed](#)]
103. Peng, D.; Reiher, M. Exact decoupling of the relativistic Fock operator. *Theor. Chem. Acc.* **2012**, *131*, 1081. [[CrossRef](#)]
104. Kaneko, H.; Hada, M.; Nakajima, T.; Nakatsuji, H. Spin-orbit effect on the magnetic shielding constant using the ab initio UHF method: Tin tetrahalides. *Chem. Phys. Lett.* **1996**, *261*, 1–6. [[CrossRef](#)]
105. Ishikawa, Y.; Nakajima, T.; Hada, M.; Nakatsuji, H. Relativistic theory of the magnetic shielding constant: A Dirac–Fock finite perturbation study. *Chem. Phys. Lett.* **1998**, *283*, 119–124. [[CrossRef](#)]
106. Fukui, H.; Baba, T.; Inomata, H. Calculation of nuclear magnetic shieldings. X. Relativistic effects. *J. Chem. Phys.* **1996**, *105*, 3175–3186. [[CrossRef](#)]
107. Fukui, H.; Baba, T.; Inomata, H. Erratum: Calculation of nuclear magnetic shieldings. X. Relativistic effects. *J. Chem. Phys.* **1996**, *105*, 3175, Erratum in *J. Chem. Phys.* **1997**, *106*, 2987–2987. [[CrossRef](#)]
108. Fukui, H.; Baba, T. Calculation of nuclear magnetic shieldings. XII. Relativistic no-pair equation. *J. Chem. Phys.* **1998**, *108*, 3854–3862. [[CrossRef](#)]
109. Ballard, C.C.; Hada, M.; Kaneko, H.; Nakatsuji, H. Relativistic study of nuclear magnetic shielding constants: Hydrogen halides. *Chem. Phys. Lett.* **1996**, *254*, 170–178. [[CrossRef](#)]
110. Sucher, J. Foundations of the relativistic theory of many-electron atoms. *Phys. Rev. A* **1980**, *22*, 348–362. [[CrossRef](#)]
111. Hess, B.A. Applicability of the no-pair equation with free-particle projection operators to atomic and molecular structure calculations. *Phys. Rev. A* **1985**, *32*, 756–763. [[CrossRef](#)]
112. Hess, B.A. Relativistic electronic-structure calculations employing a two-component no-pair formalism with external-field projection operators. *Phys. Rev.* **1986**, *33*, 3742–3748. [[CrossRef](#)] [[PubMed](#)]
113. Fukuda, R.; Hada, M.; Nakatsuji, H. Quasirelativistic theory for the magnetic shielding constant. I. Formulation of Douglas–Kroll–Hess transformation for the magnetic field and its application to atomic systems. *J. Chem. Phys.* **2003**, *118*, 1015–1026. [[CrossRef](#)]
114. Fukuda, R.; Hada, M.; Nakatsuji, H. Quasirelativistic theory for magnetic shielding constants. II. Gauge-including atomic orbitals and applications to molecules. *J. Chem. Phys.* **2003**, *118*, 1027–1035. [[CrossRef](#)]
115. Wan, J.; Fukuda, R.; Hada, M.; Nakatsuji, H. Quasi-Relativistic Study of <sup>199</sup>Hg Nuclear Magnetic Shielding Constants of Dimethylmercury, Disilylmercury and Digermylmercury. *J. Phys. Chem. A* **2001**, *105*, 128–133. [[CrossRef](#)]
116. Hada, M.; Wan, J.; Fukuda, R.; Nakatsuji, H. Quasirelativistic study of <sup>125</sup>Te nuclear magnetic shielding constants and chemical shifts. *J. Comput. Chem.* **2001**, *22*, 1502–1508. [[CrossRef](#)]
117. Wolff, S.K.; Ziegler, T. Calculation of DFT-GIAO NMR shifts with the inclusion of spin-orbit coupling. *J. Chem. Phys.* **1998**, *109*, 895–905. [[CrossRef](#)]
118. Schreckenbach, G.; Ziegler, T. Calculation of NMR Shielding Tensors Using Gauge-Including Atomic Orbitals and Modern Density Functional Theory. *J. Phys. Chem.* **1995**, *99*, 606–611. [[CrossRef](#)]
119. Schreckenbach, G.; Ziegler, T. The calculation of NMR shielding tensors based on density functional theory and the frozen-core approximation. *Int. J. Quantum Chem.* **1996**, *60*, 753–766. [[CrossRef](#)]
120. Vaara, J.; Ruud, K.; Vahtras, O.; Ågren, H.; Jokissari, J. Quadratic response calculations of the electronic spin-orbit contribution to nuclear shielding tensors. *J. Chem. Phys.* **1998**, *109*, 1212–1222. [[CrossRef](#)]
121. Vaara, J.; Ruud, K.; Vahtras, O. Second- and third-order spin-orbit contributions to nuclear shielding tensors. *J. Chem. Phys.* **1999**, *111*, 2900–2909. [[CrossRef](#)]
122. Cramer, C.J. *Essentials of Computational Chemistry, Theories and Models*, 2nd ed.; John Wiley & Sons Ltd.: Chichester, UK, 2004; pp. 1–596.
123. Jensen, F. *Introduction to Computational Chemistry*, 2nd ed.; John Wiley & Sons Ltd.: Chichester, UK, 2007; pp. 1–599.
124. Vaara, J.; Malkina, O.L.; Stoll, H.; Malkin, V.G.; Kaupp, M. Study of relativistic effects on nuclear shieldings using density-functional theory and spin-orbit pseudopotentials. *J. Chem. Phys.* **2001**, *114*, 61–71. [[CrossRef](#)]
125. Vaara, J.; Manninen, P.; Lantto, P. Perturbational and ECP calculation of relativistic effects in NMR shielding and spin-spin coupling. In *Calculation of NMR and EPR Parameters. Theory and Applications*, 1st ed.; Kaupp, M., Bühl, M., Malkin, V.G., Eds.; WILEY-VCH Verlag GmbH & Co. KGaA: Weinheim, Germany, 2004; Chapter 13, pp. 209–226.
126. Manninen, P.; Lantto, P.; Vaara, J.; Ruud, K. Perturbational ab initio calculations of relativistic contributions to nuclear magnetic resonance shielding tensors. *J. Chem. Phys.* **2003**, *119*, 2623–2637. [[CrossRef](#)]
127. Manninen, P. Breit-Pauli Hamiltonian and Molecular Magnetic Resonance Properties. Ph.D. Thesis, Department of Physical Sciences, University of Oulu, Oulu, Finland, 2004.
128. Manninen, P.; Ruud, K.; Lantto, P.; Vaara, J. Leading-order relativistic effects on nuclear magnetic resonance shielding tensors. *J. Chem. Phys.* **2005**, *122*, 114107, Erratum in *J. Chem. Phys.* **2006**, *124*, 149901. [[CrossRef](#)]

129. Jaszuński, M.; Ruud, K. Nuclear magnetic resonance shielding constants in XH<sub>4</sub> group XIV hydrides. *Mol. Phys.* **2006**, *104*, 2139–2148. [[CrossRef](#)]
130. Kudo, K.; Fukui, H. Calculation of nuclear magnetic shieldings using an analytically differentiated relativistic shielding formula. *J. Chem. Phys.* **2005**, *123*, 114102. [[CrossRef](#)]
131. Jensen, G.; Hess, B.A. Revision of the Douglas-Kroll transformation. *Phys. Rev. A* **1989**, *39*, 6016–6017. [[CrossRef](#)]
132. Barysz, M.; Sadlej, A.J. Two-component methods of relativistic quantum chemistry: From the Douglas-Kroll approximation to the exact two-component formalism. *J. Mol. Struct. THEOCHEM* **2001**, *573*, 181–200. [[CrossRef](#)]
133. Barysz, M.; Sadlej, A.J. Infinite-order two-component theory for relativistic quantum chemistry. *J. Chem. Phys.* **2002**, *116*, 2696–2704. [[CrossRef](#)]
134. Kedziera, D.; Barysz, M. Two-component relativistic methods for the heaviest elements. *J. Chem. Phys.* **2004**, *121*, 6719–6727. [[CrossRef](#)] [[PubMed](#)]
135. Kedziera, D.; Barysz, M. Non-iterative approach to the infinite-order two-component (IOTC) relativistic theory and the non-symmetric algebraic Riccati equation. *Chem. Phys. Lett.* **2007**, *446*, 176–181. [[CrossRef](#)]
136. Sun, Q.; Xiao, Y.; Liu, W. Exact Two-Component Relativistic Theory for NMR Parameters: General Formulation and Pilot Application. *J. Chem. Phys.* **2012**, *137*, 174105–174106. [[CrossRef](#)] [[PubMed](#)]
137. Autschbach, J. Relativistic calculations of magnetic resonance parameters: Background and some recent developments. *Phil. Trans. R. Soc. A* **2014**, *372*, 20120489. [[CrossRef](#)] [[PubMed](#)]
138. Dyal, K.G. Interfacing relativistic and nonrelativistic methods. I. Normalized elimination of the small component in the modified Dirac equation. *J. Chem. Phys.* **1997**, *106*, 9618–9626. [[CrossRef](#)]
139. Dyal, K.G. Interfacing relativistic and nonrelativistic methods. II. Investigation of a low-order approximation. *J. Chem. Phys.* **1998**, *109*, 4201–4208. [[CrossRef](#)]
140. Dyal, K.G.; Enevoldsen, T. Interfacing relativistic and nonrelativistic methods. III. Atomic 4-spinor expansions and integral approximations. *J. Chem. Phys.* **1999**, *111*, 10000–10007. [[CrossRef](#)]
141. Dyal, K.G. Interfacing relativistic and nonrelativistic methods. IV. One- and two-electron scalar approximations. *J. Chem. Phys.* **2001**, *115*, 9136–9143. [[CrossRef](#)]
142. Dyal, K.G. A systematic sequence of relativistic approximations. *J. Comput. Chem.* **2002**, *23*, 786–793. [[CrossRef](#)]
143. Filatov, M.; Cremer, D. Representation of the exact relativistic electronic Hamiltonian within the regular approximation. *J. Chem. Phys.* **2003**, *119*, 11526–11540. [[CrossRef](#)]
144. Filatov, M.; Cremer, D. Connection between the regular approximation and the normalized elimination of the small component in relativistic quantum theory. *J. Chem. Phys.* **2005**, *122*, 064104. [[CrossRef](#)] [[PubMed](#)]
145. Zou, W.; Filatov, M.; Cremer, D. An improved algorithm for the normalized elimination of the small-component method. *Theor. Chem. Acc.* **2011**, *130*, 633–644. [[CrossRef](#)]
146. Seino, J.; Hada, M. Magnetic shielding constants calculated by the infinite-order Douglas-Kroll-Hess method with electron-electron relativistic corrections. *J. Chem. Phys.* **2010**, *132*, 174105. [[CrossRef](#)] [[PubMed](#)]
147. Wolff, S.K.; Ziegler, T.; van Lenthe, E.; Baerends, E.J. Density functional calculations of nuclear magnetic shieldings using the zeroth-order regular approximation (ZORA) for relativistic effects: ZORA nuclear magnetic resonance. *J. Chem. Phys.* **1999**, *110*, 7689–7698. [[CrossRef](#)]
148. Chang, C.; Pelissier, M.; Durand, M. Regular Two-Component Pauli-like effective Hamiltonians in Dirac theory. *Phys. Scr.* **1986**, *34*, 394–404. [[CrossRef](#)]
149. van Lenthe, E.; Baerends, E.J.; Snijders, J.G. Relativistic regular two-component Hamiltonians. *J. Chem. Phys.* **1993**, *99*, 4597–4610. [[CrossRef](#)]
150. Hamaya, S.; Maeda, H.; Funaki, M.; Fukui, H. Relativistic calculation of nuclear magnetic shielding tensor using the regular approximation to the normalized elimination of the small component. III. Introduction of gauge-including atomic orbitals and a finite-size nuclear model. *J. Chem. Phys.* **2008**, *129*, 224103. [[CrossRef](#)]
151. Douglas, M.; Kroll, N.M. Quantum electrodynamical corrections to the fine structure of helium. *Ann. Phys.* **1974**, *82*, 89–155. [[CrossRef](#)]
152. Reiher, M. Douglas-Kroll-Hess Theory: A relativistic electrons-only theory for chemistry. *Theor. Chem. Acc.* **2006**, *116*, 241–252. [[CrossRef](#)]
153. Nakajima, T.; Hirao, K. The higher-order Douglas-Kroll transformation. *J. Chem. Phys.* **2000**, *113*, 7786–7789. [[CrossRef](#)]
154. Nakajima, T.; Hirao, K. Numerical illustration of third-order Douglas-Kroll method: Atomic and molecular properties of superheavy element 112. *Chem. Phys. Lett.* **2000**, *329*, 511–516. [[CrossRef](#)]
155. Wolf, A.; Reiher, M.; Hess, B.A. The generalized Douglas-Kroll transformation. *J. Chem. Phys.* **2002**, *117*, 9215–9226. [[CrossRef](#)]
156. Van Wüllen, C. Relation between different variants of the generalized Douglas-Kroll transformation through sixth order. *J. Chem. Phys.* **2004**, *120*, 7307–7313. [[CrossRef](#)]
157. Filatov, M.; Cremer, D. Calculation of indirect nuclear spin-spin coupling constants within the regular approximation for relativistic effects. *J. Chem. Phys.* **2004**, *120*, 11407–11422. [[CrossRef](#)] [[PubMed](#)]
158. Dyal, K.G.; van Lenthe, E. Relativistic regular approximations revisited: An infinite-order relativistic approximation. *J. Chem. Phys.* **1999**, *111*, 1366–1372. [[CrossRef](#)]

159. Wu, W.; Rehe, D.; Hrobárik, P.; Kornienko, A.Y.; Emge, T.J.; Brennan, J.G. Molecular Thorium Compounds with Dichalcogenide Ligands: Synthesis, Structure,  $^{77}\text{Se}$  NMR Study, and Thermolysis. *Inorg. Chem.* **2018**, *57*, 14821–14833. [[CrossRef](#)]
160. Brownridge, S.; Calhoun, L.; Jenkins, H.D.B.; Laitinen, R.S.; Murchie, M.P.; Passmore, J.; Pietikäinen, J.; Rautiainen, J.M.; Sanders, J.C.P.; Schrobilgen, G.J.; et al.  $^{77}\text{Se}$  NMR Spectroscopic, DFT MO, and VBT Investigations of the Reversible Dissociation of Solid  $(\text{Se}_6\text{I}_2)[\text{AsF}_6]_2 \cdot 2\text{SO}_2$  in Liquid  $\text{SO}_2$  to Solutions Containing  $1,4\text{-Se}_6\text{I}_2^{2+}$  in Equilibrium with  $\text{Se}_n^{2+}$  ( $n = 4, 8, 10$ ) and Seven Binary Selenium Iodine Cations: Preliminary Evidence for  $1,1,4,4\text{-Se}_4\text{Br}_4^{2+}$  and  $\text{cyclo-Se}_7\text{Br}^+$ . *Inorg. Chem.* **2009**, *48*, 1938–1959.
161. Ringgold, M.; Rehe, D.; Hrobárik, P.; Kornienko, A.Y.; Emge, T.J.; Brennan, J.G. Thorium Cubanes—Synthesis, Solid-State and Solution Structures, Thermolysis, and Chalcogen Exchange Reactions. *Inorg. Chem.* **2018**, *57*, 7129–7141. [[CrossRef](#)]
162. Rautiainen, J.M.; Way, T.; Schatte, G.; Passmore, J.; Laitinen, R.S.; Suontamo, R.J.; Valkonen, J. A Computational and Experimental Study of the Structures and Raman and  $^{77}\text{Se}$  NMR Spectra of  $\text{SeX}_3^+$  and  $\text{SeX}_2$  ( $X = \text{Cl, Br, I}$ ): FT-Raman Spectrum of  $(\text{SeI}_3)[\text{AsF}_6]$ . *Inorg. Chem.* **2005**, *44*, 1904–1913. [[CrossRef](#)]
163. Melo, J.I.; Ruiz de Azua, M.C.; Giribet, C.G.; Aucar, G.A.; Romero, R.H. Relativistic effects on the nuclear magnetic shielding tensor. *J. Chem. Phys.* **2003**, *118*, 471–486. [[CrossRef](#)]
164. Aucar, G.A.; Melo, J.I.; Aucar, I.A.; Maldonado, A.F. Foundations of the LRESC model for response properties and some applications. *Int. J. Quantum Chem.* **2018**, *118*, e25487. [[CrossRef](#)]
165. Melo, J.I.; Maldonado, A.F.; Aucar, G.A. Performance of the LRESC Model on top of DFT Functionals for Relativistic NMR Shielding Calculations. *J. Chem. Inf. Model.* **2020**, *60*, 722–730. [[CrossRef](#)] [[PubMed](#)]
166. Zapata-Escobar, A.D.; Maldonado, A.F.; Aucar, G.A. The LRESC-Loc Model to Analyze Magnetic Shieldings with Localized Molecular Orbitals. *J. Phys. Chem. A* **2022**, *126*, 9519–9534. [[CrossRef](#)]
167. Visscher, L.; Enevoldsen, T.; Saue, T.; Jensen, H.J.A.; Oddershede, J. Full four-component relativistic calculations of NMR shielding and indirect spin–spin coupling tensors in hydrogen halides. *J. Comput. Chem.* **1999**, *20*, 1262–1273. [[CrossRef](#)]
168. Autschbach, J. Calculation of heavy-nucleus chemical shifts. Relativistic all-electron methods. In *Calculation of NMR and EPR Parameters. Theory and Applications*, 1st ed.; Kaupp, M., Bühl, M., Malkin, V.G., Eds.; WILEY-VCH Verlag GmbH & Co. KGaA: Weinheim, Germany, 2004; Chapter 14, pp. 227–248.
169. Autschbach, J. Perspective: Relativistic effects. *J. Chem. Phys.* **2012**, *136*, 150902. [[CrossRef](#)] [[PubMed](#)]
170. Autschbach, J. Relativistic Effects on NMR Parameters. In *High Resolution NMR Spectroscopy. Understanding Molecules and Their Electronic Structures*, 1st ed.; Contreras, R.H., Ed.; Elsevier B. V.: London, UK, 2013; Volume 3, Chapter 4, pp. 69–117.
171. Autschbach, J.; Ziegler, T. Relativistic computation of NMR shieldings and spin-spin coupling constants. In *Encyclopedia of Nuclear Magnetic Resonance: Advances in NMR*, 1st ed.; Grant, D.M., Harris, R.K., Eds.; John Wiley and Sons: Chichester, UK, 2002; Volume 9, pp. 306–323.
172. Oprea, C.I. Theoretical Calculations of Heavy Atom Effects in Magnetic Resonance Spectroscopy. Ph.D. Thesis, Theoretical Chemistry School of Biotechnology Royal Institute of Technology, Stockholm, Sweden, 2006.
173. Gómez, S.S.; Romero, R.H.; Aucar, G.A. Relativistic mass-corrections to the heavy atom nuclear magnetic shieldings. Analysis of contributions in terms of localized orbitals. *Chem. Phys. Lett.* **2003**, *367*, 265–269. [[CrossRef](#)]
174. Gómez, S.S.; Melo, J.I.; Romero, R.H.; Aucar, G.A.; Azúa, M.R. Relativistic corrections to the diamagnetic term of the nuclear magnetic shielding: Analysis of contributions from localized orbitals. *J. Chem. Phys.* **2005**, *122*, 064103. [[CrossRef](#)] [[PubMed](#)]
175. Gómez, S.S.; Maldonado, A.; Aucar, G.A. Relativistic effects on the nuclear magnetic shieldings of rare-gas atoms and halogen in hydrogen halides within relativistic polarization propagator theory. *J. Chem. Phys.* **2005**, *123*, 214108. [[CrossRef](#)] [[PubMed](#)]
176. Lantto, P.; Romero, R.H.; Gómez, S.S.; Aucar, G.A.; Vaara, J. Relativistic heavy-atom effects on heavy-atom nuclear shieldings. *J. Chem. Phys.* **2006**, *125*, 184113. [[CrossRef](#)]
177. Melo, J.I.; Maldonado, A.; Aucar, G.A. Relativistic effects on the shielding of  $\text{SnH}_2\text{XY}$  and  $\text{PbH}_2\text{XY}$  ( $X, Y = \text{F, Cl, Br}$  and  $\text{I}$ ) heavy atom-containing molecules. *Theor. Chem. Acc.* **2011**, *129*, 483–494. [[CrossRef](#)]
178. Melo, J.I.; Maldonado, A.; Aucar, G.A. Relativistic effects on nuclear magnetic shieldings of  $\text{CH}_n\text{X}_4-n$  and  $\text{CHXYZ}$  ( $X, Y, Z = \text{H, F, Cl, Br, I}$ ). *J. Chem. Phys.* **2012**, *137*, 214319. [[CrossRef](#)] [[PubMed](#)]
179. Maldonado, A.; Aucar, G.A. Relativistic and Electron-Correlation Effects on the Nuclear Magnetic Resonance Shieldings of Molecules Containing Tin and Lead Atoms. *J. Phys. Chem. A* **2014**, *118*, 7863–7875. [[CrossRef](#)] [[PubMed](#)]
180. Maldonado, A.; Melo, J.I.; Aucar, G.A. Theoretical analysis of NMR shieldings of group-11 metal halides on  $\text{MX}$  ( $M = \text{Cu, Ag, Au}$ ;  $X = \text{H, F, Cl, Br, I}$ ) molecular systems, and the appearance of quasi-instabilities on  $\text{AuF}$ . *Phys. Chem. Chem. Phys.* **2015**, *17*, 25516–25524. [[CrossRef](#)]
181. Gimenez, C.A.; Koziol, K.; Aucar, G.A. Quantum electrodynamics effects on NMR magnetic shielding constants of He-like and Be-like atomic systems. *Phys. Rev. A* **2016**, *93*, 032504. [[CrossRef](#)]
182. Jofré, M.T.; Koziol, K.; Aucar, I.A.; Gaul, K.; Berger, R.; Aucar, G.A. Relativistic and QED corrections to one-bond indirect nuclear spin–spin couplings in  $\text{X}^{22+}$  and  $\text{X}^{32+}$  ions ( $X = \text{Zn, Cd, Hg}$ ). *J. Chem. Phys.* **2022**, *157*, 064103. [[CrossRef](#)]
183. Rusakova, I.L.; Krivdin, L.B. Relativistic effects in the NMR spectra of compounds containing heavy chalcogens. *Mendeleev Commun.* **2018**, *28*, 1–13. [[CrossRef](#)]
184. Rusakova, I.L.; Rusakov, Y.Y. On the heavy atom on light atom relativistic effect in the NMR shielding constants of phosphine tellurides. *Magn. Reson. Chem.* **2019**, *57*, 1071–1083. [[CrossRef](#)]

185. Kaupp, M. Relativistic effects on NMR chemical shifts. In *Relativistic Electronic Structure Theory, Part 2: Applications. Theoretical and Computational Chemistry*, 1st ed.; Schwerdtfeger, P., Ed.; Elsevier B. V.: Amsterdam, The Netherlands, 2004; Volume 14, Chapter 9, pp. 552–597.
186. Kaupp, M.; Malkina, O.L.; Malkin, V.G.; Pyykkö, P. How Do Spin-Orbit-Induced Heavy-Atom Effects on NMR Chemical Shifts Function? Validation of a Simple Analogy to Spin-Spin Coupling by Density Functional Theory (DFT) Calculations on Some Iodo Compounds. *Chem. Eur. J.* **1998**, *4*, 118–126. [[CrossRef](#)]
187. Rusakov, Y.Y.; Rusakova, I.L. Long-range relativistic heavy atom effect on  $^1\text{H}$  NMR chemical shifts of selenium- and tellurium-containing compounds. *Int. J. Quantum Chem.* **2018**, *119*, e25809. [[CrossRef](#)]
188. Jameson, C.J.; Mason, J. The Parameters of NMR Spectroscopy. In *Multinuclear NMR*, 1st ed.; Mason, J., Ed.; Plenum Press: New York, NY, USA, 1987; pp. 3–50. [[CrossRef](#)]
189. Jameson, C.J.; Mason, J. The Chemical Shift. In *Multinuclear NMR*, 1st ed.; Mason, J., Ed.; Plenum Press: New York, NY, USA, 1987; pp. 51–88. [[CrossRef](#)]
190. Schneider, W.G.; Bernstein, H.J.; Pople, J.A. Proton Magnetic Resonance Chemical Shift of Free (Gaseous) and Associated (Liquid) Hydride Molecules. *J. Chem. Phys.* **1958**, *28*, 601–607. [[CrossRef](#)]
191. Kidd, R.G. Nuclear Shielding of the Transition Metals. *Ann. Rep. NMR Spectrosc.* **1980**, *10A*, 1–79. [[CrossRef](#)]
192. Kidd, R.G. The Oxidation-State Dependence of Transition-Metal Shieldings. *Ann. Rep. NMR Spectrosc.* **1991**, *23*, 85–139. [[CrossRef](#)]
193. Takashima, H.; Hada, M.; Nakatsuji, H. Spin-orbit effect on the magnetic shielding constant using the ab initio UHF method: Gallium and indium tetrahalides. *Chem. Phys. Lett.* **1995**, *235*, 13–16. [[CrossRef](#)]
194. Nakatsuji, H.; Nakajima, T.; Hada, M.; Takashima, H.; Tanaka, S. Spin-orbit effect on the magnetic shielding constant using the ab initio UHF method: Silicon tetrahalides. *Chem. Phys. Lett.* **1995**, *247*, 418–424. [[CrossRef](#)]
195. Nakatsuji, H.; Hada, M.; Tejima, T.; Nakajima, T.; Sugimoto, M. Spin-orbit effect on the magnetic shielding constant using the ab initio UHF method. Electronic mechanism in the aluminum compounds,  $\text{AlX}_4^-$  ( $X = \text{H, F, Cl, Br}$  and  $\text{I}$ ). *Chem. Phys. Lett.* **1996**, *249*, 284–289. [[CrossRef](#)]
196. Nakatsuji, H.; Hada, H.; Kaneko, H.; Ballard, C.C. Relativistic study of nuclear magnetic shielding constants: Mercury dihalides. *Chem. Phys. Lett.* **1996**, *255*, 195–202. [[CrossRef](#)]
197. Hada, M.; Kaneko, H.; Nakatsuji, H. Relativistic study of nuclear magnetic shielding constants: Tungsten hexahalides and tetraoxide. *Chem. Phys. Lett.* **1996**, *261*, 7–12. [[CrossRef](#)]
198. Viesser, R.V.; Ducati, L.C.; Tormena, C.F.; Autschbach, J. The halogen effect on the  $^{13}\text{C}$  NMR chemical shift in substituted benzenes. *Phys. Chem. Chem. Phys.* **2018**, *20*, 11247–11259. [[CrossRef](#)]
199. Nakagawa, N.; Sinada, S.; Obinata, S. Heavy atom-derived spin polarization shifts. In Proceedings of the “The 6th NMR Symposium”, Japan, Kyoto, 1967; pp. 8–12.
200. Lohr, L.L., Jr.; Pyykkö, P. Relativistically parameterized extended Hückel theory. *Chem. Phys. Lett.* **1979**, *62*, 333–338. [[CrossRef](#)]
201. Hoffmann, R. An Extended Hückel Theory. I. Hydrocarbons. *J. Chem. Phys.* **1963**, *39*, 1397–1412. [[CrossRef](#)]
202. Kaupp, M.; Malkina, O.L.; Malkin, V.G. Interpretation of  $^{13}\text{C}$  NMR chemical shifts in halomethyl cations. On the importance of spin-orbit coupling and electron correlation. *Chem. Phys. Lett.* **1997**, *265*, 55–59. [[CrossRef](#)]
203. Malkin, V.G.; Malkina, O.L.; Casida, M.E.; Salahub, D.R. Nuclear Magnetic Resonance Shielding Tensors Calculated with a Sum-over-States Density Functional Perturbation Theory. *J. Am. Chem. Soc.* **1994**, *116*, 5898–5908. [[CrossRef](#)]
204. Malkin, V.G.; Malkina, O.L.; Eriksson, L.A.; Salahub, D.R. The calculation of NMR and ESR spectroscopy parameters using density functional theory. In *Theoretical and Computational Chemistry. Modern Density Functional Theory: A Tool for Chemistry*, 1st ed.; Seminario, J.M., Politzer, P., Eds.; Elsevier Science: Amsterdam, The Netherlands, 1995; Volume 2, Chapter 9, pp. 273–348.
205. Pople, J.A.; McIver, J.W., Jr.; Ostlund, N.S. Self-Consistent Perturbation Theory. II. Nuclear-Spin Coupling Constants. *J. Chem. Phys.* **1968**, *49*, 2965–2970. [[CrossRef](#)]
206. Malkina, O.L.; Schimmelpfennig, B.; Kaupp, M.; Hess, B.A.; Chandra, P.; Wahlgren, U.; Malkin, V.G. Spin-orbit corrections to NMR shielding constants from density functional theory. How important are the two-electron terms? *Chem. Phys. Lett.* **1998**, *296*, 93–104. [[CrossRef](#)]
207. Kaupp, M.; Aubauer, C.; Engelhardt, G.; Klapötke, T.M.; Malkina, O.L. The  $\text{PI}_4^+$  cation has an extremely large negative  $^{31}\text{P}$  nuclear magnetic resonance chemical shift, due to spin-orbit coupling: A quantum-chemical prediction and its confirmation by solid-state nuclear magnetic resonance spectroscopy. *J. Chem. Phys.* **1999**, *110*, 3897–3902. [[CrossRef](#)]
208. Kaupp, M.; Malkina, O.L.; Malkin, V.G. The Role of  $\pi$ -Type Nonbonding Orbitals for Spin-Orbit Induced NMR Chemical Shifts: DFT Study of  $^{13}\text{C}$  and  $^{19}\text{F}$  Shifts in the Series  $\text{CF}_3\text{IF}_n$  ( $n = 0, 2, 4, 6$ ). *J. Comput. Chem.* **1999**, *20*, 1304–1313. [[CrossRef](#)]
209. Perdew, J.P.; Wang, Y. Accurate and simple analytic representation of the electron-gas correlation energy. *Phys. Rev. B* **1992**, *45*, 13244–13249. [[CrossRef](#)] [[PubMed](#)]
210. Perdew, J.P.; Chevary, J.A.; Vosko, S.H.; Jackson, K.A.; Pederson, M.R.; Singh, D.J.; Fiolhais, C. Atoms, molecules, solids, and surfaces: Applications of the generalized gradient approximation for exchange and correlation. *Phys. Rev. B* **1992**, *46*, 6671–6687. [[CrossRef](#)]
211. Partridge, H. Near Hartree-Fock quality GTO basis sets for the first- and third-row atoms. *J. Chem. Phys.* **1989**, *90*, 1043–1047. [[CrossRef](#)]
212. Partridge, H.; Faegri, K. High-quality Gaussian basis sets for fourth-row atoms. *Theor. Chim. Acta* **1992**, *82*, 207–212. [[CrossRef](#)]
213. Partridge, H. Near Hartree-Fock quality GTO basis sets for the second-row atoms. *J. Chem. Phys.* **1987**, *87*, 6643–6647. [[CrossRef](#)]

214. Kantola, A.M.; Lantto, P.; Vaara, J.; Jokisaari, J. Carbon and proton shielding tensors in methyl halides. *Phys. Chem. Chem. Phys.* **2010**, *12*, 2679–2692. [[CrossRef](#)] [[PubMed](#)]
215. Bartlett, R.J.; Silver, D.M. Correlation energy in LiH, BH, and HF with many-body perturbation theory using Slater-type atomic orbitals. *Int. J. Quantum Chem.* **1974**, *S8*, 271–276. [[CrossRef](#)]
216. Binkley, J.S.; Pople, J.A. Møller–Plesset theory for atomic ground state energies. *Int. J. Quantum Chem.* **1975**, *9*, 229–236. [[CrossRef](#)]
217. Bartlett, R.J. Many-body perturbation theory and coupled cluster theory for electron correlation in molecules. *Annu. Rev. Phys. Chem.* **1981**, *32*, 359–401. [[CrossRef](#)]
218. Gauss, J.; Stanton, J.F. Analytic CCSD(T) second derivatives. *Chem. Phys. Lett.* **1997**, *276*, 70–77. [[CrossRef](#)]
219. Knizia, G.; Adler, T.B.; Werner, H.-J. Simplified CCSD(T)-F12 methods: Theory and benchmarks. *J. Chem. Phys.* **2009**, *130*, 054104. [[CrossRef](#)]
220. Stanton, J.F.; Gauss, J.; Siehl, H.-U. CCSD(T) calculation of NMR chemical shifts: Consistency of calculated and measured  $^{13}\text{C}$  chemical shifts in the 1-cyclopropylcyclopropylidenemethyl cation. *Chem. Phys. Lett.* **1996**, *262*, 183–186. [[CrossRef](#)]
221. Rasul, G.; Surya Prakash, G.K.; Olah, G.A. Comparative study of the hypercoordinate ions  $\text{C}_7\text{H}_9^+$  and  $\text{C}_8\text{H}_9^+$  by the ab initio/GIAO-CCSD(T) method. *J. Phys. Chem. A* **2006**, *110*, 11320–11323. [[CrossRef](#)]
222. Kupka, T.; Stachów, M.; Kaminsky, J.; Sauer, S.P.A. Estimation of isotropic nuclear magnetic shieldings in the CCSD(T) and MP2 complete basis set limit using affordable correlation calculations. *Magn. Reson. Chem.* **2013**, *51*, 482–489. [[CrossRef](#)]
223. Lee, C.; Yang, W.; Parr, R.G. Development of the Colle-Salvetti correlation-energy formula into a functional of the electron density. *Phys. Rev. B* **1988**, *37*, 785–789. [[CrossRef](#)]
224. Becke, A.D. Density-functional thermochemistry. III. The role of exact exchange. *J. Chem. Phys.* **1993**, *98*, 5648–5652. [[CrossRef](#)]
225. Becke, A.D. A new mixing of Hartree–Fock and local density-functional theories. *J. Chem. Phys.* **1993**, *98*, 1372–1377. [[CrossRef](#)]
226. Casella, G.; Bagno, A.; Komorovsky, S.; Repisky, M.; Saielli, G. Four-Component Relativistic DFT Calculations of  $^{13}\text{C}$  Chemical Shifts of Halogenated Natural Substances. *Chem. Eur. J.* **2015**, *21*, 18834–18840. [[CrossRef](#)] [[PubMed](#)]
227. Neto, A.C.; Ducati, L.C.; Rittner, R.; Tormena, C.F.; Contreras, R.H.; Frenking, G. Heavy Halogen Atom Effect on  $^{13}\text{C}$  NMR Chemical Shifts in Monohalo Derivatives of Cyclohexane and Pyran. Experimental and Theoretical Study. *J. Chem. Theory Comput.* **2009**, *5*, 2222–2228. [[CrossRef](#)] [[PubMed](#)]
228. Hyvärinen, M.; Vaara, J.; Goldammer, A.; Kutzky, B.; Hegetschweiler, K.; Kaupp, M.; Straka, M. Characteristic Spin-Orbit Induced  $^1\text{H}(\text{CH}_2)$  Chemical Shifts upon Deprotonation of Group 9 Polyamine Aqua and Alcohol Complexes. *J. Am. Chem. Soc.* **2009**, *131*, 11909–11918. [[CrossRef](#)]
229. Hegetschweiler, K.; Kuppert, D.; Huppert, J.; Straka, M.; Kaupp, M. Spin-Orbit-Induced Anomalous pH-Dependence in  $^1\text{H}$  NMR Spectra of CoIII Amine Complexes: A Diagnostic Tool for Structure Elucidation. *J. Am. Chem. Soc.* **2004**, *126*, 6728–6738. [[CrossRef](#)]
230. Viesser, R.V.; Ducati, L.C.; Autschbach, J.; Tormena, C.F. Effects of stereoelectronic interactions on the relativistic spin–orbit and paramagnetic components of the  $^{13}\text{C}$  NMR shielding tensors of dihaloethenes. *Phys. Chem. Chem. Phys.* **2015**, *17*, 19315–19324. [[CrossRef](#)]
231. Demissie, T.B.; Repisky, M.; Komorovsky, S.; Isaksson, J.; Svendsen, J.S.; Dodziuk, H.; Ruud, K. Four-component relativistic chemical shift calculations of halogenated organic compounds. *J. Phys. Org. Chem.* **2013**, *26*, 679–687. [[CrossRef](#)]
232. Perdew, J.P.; Burke, K.; Ernzerhof, M. Generalized Gradient Approximation Made Simple. *Phys. Rev. Lett.* **1996**, *77*, 3865–3868. [[CrossRef](#)]
233. Perdew, J.P.; Burke, K.; Ernzerhof, M. Generalized Gradient Approximation Made Simple. *Phys. Rev. Lett.* **1996**, *77*, 3865–3868, Erratum in *Phys. Rev. Lett.* **1997**, *78*, 1396–1396. [[CrossRef](#)] [[PubMed](#)]
234. Slater, J.C.; Phillips, J.C. *Quantum Theory of Molecules and Solids: The Self-Consistent Field for Molecules and Solids*, 1st ed.; McGraw-Hill: New York, NY, USA, 1974; Volume 4, pp. 1–583. [[CrossRef](#)]
235. Vosko, S.H.; Wilk, L.; Nusair, M. Accurate spin-dependent electron liquid correlation energies for local spin density calculations: A critical analysis. *Can. J. Phys.* **1980**, *59*, 1200–1211. [[CrossRef](#)]
236. Becke, A.D. Density-functional exchange-energy approximation with correct asymptotic behavior. *Phys. Rev. A* **1988**, *38*, 3098–3100. [[CrossRef](#)] [[PubMed](#)]
237. Perdew, J. Density-functional approximation for the correlation energy of the inhomogeneous electron gas. *Phys. Rev. B* **1986**, *33*, 8822–8824. [[CrossRef](#)]
238. Burke, K.; Perdew, J.P.; Wang, Y. Derivation of a Generalized Gradient Approximation: The PW91 Density Functional. In *Electronic Density Functional Theory*, 1st ed.; Dobson, J.F., Vignale, G., Das, M.P., Eds.; Springer: Boston, MA, USA, 1998; pp. 81–111. [[CrossRef](#)]
239. Irwin, J.J.; Shoichet, B.K. ZINC—A free database of commercially available compounds for virtual screening. *J. Chem. Inf. Mod.* **2004**, *45*, 177–182. [[CrossRef](#)]
240. Bolton, E.E.; Wang, Y.; Thiessen, P.A.; Bryant, S.H. Chapter 12—PubChem: Integrated Platform of Small Molecules and Biological Activities. *Annu. Rep. Comput. Chem.* **2008**, *4*, 217–241. [[CrossRef](#)]
241. Samultsev, D.O.; Rusakov, Y.Y.; Krivdin, L.B. Normal halogen dependence of  $^{13}\text{C}$  NMR chemical shifts of halogenomethanes revisited at the four-component relativistic level. *Magn. Reson. Chem.* **2016**, *54*, 787–792. [[CrossRef](#)]
242. Handy, N.C.; Cohen, A.J. Left-right correlation energy. *Mol. Phys.* **2001**, *99*, 403–412. [[CrossRef](#)]

243. Perdew, J.P. Unified Theory of Exchange and Correlation Beyond the Local Density Approximation. In *Electronic Structure of Solids*, 91 ed.; Ziesche, P., Eschig, H., Eds.; Akademie Verlag: Berlin, Germany, 1991; pp. 11–20.
244. Glaser, R.; Chen, N.; Wu, N.; Knotts, N.; Kaupp, M.  $^{13}\text{C}$  NMR Study of Halogen Bonding of Haloarenes: Measurements of Solvent Effects and Theoretical Analysis. *J. Am. Chem. Soc.* **2004**, *126*, 4412–4419. [[CrossRef](#)]
245. Radula-Janik, K.; Kupka, T.; Ejsmont, K.; Daszkiewicz, Z.; Sauer, S.P.A. Halogen effect on structure and  $^{13}\text{C}$  NMR chemical shift of 3,6-disubstituted-N-alkyl carbazoles. *Magn. Reson. Chem.* **2013**, *51*, 630–635. [[CrossRef](#)]
246. Zhao, J.; Truhlar, D.G. Improved Description of Nuclear Magnetic Resonance Chemical Shielding Constants Using the M06-L Meta-Generalized-Gradient-Approximation Density Functional. *J. Phys. Chem. A* **2008**, *122*, 6794–6799. [[CrossRef](#)] [[PubMed](#)]
247. Standara, S.; Maliňáková, K.; Marek, R.; Marek, J.; Hocek, M.; Vaara, J.; Straka, M. Understanding the NMR chemical shifts for 6-halopurines: Role of structure, solvent and relativistic effects. *Phys. Chem. Chem. Phys.* **2010**, *12*, 5126–5139. [[CrossRef](#)] [[PubMed](#)]
248. Ariai, J.; Saielli, G. “Through-Space” Relativistic Effects on NMR Chemical Shifts of Pyridinium Halide Ionic Liquids. *ChemPhysChem* **2018**, *20*, 108–115. [[CrossRef](#)] [[PubMed](#)]
249. Vicha, J.; Švec, P.; Růžičková, Z.; Samsonov, M.A.; Bártová, K.; Růžička, A.; Straka, M.; Dračínský, M. Experimental and Theoretical Evidence of Spin-Orbit Heavy Atom on the Light Atom  $^1\text{H}$  NMR Chemical Shifts Induced through  $\text{H}\cdots\text{I}$ –Hydrogen Bond. *Chem. Eur. J.* **2020**, *26*, 8698–8702. [[CrossRef](#)] [[PubMed](#)]
250. Pickard, C.J.; Mauri, F. All-electron magnetic response with pseudopotentials: NMR chemical shifts. *Phys. Rev. B* **2001**, *63*, 245101. [[CrossRef](#)]
251. Bonhomme, C.; Gervais, C.; Babonneau, F.; Coelho, C.; Pourpoint, F.; Azais, T.; Ashbrook, S.E.; Griffin, J.M.; Yates, J.R.; Mauri, F.; et al. First-Principles Calculation of NMR Parameters Using the Gauge Including Projector Augmented Wave Method: A Chemist’s Point of View. *Chem. Rev.* **2012**, *112*, 5733–5779. [[CrossRef](#)]
252. Rodriguez, J.I. An efficient method for computing the QTAIM topology of a scalar field: The electron density case. *J. Comput. Chem.* **2013**, *34*, 681–686. [[CrossRef](#)]
253. Nakanishi, W.; Hayashi, S.; Narahara, K. Atoms-in-Molecules Dual Parameter Analysis of Weak to Strong Interactions: Behaviors of Electronic Energy Densities versus Laplacian of Electron Densities at Bond Critical Points. *J. Phys. Chem. A* **2008**, *112*, 13593–13599. [[CrossRef](#)]
254. Vicha, J.; Foroutan-Nejad, C.; Pawlak, T.; Munzarová, M.L.; Straka, M.; Marek, R. Understanding the electronic factors responsible for ligand spin-orbit NMR shielding in transition-metal complexes. *J. Chem. Theory Comput.* **2015**, *11*, 1509–1517. [[CrossRef](#)]
255. Jaszunski, M.; Olejniczak, M. NMR shielding constants in  $\text{SeH}_2$  and  $\text{TeH}_2$ . *Mol. Phys.* **2013**, *111*, 1355–1363. [[CrossRef](#)]
256. Rusakov, Y.Y.; Rusakova, I.L.; Krivdin, L.B. On the significant relativistic heavy atom effect on  $^{13}\text{C}$  NMR chemical shifts of  $\beta$ - and  $\gamma$ -carbons in seleno- and telluroketones. *Mol. Phys.* **2017**, *115*, 3117–3127. [[CrossRef](#)]
257. Rusakov, Y.Y.; Rusakova, I.L.; Krivdin, L.B. Relativistic heavy atom effect on the  $^{31}\text{P}$  NMR parameters of phosphine chalcogenides. Part 1. Chemical shifts. *Magn. Reson. Chem.* **2018**, *56*, 1061–1073. [[CrossRef](#)] [[PubMed](#)]
258. Lantto, P.; Kangasvieri, S.; Vaara, J. Electron correlation and relativistic effects in the secondary NMR isotope shifts of  $\text{CSe}_2$ . *Phys. Chem. Chem. Phys.* **2013**, *15*, 17468–17478. [[CrossRef](#)] [[PubMed](#)]
259. Kellö, V.; Sadlej, A.J. Medium-size polarized basis sets for high-level-correlated calculations of molecular electric properties. *Theor. Chim. Acta* **1992**, *83*, 351–366. [[CrossRef](#)]
260. Berger, R.J.F.; Rettenwander, D.; Spirk, S.; Wolf, C.; Patzschke, M.; Ertl, M.; Monkowius, U.; Mitzel, N.W. Relativistic effects in triphenylbismuth and their influence on molecular structure and spectroscopic properties. *Phys. Chem. Chem. Phys.* **2012**, *14*, 15520–15524. [[CrossRef](#)]
261. Bast, R.; Jensen, H.J.A.; Saue, T. Relativistic adiabatic time-dependent density functional theory using hybrid functionals and noncollinear spin magnetization. *Int. J. Quantum Chem.* **2009**, *109*, 2091–2112. [[CrossRef](#)]
262. Lévy-Leblond, J.-M. Nonrelativistic particles and wave equations. *Commun. Math. Phys.* **1967**, *6*, 286–311. [[CrossRef](#)]
263. Rusakov, Y.Y.; Rusakova, I.L. Relativistic heavy atom effect on  $^{13}\text{C}$  NMR chemical shifts initiated by adjacent multiple chalcogens. *Magn. Reson. Chem.* **2018**, *56*, 716–726. [[CrossRef](#)]
264. Rusakov, Y.Y.; Rusakova, I.L.; Krivdin, L.B. On the HALA effect in the NMR carbon shielding constants of the compounds containing heavy p-elements. *Int. J. Quantum Chem.* **2016**, *116*, 1404–1412. [[CrossRef](#)]
265. Demissie, T.B. Relativistic effects on the NMR parameters of Si, Ge, Sn, and Pb alkynyl compounds: Scalar versus spin-orbit effects. *J. Chem. Phys.* **2017**, *147*, 174301. [[CrossRef](#)]
266. Vicha, J.; Marek, R.; Straka, M. High-Frequency  $^1\text{H}$  NMR Chemical Shifts of SnII and PbII Hydrides Induced by Relativistic Effects: Quest for PbII Hydrides. *Inorg. Chem.* **2016**, *55*, 10302–10309. [[CrossRef](#)]
267. Vicha, J.; Marek, R.; Straka, M. High-Frequency  $^{13}\text{C}$  and  $^{29}\text{Si}$  NMR Chemical Shifts in Diamagnetic Low-Valence Compounds of TII and PbII: Decisive Role of Relativistic Effects. *Inorg. Chem.* **2016**, *55*, 1770–1781. [[CrossRef](#)]
268. Gómez, S.S.; Aucar, G.A. Relativistic effects on the nuclear magnetic resonance shielding of FX (X = F, Cl, Br, I, and At) molecular systems. *J. Chem. Phys.* **2011**, *134*, 204314. [[CrossRef](#)]
269. Field-Theodore, T.E.; Olejniczak, M.; Jaszunski, M.; Wilson, D.J.D. NMR shielding constants in group 15 trifluorides. *Phys. Chem. Chem. Phys.* **2018**, *20*, 23025–23033. [[CrossRef](#)]
270. Perdew, J.P.; Ernzerhof, M.; Burke, K. Rationale for mixing exact exchange with density functional approximations. *J. Chem. Phys.* **1996**, *105*, 9982–9985. [[CrossRef](#)]

271. Ernzerhof, M.; Scuseria, G.E. Assessment of the Perdew–Burke–Ernzerhof exchange–correlation functional. *J. Chem. Phys.* **1999**, *110*, 5029–5036. [[CrossRef](#)]
272. Adamo, C.; Barone, V. Toward reliable density functional methods without adjustable parameters: The PBE0 model. *J. Chem. Phys.* **1999**, *110*, 6158–6170. [[CrossRef](#)]
273. Keal, T.W.; Tozer, D.J. The exchange–correlation potential in Kohn–Sham nuclear magnetic resonance shielding calculations. *J. Chem. Phys.* **2003**, *119*, 3015–3024. [[CrossRef](#)]
274. Keal, T.W.; Tozer, D.J. A semiempirical generalized gradient approximation exchange–correlation functional. *J. Chem. Phys.* **2004**, *121*, 5654–5660. [[CrossRef](#)]
275. Keal, T.W.; Tozer, D.J.; Helgaker, T. GIAO shielding constants and indirect spin–spin coupling constants: Performance of density functional methods. *Chem. Phys. Lett.* **2004**, *391*, 374–379. [[CrossRef](#)]
276. Teale, A.M.; Tozer, D.J. Exchange representations in Kohn–Sham NMR shielding calculations. *Chem. Phys. Lett.* **2004**, *383*, 109–114. [[CrossRef](#)]
277. Sugimoto, M.; Kanayama, M.; Nakatsuji, H. Theoretical study on metal NMR chemical shifts. Gallium compounds,  $\text{GaCl}_{4-n}\text{Br}_n^-$  ( $n = 0 - 4$ ). *J. Phys. Chem.* **1993**, *97*, 5868–5874. [[CrossRef](#)]
278. Fedorov, S.V.; Rusakov, Y.Y.; Krivdin, L.B. Relativistic Environmental Effects in  $^{29}\text{Si}$  NMR Chemical Shifts of Halosilanes: Light Nucleus, Heavy Environment. *J. Phys. Chem. A* **2015**, *119*, 5778–5789. [[CrossRef](#)]
279. Dylla, K.G. Relativistic and nonrelativistic finite nucleus optimized triple-zeta basis sets for the 4p, 5p and 6p elements. *Theor. Chem. Acc.* **2002**, *108*, 335–340. [[CrossRef](#)]
280. Dylla, K.G. Relativistic quadruple-zeta and revised triple-zeta and double-zeta basis Sets for the 4p, 5p, and 6p elements. *Theor. Chem. Acc.* **2006**, *115*, 441–447. [[CrossRef](#)]
281. Bühl, M.; Kaupp, M.; Malkina, O.L.; Malkin, V.G. The DFT Route to NMR Chemical Shifts. *J. Comput. Chem.* **1999**, *20*, 91–105. [[CrossRef](#)]
282. Chernyshev, K.A.; Krivdin, L.B. Quantum–chemical calculations of NMR chemical shifts of organic molecules: II. Influence of medium, relativistic effects, and vibrational corrections on phosphorus magnetic shielding constants in the simplest phosphines and phosphine chalcogenides. *Rus. J. Org. Chem.* **2011**, *47*, 355–362. [[CrossRef](#)]
283. Chernyshev, K.A.; Krivdin, L.B.; Fedorov, S.V.; Arbuzova, S.N.; Ivanova, N.I. Quantum Chemical Calculations of NMR Chemical Shifts of Organic Molecules: XI.\* Conformational and Relativistic Effects on the  $^{31}\text{P}$  and  $^{77}\text{Se}$  Chemical Shifts of Phosphine Selenides. *Russ. J. Org. Chem.* **2013**, *49*, 1420–1427. [[CrossRef](#)]
284. Fedorov, S.V.; Rusakov, Y.Y.; Krivdin, L.B. Towards the versatile DFT and MP2 computational schemes for  $^{31}\text{P}$  NMR chemical shifts taking into account relativistic corrections. *Magn. Reson. Chem.* **2014**, *52*, 699–710. [[CrossRef](#)]
285. Hocek, M.; Masojdková, M.; Holý, A. Synthesis of Acyclic Nucleotide Analogues Derived from 6-Hetarylpurines via Cross-Coupling Reactions of 9-[2-(Diethoxyphosphorylmethoxy)ethyl]-6-iodopurine with Hetaryl Organometallic Reagents. *Collect. Czech. Chem. Commun.* **1997**, *62*, 136–146. [[CrossRef](#)]
286. Samultsev, D.O.; Rusakov, Y.Y.; Krivdin, L.B. Relativistic effects of chlorine in  $^{15}\text{N}$  NMR chemical shifts of chlorine-containing amines. *Russ. J. Org. Chem.* **2017**, *53*, 1738–1739. [[CrossRef](#)]
287. Samultsev, D.O.; Rusakov, Y.Y.; Krivdin, L.B. On the long-range relativistic effects in the  $^{15}\text{N}$  NMR chemical shifts of halogenated azines. *Magn. Reson. Chem.* **2017**, *55*, 990–995. [[CrossRef](#)]
288. Jensen, F. Basis Set Convergence of Nuclear Magnetic Shielding Constants Calculated by Density Functional Methods. *J. Chem. Theory Comput.* **2008**, *4*, 719–727. [[CrossRef](#)]
289. Karplus, M. Contact Electron-Spin Coupling of Nuclear Magnetic Moments. *J. Chem. Phys.* **1959**, *30*, 11–15. [[CrossRef](#)]
290. Rusakova, I.L.; Krivdin, L.B. Karplus dependence of spin–spin coupling constants revisited theoretically. Part 1: Second-order double perturbation theory. *Phys. Chem. Chem. Phys.* **2013**, *15*, 18195–18203. [[CrossRef](#)]
291. Schraml, J.  $^{13}\text{C}$ -NMR spectra of monosubstituted and symmetrically 1,2-disubstituted ethenes. *Collect. Czech. Chem. Commun.* **1976**, *41*, 3063–3076. [[CrossRef](#)]
292. Savitsky, G.; Namikawa, K. Carbon-13 Chemical Shifts and Geometric Isomerism About the Ethylenic Double Bond. *J. Phys. Chem.* **1963**, *67*, 2754–2756. [[CrossRef](#)]
293. Maciel, G.E.; Ellis, P.D.; Natterstad, J.J.; Savitsky, G.B. The effect of geometric isomerism on the carbon-13 chemical shift of diiodoethylene and related compounds. *J. Magn. Reson.* **1969**, *1*, 589–605. [[CrossRef](#)]
294. Minaev, B.; Vaara, J.; Ruud, K.; Vahtras, O.; Ågren, H. Internuclear distance dependence of the spin–orbit coupling contributions to proton NMR chemical shifts. *Chem. Phys. Lett.* **1998**, *295*, 455–461. [[CrossRef](#)]
295. Minaev, B.F. Theoretical Analysis and Prognostication of Spin–Orbit Coupling Effects in Molecular Spectroscopy and Chemical Kinetics. Ph.D. Thesis, N.N. Semenov Institute of Chemical Physics, Moscow, Russia, 1981.
296. Bacskey, G.B. On the calculation of nuclear spin–spin coupling constants. The bond length dependence of the Fermi contact term in  $\text{H}_2$  and  $\text{HD}$ . *Chem. Phys. Lett.* **1995**, *242*, 507–513. [[CrossRef](#)]
297. Crompt, B.; Carrington, T., Jr.; Salahub, D.R.; Malkina, O.L.; Malkin, V.G. Effect of rotation and vibration on nuclear magnetic resonance chemical shifts: Density functional theory calculations. *J. Chem. Phys.* **1999**, *110*, 7153–7159. [[CrossRef](#)]
298. Jameson, C.J.; Jameson, A.K.; Burrell, P.M.  $^{19}\text{F}$  nuclear magnetic shielding scale from gas phase studies. *J. Chem. Phys.* **1980**, *73*, 6013–6020. [[CrossRef](#)]

299. Lantto, P.; Vaara, J.; Kantola, A.M.; Telkki, V.-V.; Schimmelpfennig, B.; Ruud, K.; Jokisaari, J. Relativistic Spin-Orbit Coupling Effects on Secondary Isotope Shifts of  $^{13}\text{C}$  Nuclear Shielding in  $\text{CX}_2$  ( $X = \text{O}, \text{S}, \text{Se}, \text{Te}$ ). *J. Am. Chem. Soc.* **2002**, *124*, 2762–2771. [[CrossRef](#)] [[PubMed](#)]
300. Hess, B.A.; Marian, C.M.; Wahlgren, U.; Gropen, O. A mean-field spin-orbit method applicable to correlated wavefunctions. *Chem. Phys. Lett.* **1996**, *251*, 365–371. [[CrossRef](#)]
301. Jakubowska, K.; Pecul, M.; Ruud, K. Vibrational Corrections to NMR Spin–Spin Coupling Constants from Relativistic Four-Component DFT Calculations. *J. Phys. Chem. A* **2022**, *126*, 7013–7020. [[CrossRef](#)] [[PubMed](#)]

**Disclaimer/Publisher’s Note:** The statements, opinions and data contained in all publications are solely those of the individual author(s) and contributor(s) and not of MDPI and/or the editor(s). MDPI and/or the editor(s) disclaim responsibility for any injury to people or property resulting from any ideas, methods, instructions or products referred to in the content.